Overview and Validation of the VENTURE Core Models used in Support of the WPI Fuel Transfer Project

Dr. John R. White, Jeremy Marcyoniak, and Michael Pike

Chemical and Nuclear Engineering Department
University of Massachusetts Lowell
Lowell, MA 01854

September 1, 2012

Introduction

Upon closing of the Worcester Polytechnic Institute (WPI) research reactor, arrangements have been made to transfer the slightly used WPI fuel elements to UMass-Lowell for use in our on-campus 1 MW pool-type research reactor. The UMass-Lowell research reactor (UMLRR) and WPI fuel assemblies are quite similar in overall size and shape, so the elements should fit nicely within the UMLRR grid support structure (the assembly size is approximately 3″×3″×30″ not including the end box extensions). However, although the WPI and UMLRR elements are the same size and both contain low enriched uranium (LEU) fuel, the material composition of the fuel meat is different -- the WPI fuel plates contain uranium-aluminide fuel (UAl_x-Al) and the UMLRR plates have uranium-silicide fuel (U_3Si_2-Al). In addition, the U235 loading is quite different (167 g for the WPI element vs. 200 g for the UMLRR assembly) and there are also some small differences in meat thickness, plate thickness, water gap thickness, etc. Thus, because of the number of variations to consider, a formal comparison and safety evaluation for combined use of the UMLRR and WPI fuel elements within the UMass-Lowell research reactor is needed -- and a series of reactor physics and thermal analysis computations will be required to perform the desired comparative analyses.

At UMass-Lowell, the VENTURE code is the primary tool used to do 2-D and 3-D core physics studies, with focus on computing reactivity effects and spatial power distributions (or thermal flux profiles) within a variety of core configurations. A set of consistent 2-D and 3-D VENTURE models was generated in 1999 for support of the conversion of HEU to LEU fuel in the UMLRR. The actual conversion was successfully completed in August 2000 and the models generated at that time have proved to be adequate for predicting the overall core physics behavior. References 1 – 4, for example, overview the actual models, document some of the preliminary design work used to support the conversion effort, and report upon some comparisons of calculation vs. measurement that were made during startup testing of the LEU core. Also, in the 10+ years of operation of the LEU core, the existing VENTURE models have served quite nicely in supporting general operation and use of the reactor.

However, after review of the existing models for use in the current effort, it became clear that some changes and updates were needed to support the WPI fuel transfer project and for future support of routine reactor operations within the UMLRR. In particular, there were several changes that could be made that would either simplify the model, make it more useful, or improve upon the overall accuracy of the computational results. Thus, the decision was made to

overhaul the existing VENTURE models -- and the goal of this report is simply to highlight these changes and to provide full documentation for validation of the new model. The new models will be used to support the current WPI fuel transfer project as well as provide general computational support for continued operation of the UMLRR for many years into the future.

The M-1-3 and M-2-5 UMLRR Core Configurations

The UMass-Lowell Research Reactor (UMLRR) contains a 7x9 grid of fuel assemblies, graphite reflector elements, radiation baskets, and corner posts. It also has two grid locations reserved for an external neutron source and a low-worth regulating rod for fine reactivity control. Four large control blade assemblies are used for gross reactivity control and for reactor shutdown. From the top view, the reactor is enclosed by an aluminum core box and a large pool of demineralized water surrounds the system on three sides, with a 3 inch lead shield and large graphite thermal column on the remaining side. A specific arrangement of fuel elements, graphite reflector blocks, and radiation baskets make up a particular core configuration.

The basic layout for the LEU startup core arrangement, including the six beam ports and thermal column, is sketched in Fig. 1. This reference configuration is referred to as the M-1-3 core and it contains 19 full fuel assemblies and 2 partial assemblies arranged roughly in the center of the 7x9 grid. Directly in the middle of the core is a central irradiation zone known as the flux trap. The flux trap is similar to a radiation basket, except that the region between the inner irradiation tube and the outer aluminum can is filled with graphite.

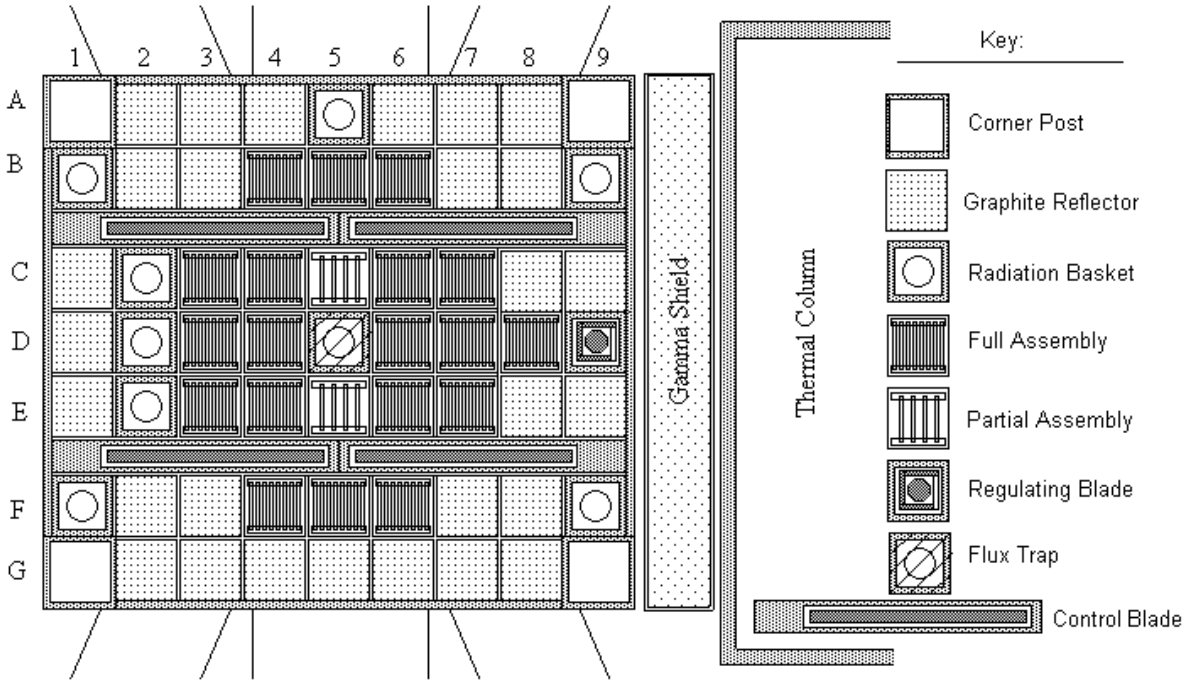

Fig. 1 Rough sketch of the LEU startup core configuration for the UMLRR (M-1-3 core).

During startup testing in Fall 2000, a series of reactivity evaluations and flux profile measurements were taken within the beginning-of-life (BOL) M-1-3 configuration to support routine operation of the new LEU core. In addition, formal comparison to the VENTURE calculations was made and the results of these model validation studies are summarized in Refs. 3 and 4. Now, 10+ years later, these results are still important since they can be used to help validate any new models that may be developed for the UMLRR. Thus, whenever any substantial model changes are made or a new cross section library is developed, the M-1-3 configuration is always modeled and evaluated as an important part of the overall validation effort.

During the latter part of 2001, a new ex-core fast neutron irradiation facility was installed within the UMLRR pool (see Refs. 5 and 6 for details). The purpose of this new experimental facility is to provide a large-volume irradiation location that has a relatively high fast neutron flux, with correspondingly low thermal neutron and gamma fluence rates. The fast neutron irradiator (FNI) replaced the three beam ports on the far side of the core (next to row A of the core grid structure). The FNI was purposely placed outside the core region for relatively easy access to the large experimental location and to minimize any effect on core operation during use of the new facility. The new irradiation facility did, however, require some changes to the actual in-core assembly configuration -- to optimize performance of the FNI and to counter reactivity effects caused by the composite facility changes. In particular, three key changes were made, including movement of the source holder from grid position A5 to G5, movement of the partial fuel elements from C5 and E5 to C3 and E3, and replacement of five graphite reflectors in row A with newly-designed lead-void assemblies (these elements eliminate the fast neutron moderation associated with graphite and they provide a first level of gamma shielding for the FNI). The resulting configuration, including the FNI grid and shield blocks, is referred to as the M-2-5 configuration and this is also the current operating layout for the UMLRR (in Aug. 2012). This post-FNI configuration is sketched in Fig. 2.

It should be noted that the VENTURE diffusion theory code is typically only used for incore physics analyses where the flux is not strongly anisotropic (due to the distributed fission source within the core region). However, in the excore FNI, beam port, and thermal column facilities, transport theory is required so that explicit treatment of the outgoing angular fluxes can be modeled. However, for the diffusion theory core models that focus on computing reactivity and power distributions, only a rough representation of these excore experimental facilities is needed to properly account for the core leakage at the core-excore boundary. Thus, in the VENTURE 2-D and 3-D core models discussed here, only those portions of the excore facilities that have any affect on the core are modeled with any detail (the reader is referred to Refs. 2, 5, and 6 for more information on some of our existing excore modeling efforts).

Also of note is that, during the approximately 12-year period since startup (Aug. 2000 through July 2012), the LEU core has about 1240 MWhr of total burnup (i.e. equivalent to about 52 full power days at 1 MW operation) -- where we note that the operation of the UMLRR is usually very intermittent and much of it occurs at low power in increments of only a few hours for a variety of training and educational purposes. Since it is not possible (and not necessary) to include all this operational detail, the burnup data is usually recorded in increments of MWD per month as shown in Fig. 3. This burnup rate data, when integrated over time, gives the cumulative burnup curve shown in Fig. 4 -- this gives the total core burnup at any point since

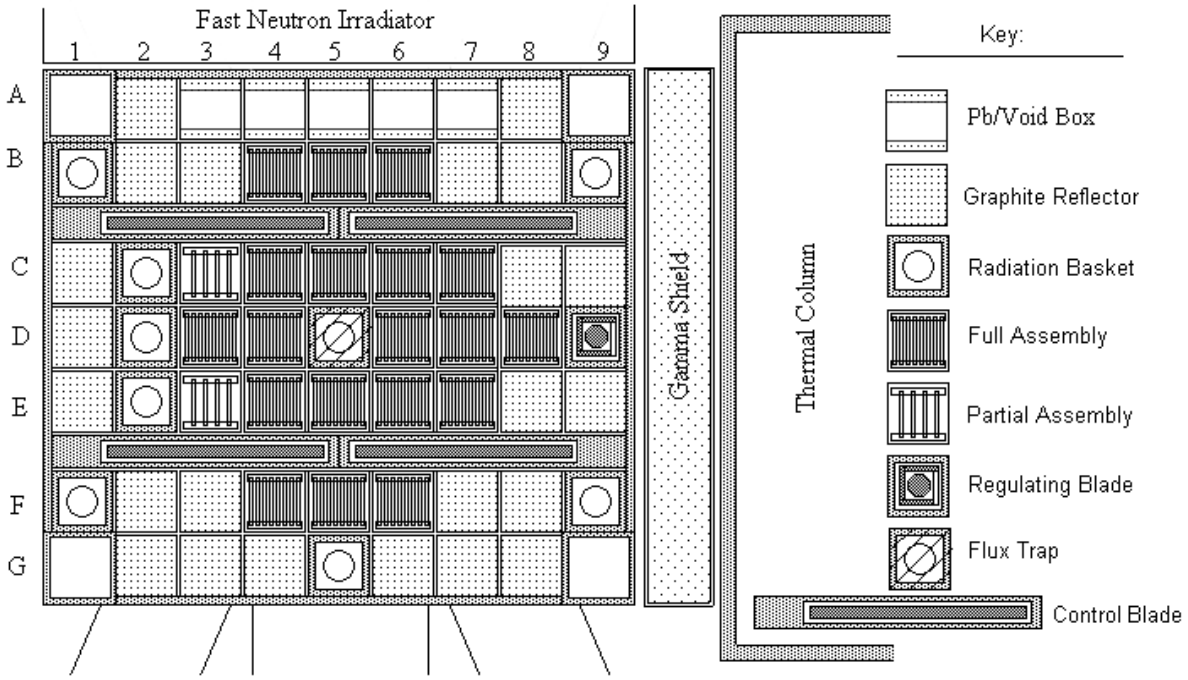

Fig. 2 Rough sketch of the post-FNI configuration for the UMLRR (M-2-5 core).

the start of LEU operation in Aug. 2000. Note that the extended down time (roughly Feb. 2001 to Nov. 2001) after only about six months of operations (as seen in Figs. 3 and 4) was due to the complete overhaul and upgrade of the data acquisition and control system within the UMLRR facility and for the installation of the excore fast neutron irradiator. In particular, the M-1-3 core only had about 4 MWD of burnup when the new M-2-5 configuration was installed. Thus, most of the full operating history to date has been associated with a single core layout -- that is, the M-2-5 configuration.

From a model validation perspective, the BOL M-1-3 model represents a fresh core and it has the most measured data available (reactivity evaluations and some thermal flux mappings) to support model evaluation -- thus, this configuration is the easiest and best to use for initial model validation. Next in line for model evaluation is the initial M-2-5 configuration, but only reactivity evaluations (i.e. measured blade worth curves) are available for this configuration. However, because of the low burnup level (about 4 MWD), approximating this configuration with fresh fuel densities gives a reasonable representation of reality. In contrast, for the current configuration with its roughly 50 MWD cumulative burnup, fuel depletion calculations are required to achieve a reasonable representation of the core physics. But, since the VENTURE model after 50 MWD of burnup represents current operations, this also creates an opportunity to perform additional measurements within the reactor to evaluate the overall suitability of the various modeling approximations. In particular, a series of reactivity worths measurements associated with various element interchanges have been made and compared to predictions from the VENTURE 3-D model -- and this represents our best validation of current operations (the results of these reactivity evaluations are given in a later section of this report).

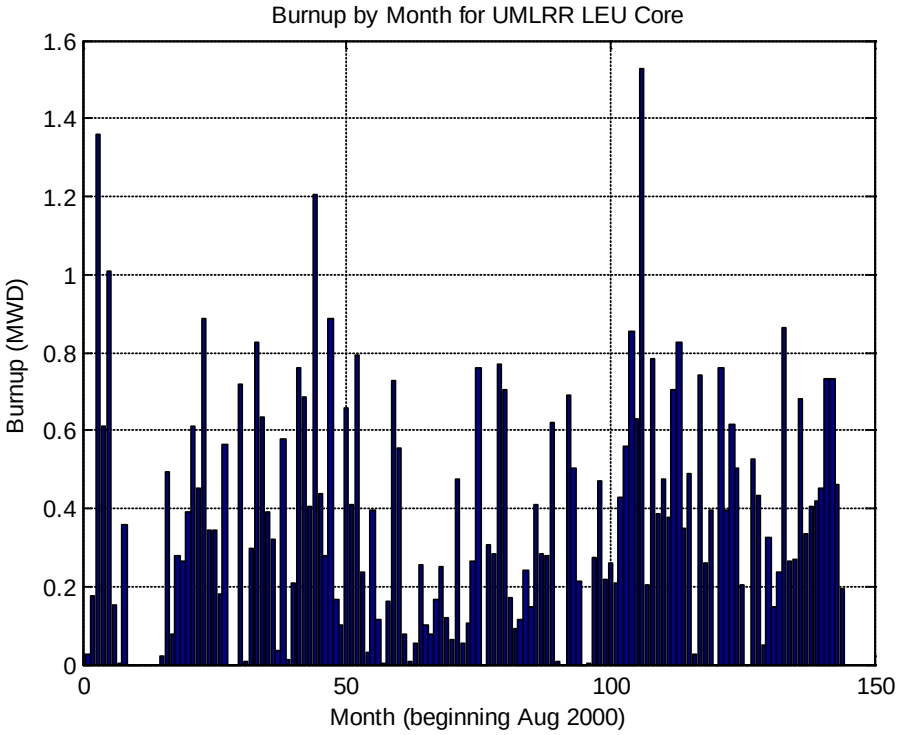

Fig. 3 Burnup rate history for the UMLRR LEU core.

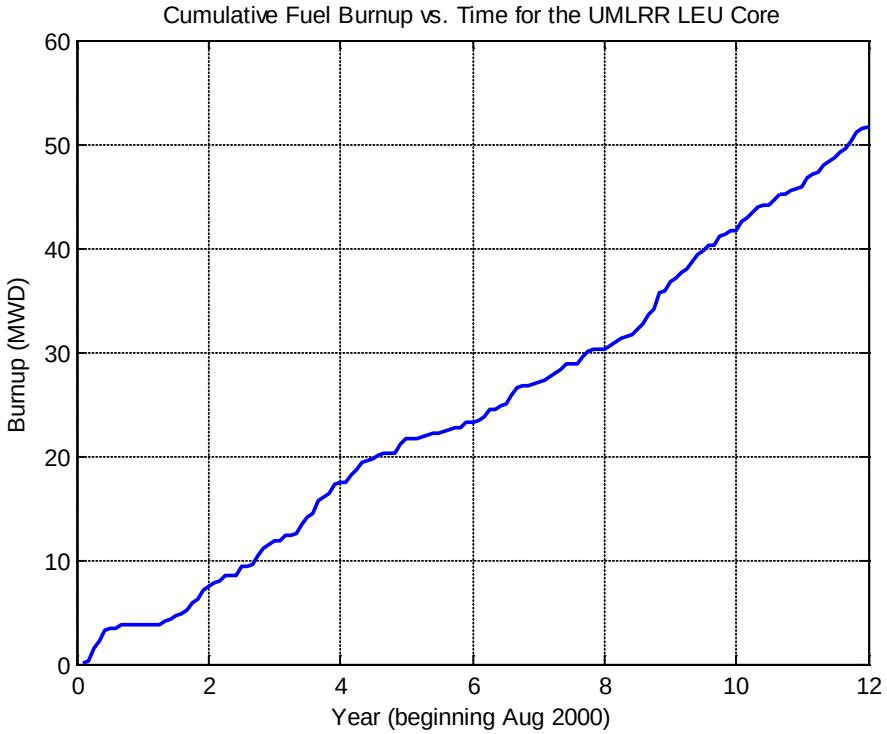

Fig. 4 Cumulative burnup history for the UMLRR LEU core.

The VENTURE 2-D and 3-D Models (2011/2012 versions)

Putting together a computational model for any reactor system requires precise information about the geometry and material composition of the actual system. It also requires a number of decisions by the model builder concerning the mesh grid layout, the zone placement, and the degree of detail that can be modeled efficiently and accurately within the limitations of the available computer tools. These decisions often require that tradeoffs be made in the model details, and these usually result in the consolidation of the fine heterogeneous geometry details into larger homogeneous regions. The homogeneous zones must use properly averaged material densities to approximate the actual materials present in the real system. They also require a problem-dependent set of microscopic cross sections that account for the heterogeneous detail that is lost when developing a homogeneous model -- and the detailed procedure for the generation of a suitable library for the current VENTURE models follows closely the same process outlined in Ref. 7 (although newer versions of the codes and base fine-group cross sections have been used -- that is, SCALE 6.0 and SCALE 6.1 with their associated 238 group ENDFB-VII libraries).

As noted previously, a new set of VENTURE 2-D and 3-D models was needed to help streamline our in-house analysis capability and to improve upon the accuracy of the computational results, where possible. The starting point for the current development was the models from the 1999 HEU to LEU conversion effort (Ref. 1). The primary areas of focus for the simplifications and enhancements include:

1. The 1999 model had capability to model the regulating blade in both the D8 and D9 grid locations. However, the decision was made to leave the regulating blade in D9, so the added complexity in D8 is no longer warranted. This simplifies the zone layout in grid D8.
2. The initial 3-D model had significant additional zone detail in the first two columns on the left side of the core. In 1999 we were considering the development of a large experimental facility for fast neutron irradiations, and one possibility was to design something that could fit into the six grid positions on the left side of the core in Rows C – D (see Fig. 1 or 2). However, since the FNI facility was eventually placed in the excore region as seen in Fig. 2, the extra zone detail on the left side of the core grid is no longer required -- which again simplifies the overall model.
3. The 1999 reference 3-D model had 17 axial layers, many of which were included to allow for blade movement in the axial direction in discrete increments (and to allow for variation in burnup in the axial direction). Focusing on the control model, each control zone can either have water or control material present to account for the axial positioning of the control blades and regulating blade. This capability, in particular, is used to predict the expected blade worth curves for the system and to have some flexibility in positioning the control blades to approximate the actual critical height of the blades. However, since the critical height typically varies roughly between 15 – 18 inches out between refuelings and/or configuration changes, we decided to add a few additional layers within this axial region so that a finer resolution of the blade position could be achieved within the 3-D model. Thus, two additional axial layers were added in the current model, giving an overall 19-layer 3-D model. The normal blade traverse in the UMLRR covers approximately 26 inches and there are now 13 (non-uniform) layers within this range for the new model -- which gives a fair

amount of flexibility for computing the blade worth curves and for positioning the blades appropriately to simulate the critical state of the reactor.

4. The final and most important major change to the previous 3-D model was a refinement of the computational mesh grid layout. The 1999 models had different mesh layouts in the x and y directions for the 2-D and 3-D models -- primarily because a fine-mesh 3-D model was just too large for routine use with the computer capability from about a decade ago. In particular, the base 3-D model developed in 1999 had a 130×121×65 mesh grid in the three coordinate directions (slightly over 1 million mesh points total), spanning 225 cm in the x direction, 200 cm in the y direction, and 175 cm in the z-dimension. This 3-D grid layout gave a mesh spacing of roughly 1 – 2 cm per mesh in the x-y plane and a Δz of about 2 – 3 cm in the axial direction.

   The largest ramification of this mesh layout selection was the specification of the edge region boundaries for the 3-zone center/edge/side fuel assembly layout. Since the smallest mesh in the model was about 0.844 cm (which corresponds to the thickness of the side plate region), the edge region was modeled with this same thickness. Note, however, that a single edge plate with the small water gap outside the assembly is only about 0.50 cm thick. Thus, this modeling compromise required that a portion of the central fuel region be homogenized within the edge region. Clearly, this is quite awkward and it certainly leads to increased uncertainty in the peak power density computed with this model (since the peak often occurs in or near this region).

   The new 2011 model developed as part of the current WPI fuel transfer project avoids this homogenization procedure by reducing the minimum mesh spacing to about 0.5 cm -- which allows modeling the edge region as a single plate/water region as shown in Fig. 5 (note that this figure was taken directly from Ref. 8 and the reader is encouraged to see that report for a more detailed discussion of the current fuel assembly model). And, of course, along with a reduction in the minimum mesh spacing, a general mesh refinement was applied throughout the full model. After a few iterations, we converged on a final 3-D model with a 232×213×136 mesh grid layout for the 2011 model (about 6.7 million mesh). This better overall spatial resolution and the more straightforward treatment of the fuel edge region should lead to significantly better estimates of power peaking factors within the new model -- while maintaining a reasonable run-time of well less than 1 hour on a standard laptop PC.

With the above simplifications and improvements in mind, we can now describe the current 2011 UMLRR VENTURE models in some detail. As noted, there are 19 axial layers, with each layer representing a 2-D x-y model at a particular z location. For each x-y plane in the active core region, the outer ring of grid locations and the inner 5×7 grid array are treated differently, with the inner region having more zone detail per grid location than the outer ring of assemblies. In particular, the outer grid locations typically include graphite reflectors, radiation baskets, lead-void assemblies, or the structural corner posts. These assemblies are usually modeled adequately using a simple 1-zone or 2-zone homogeneous representation -- thus, not much zone detail is needed for these grid locations (except for the regulating blade in D9, of course).

In contrast, however, most of the interior grid locations will probably contain a fuel assembly, which is broken into a 5-region, 3-zone symmetric configuration (as seen in Fig. 5). Thus, each interior grid location has two sides (top and bottom), two edges (left and right), and a center region. This zone layout and the specific dimensions used are consistent with the existing

UMLRR LEU fuel assembly geometry and also with the WPI fuel assembly (see a detailed description/comparison of the two assembly designs in Ref. 8). This arrangement allows explicit modeling of the side plate and central fueled regions of the fuel assembly. It also allows for a better treatment of the aluminum end plates and the slightly increased water content associated with the assembly gap.

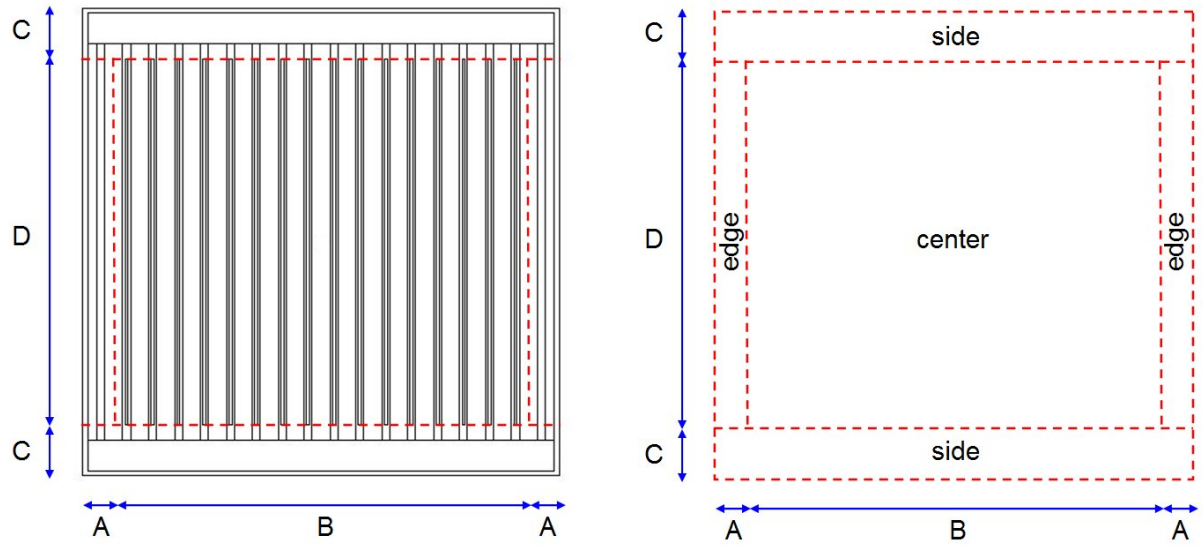

Region Dimensions (cm)		
A = 0.4995	B = 6.7734	2A+B = 7.7724
C = 0.8437	D = 6.0850	2C+D = 7.7724

Fig. 5 Detailed assembly geometry and 3-zone homogeneous representation (from Ref. 8).

In the axial direction, the 19 planes allow a relatively detailed axial representation for control movement (13 positions over a 26″ traverse), and for fuel burnup and irradiation sample placement (5 axial regions over a 23.5″ length). In addition, there are 4 axial layers above and 4 layers below the active fuel to model the various mixtures of structure and water in these regions of the system. The definition of several edit regions have also been added to the base 3-D model (mostly in the central Layer 11 region) to allow a rough characterization of the various experimental facilities for different arrangements of fuel elements and graphite or water reflector assemblies. Note also that the 2-D XY VENTURE model -- which is used primarily as a quick scoping tool -- is essentially equivalent to Layer 11 from the 3-D model. The standalone 2-D model uses a simple axial buckling approximation to represent axial leakage effects, but otherwise it is nearly identical to the central region of the 3-D model. Overall the new VENTURE models (2011 version) are quite flexible and hopefully they can serve as a focal point for operational support and core follow/burnup analyses for the LEU core for the foreseeable future -- and, of course, also serve as the primary computational tool for the physics evaluations needed to support the use of the WPI fuel within the UMLRR.

Getting the actual geometry and homogenized material information into the VENTURE code requires specification of three key arrays: a region grid layout, a zone-by-region map, and a material-by-zone array. The new x-y planar model uses a 75×69 region layout (75 y-directed regions and 69 x-directed regions) and a fine-mesh grid containing 232 discrete nodes in the x direction and 213 nodes in the y direction. A zone-by-region map is then given which identifies a specific zone number with each region in the 2-D grid structure. For the current 3-D model, there are 19 of these 2-D zone-by-region maps, where the zone numbers range from 1 to 764 for the pre-FNI cores and from 1 – 775 for the post-FNI configurations (note that, for ease and flexibility in modeling, a few zones numbers were not used). Attention to detail in specifying the full zone and mesh maps allows one to build a relatively flexible geometry that can handle a variety of material configurations. This modeling step is quite important, because a little added flexibility here can save lots of analysis time if several material layouts need to be considered.

Because of the major geometry change associated with the pre-FNI and post-FNI configurations in the UMLRR (i.e. recall that three beam ports were replaced with the FNI facility and support structure), two separate sets of zone maps and material maps have been prepared -- one for the M-1-3 pre-FNI configuration and one for the M-2-5 post-FNI layout. Note, however, that the actual geometry (region and mesh boundaries) is identical for the two models. Concerning the zone layout, only the zone description and placement in the region outside of Row A of the core grid is different in the two models, where we note that a few additional zone numbers are used in the post-FNI configuration. In practice, the details needed to generate the information required for the full model are usually recorded within an Excel file and then these data are transferred to a set of Matlab routines that allow visualization and debugging of the geometry and material composition information -- and they can also write a substantial portion of the actual VENTURE input file.

In addition to a flexible geometry, one also needs to specify a particular material composition to be placed in each zone (i.e. the so-called material-by-zone map). Homogenized atom densities for 40 materials were computed for the 3-D model based on the nominal region densities and region volume fractions within the given homogeneous zone. These materials include the primary core and reflector components (fuel, radiation baskets, graphite reflectors, core box, water reflector, flux trap, etc.) as well as several mixtures that represent the radial and axial excore structures for the full 3-D geometric model.

Appendices I – III contain much of the detailed information (geometry and material composition) needed to build the VENTURE models for the M-1-3 and M-2-5 cores. The first two appendices highlight the geometry and zone detail, respectively, for the M-1-3 and M-2-5 configurations, and Appendix III identifies the material information needed for both configurations. With this information properly inserted into three Matlab data files (i.e. the so-called **vgeo**, **vmat**, and **vden** files), an in-house Matlab plotting program called **plot_vgeo** can generate a variety of 2-D zone and material maps for the configuration of interest and write out much of this information in a format that is directly compatible with the VENTURE input. The data files required by **plot_vgeo** define a set of internal variables used by the code to specialize the plots and output file for a specific case of interest, as follows:

***_vgeo file** -- defines the region boundaries in all three directions, the number of fine mesh by region, and the zone-by-region map for each layer of the 3-D model.

***_vmat file** -- defines the material list and the material-by-zone map.

***_vden file** -- defines the nuclei atom densities (atom/b-cm) by material

The **plot_vgeo** program allows one to plot a combination zone and material map for any XY, XZ, or YZ plane within the model, and the following set of six sketches represent selected output from this Matlab code for both the M-1-3 and M-2-5 configurations. In particular, three such pictures from the M-1-3 critical configuration are given in Figs. 6 – 8 and three similar material maps for the M-2-5 core layout are shown in Figs. 9 – 11 as examples of the code's plotting capability and also to illustrate the level of detail that is treated in the overall 3-D models for these two UMLRR configurations. In each case, the three cuts are taken near the core midplane in each of the respective three directions. Note that both models have the control blades at the 14.86 inches withdrawn position (the actual critical heights were 15.3″ and 14.9″, respectively, for the M-1-3 and M-2-5 BOL initial cores) and the regulating blade at 8.96″ withdrawn. Any other row (y location for XZ cuts), column (x location for YZ cuts), or layer (z location for an XY view) can also be chosen to help visualize the full geometry model and material layout.

It should be noted that, as seen in the XY cuts in Figs. 6 and 9, the angled 6″ beam ports in the UMLRR were modeled with a relatively coarse stair-step approximation to minimize the number of region boundaries specified within VENTURE. Since the regions of interest in all our anticipated studies with VENTURE occur within the core or at the beam port/core box interface, the jagged edges used to represent the beam port sides should not seriously affect subsequent analyses. Also, as apparent for the M-2-5 configuration, only the first three rows of the FNI grid arrangement are modeled, and this is simply treated as three long rows of shield blocks, containing an outer homogeneous layer of aluminum structure, a water gap, and a thin borated-aluminum liner on either side of the lead shield material within each block. Since nothing beyond this 9″ shield region has any affect on the core behavior, the remaining FNI regions are simply filled with water. Thus, as with any modeling effort, less detail can be incorporated in the computational model, where appropriate, to simplify the overall model-building process. Here, these two simplifications (i.e. the stair-step beam tubes and simplified FNI region) have minimal affect on the computed core performance characteristics, since adequate detail has been included at the important core-excore interfaces -- and that is all that is really needed here.

Finally, we note that, on option, the **plot_vgeo** code can also write a significant portion of the actual VENTURE input file. This feature has saved countless hours of VENTURE input preparation and debugging -- and it works equally well for both the 2-D and 3-D models. Thus, the in-house **plot_vgeo** code represents a significant enhancement in our ability to generate base models and to modify existing models in a more efficient manner.

Depletion Considerations

One of the key goals of the current validation effort was the evaluation of the burnup model available within the VENTURE system. As noted above, through June 2012, the UMLRR LEU fuel has produced about 50 MWD of energy, and treating this properly is important during the overall modeling process and when trying to predict the performance characteristics of the current burnt M-2-5 configuration. Thus, here we will describe briefly the depletion model within VENTURE, and the actual burnup-related results, with comparison to measured data for the M-2-5 configuration, will come in a later section of this report.

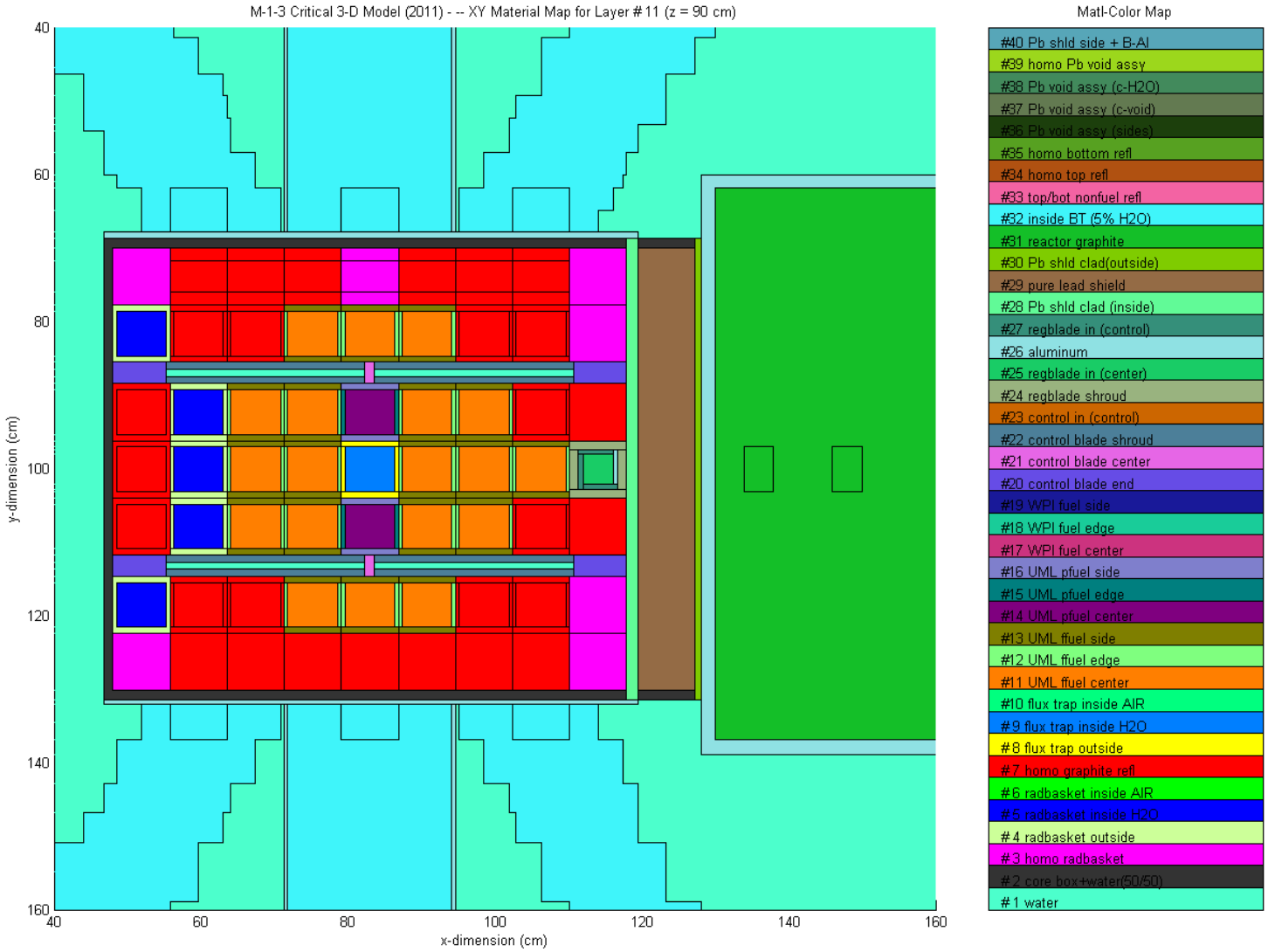

Fig. 6 XY zone/material map near the core midplane for the M-1-3 model.

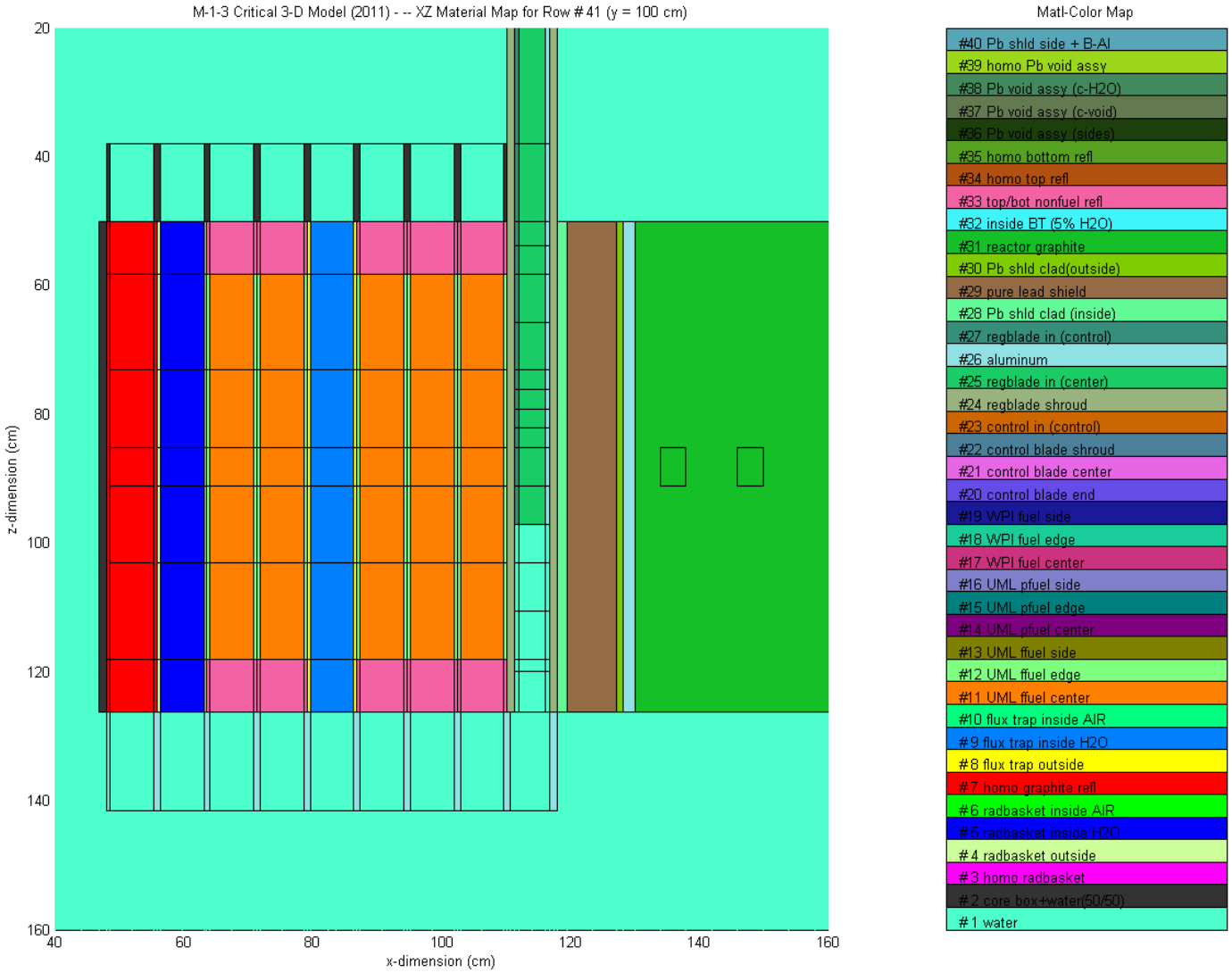

Fig. 7 XZ zone/material map near the core midplane for the M-1-3 model.

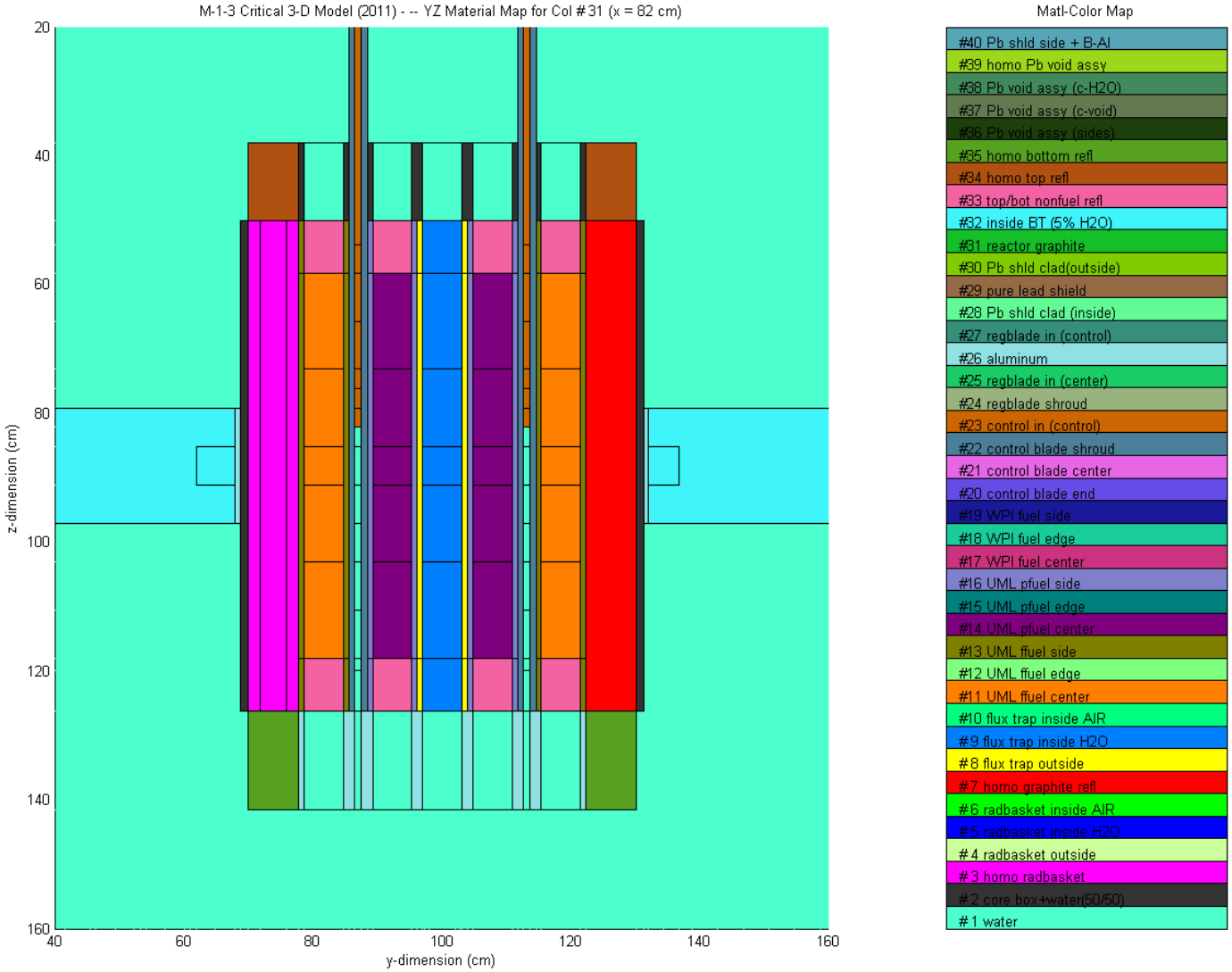

Fig. 8 YZ zone/material map near the core midplane for the M-1-3 model.

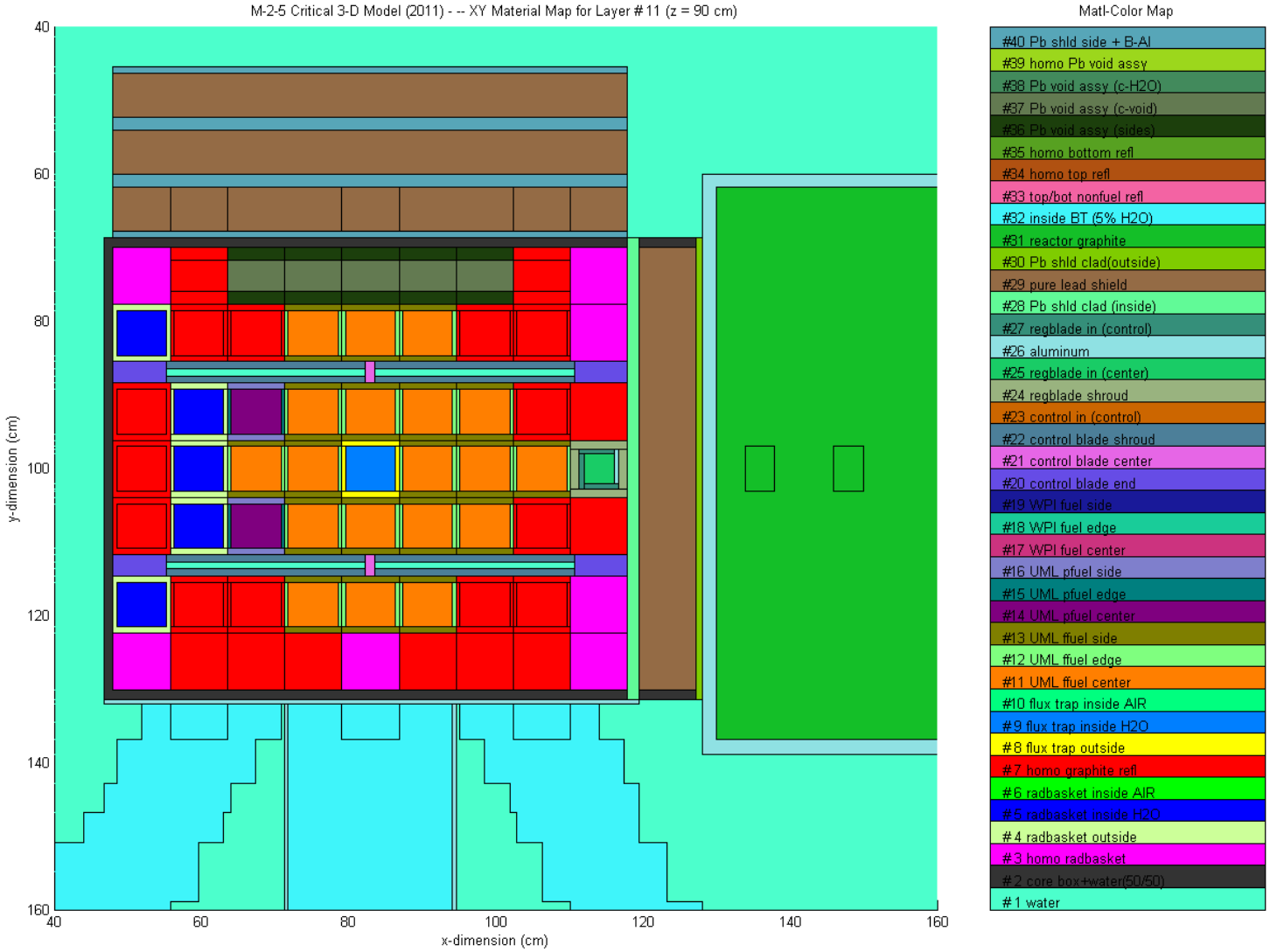

Fig. 9 XY zone/material map near the core midplane for the M-2-5 model.

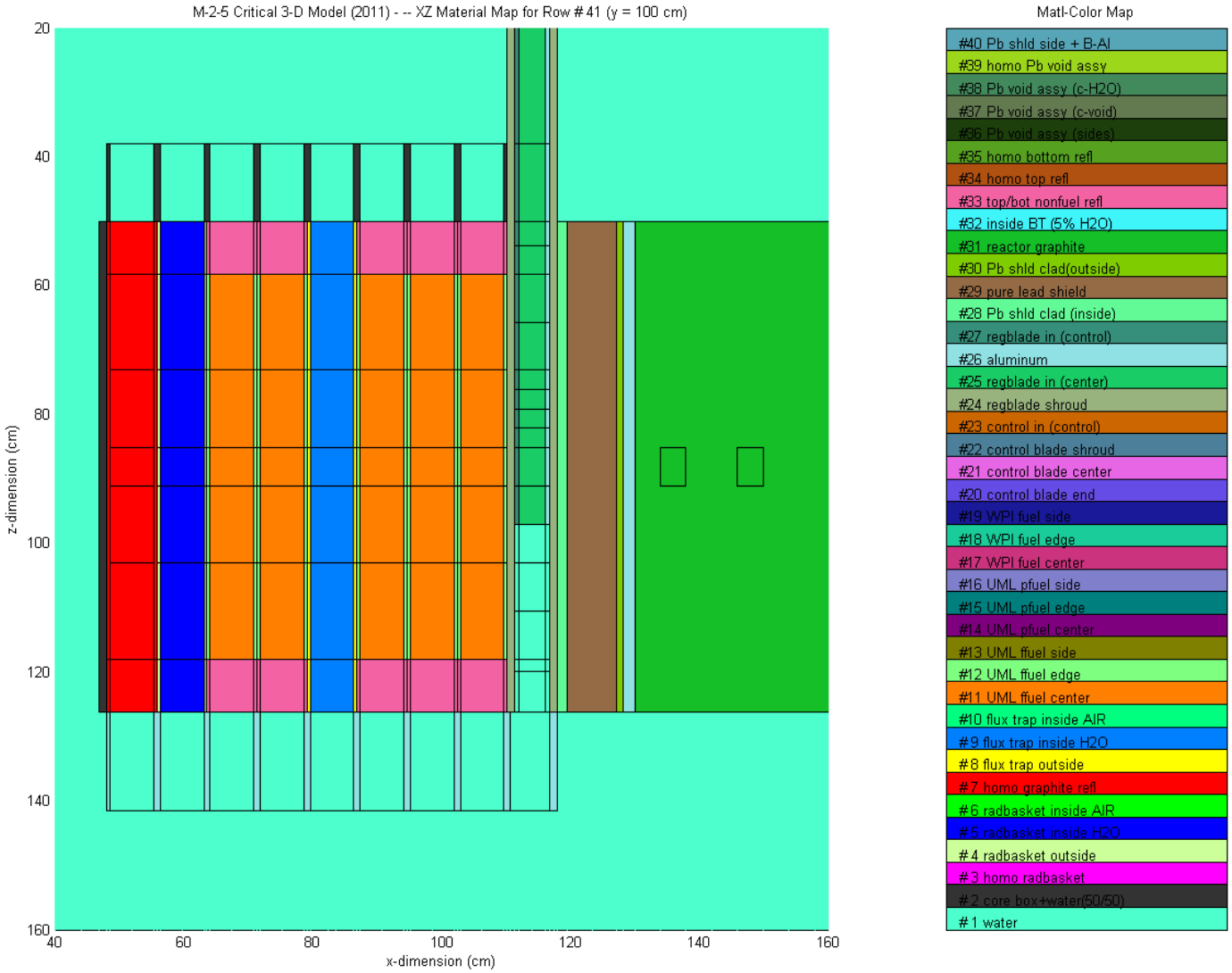

Fig. 10 XZ zone/material map near the core midplane for the M-2-5 model.

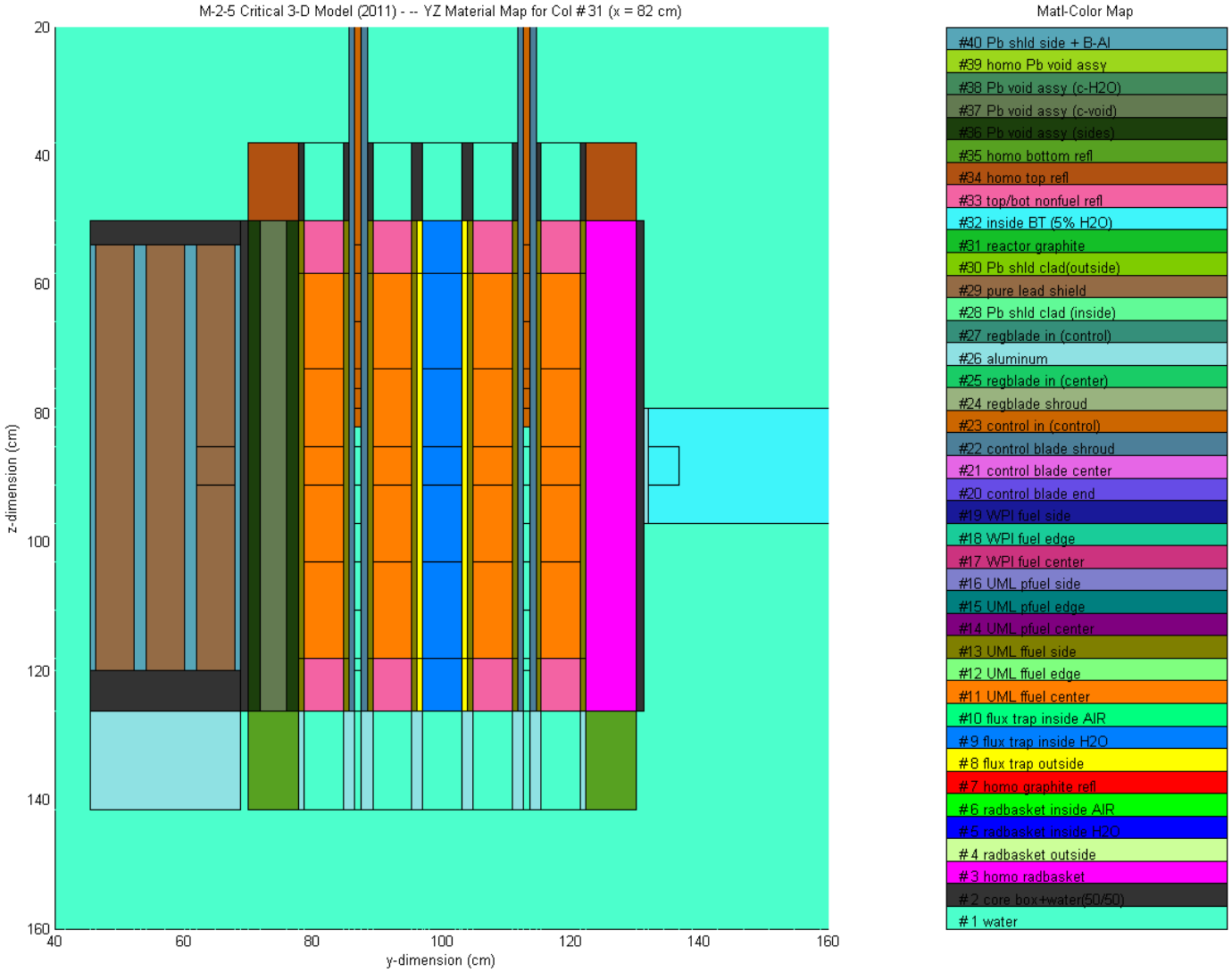

Fig. 11 YZ zone/material map near the core midplane for the M-2-5 model.

The BURNER code is the VENTURE module that does the desired depletion calculations. The VENTURE/BURNER code sequence uses a quasi-static approximation, where the flux distribution is assumed to be unchanged over a given time interval. A new VENTURE neutronics calculation is done at the beginning of each time interval and a renormalization of the flux to the specified power is done at substep boundaries. During the interval, BURNER uses the matrix exponential technique to solve the point depletion equations using the average flux in each zone containing fuel material. Thus, a sequence of a VENTURE flux calculation and BURNER depletion computation allows one to easily track the nuclide inventory in each fuel region versus burnup. In the current setup, for short-term detailed depletion analyses, a new flux calculation is done every 5 full-power days and two renormalizations are done for each major time step -- which gives a good representation of the flux redistribution and normalization with burnup. For scoping studies involving longer depletion times, times steps as large as 30 days is used with two renormalizations per interval.

For the BURNER depletion calculations, the time-varying nuclide vector contains the major actinides up through Am241 (including U235, U236, U237, U238, Np237, Np238, Np239, Pu238, Pu239, Pu240, Pu241, Pu242, and Am241), the key isotopes associated with the Xe135, Sm149, and Sm151 fission product chains (I135, Xe135, Pm149, Sm149, Pm151, and Sm151), and a single effective lumped fission product (called FISSP or FISSPN in the library) to represent all the remaining non-saturating fission product isotopes. Note that the FISSP isotope is included as a simple absorber which has a fast absorption cross section of 2.6 b and a thermal cross section of 14 b. This specific treatment of the fission products (three individual saturating nuclides and one effective non-saturating lumped fission product) was identified in a separate study (see Ref. 9) to be a sufficient treatment of the fission product reactivity effect within the UMLRR.

One final dummy material called MWD was included to track the total energy produced in each fuel zone in the model. This artificial isotope has zero cross sections (so it does not affect the flux calculations) but it has a special yield value of 370.8 MWD/fission. This value was obtained as follows:

$$\left(\frac{200\,\text{MeV}}{\text{fission}}\right)\left(\frac{1.602\,\text{x}\,10^{-19}\,\text{J}}{\text{eV}}\right)\left(\frac{1\,\text{day}}{86400\,\text{sec}}\right) = 3.708\,\text{x}10^{-22}\,\frac{\text{MWD}}{\text{fission}}$$

The yield is set at 370.8 MWD/fission in the code input since a factor of 10^{24} is applied internally to convert the typical atom density from units of atoms/b-cm to atoms/cm^3.

Thus, the final burnup model includes 21 isotopes that are followed for each fuel zone in the model. In the current VENTURE model, each fuel assembly has five axial zones and a 3-zone radial layout. However, the side plate region does not contain any depletable isotopes, and the edges may or may not have fuel (recall that the current UMLRR element has 16 fuel plates and two aluminum edge plates, but that the WPI assembly has a full complement of 18 fuel plates). Thus, with 21 assemblies, there may be as many as $2\times5\times21 = 210$ burnable zones within the model (there are only 105 fuel zones for the current M-2-5 core with only the original UMLRR fuel elements present).

This basic setup was used to deplete the beginning-of-life (BOL) UMLRR core to arrive at a configuration that represents current operation (in Aug. 2012). The results of the burnup

calculations and comparison to measured data are given in a subsequent section of this report (see below).

A Note on the various Cross Section and Model Versions Used within this Study

It should be noted that most of the results summarized in the subsequent sections of this report used the 2011 version of the VENTURE model (as previously described) with 2-group cross sections derived from the 238-group ENBFB-VII libraries included as part of the SCALE 6.0 package. Much of this work was done during the summer and fall of 2011. However, in parallel with these analyses, a study of how best to represent fission products within the UMLRR depletion models was also being conducted. As summarized above and in Ref. 9, we selected a model that includes three individual saturating nuclides (Xe135, Sm149, and Sm151) and one effective non-saturating lumped fission product. Prior to this model change, we only followed Xe135 and Sm149 as explicit saturating isotopes, along with a FP lump with a very approximate effective cross section. Thus, the primary difference in the so-called 2011 and 2012 model versions is simply in the treatment of the FPs within the models -- all the geometry, mesh layouts, BOL material compositions, etc. are identical. Thus, this change has absolutely no effect on the beginning of life (BOL) M-1-3 and M-2-5 configurations, and has only a minor (essentially negligible) effect on the M-2-5 model at 50 MWD burnup (since the burnup is so low).

However, in summer 2012, the SCALE package was upgraded from version 6.0 to 6.1. In addition to a number of enhancements and fixes, both the CENTRM pointwise cross sections and the 238-group multigroup libraries were changed (see details in Ref. 10). Although small, these modifications lead to slightly different collapsed few-group cross sections which, in turn, give slightly different VENTURE results. However, since the calculations give essentially the same results (although not identical), we consider our analyses with both the VENTURE 2011 and 2012 models and the SCALE 6.0 and 6.1 cross sections as "essentially the same calculations". Thus, no distinction between these models/cross section sets is made, since they give essentially the same results. For example, for the BOL M-2-5 core configuration the SCALE 6.0 data give k = 0.97804 with a peak power density of 47.28 W/cm^3 and the SCALE 6.1 data give k = 0.97917 with P_{max} = 47.31 W/cm^3 -- and, as stated above, these are essentially the same result.

Summary Results/Validation for the M-1-3 BOL Configuration

As mentioned previously, several measurements were made in the LEU startup core, and comparison to these experimental results represents an excellent way to assess the validity and usefulness of a new computer model of the UMLRR. In particular, several reactivity evaluations, a full series of blade worth curve measurements, and a set of axial thermal flux profiles were determined for the M-1-3 startup core (see Refs. 4 and 5), and these data are used here to evaluate the new 2011 version of our 3-D VENTURE model for the M-1-3 configuration.

Critical Blade Height: The axial location of the four large control blades (all banked at the same level) and the position of the regulating blade when the reactor is just critical (i.e. k = 1.00) at low power is referred to as the critical blade height. The low power critical state in the M-1-3 startup core was achieved with the control blades at 15.3″ out and the regulating blade at about 8″ withdrawn. Unfortunately, the closest discrete axial locations in the VENTURE model for the four large control blades were at 14.86″ and 16.04″ withdrawn, with the low-worth regulating blade at 8.96″ out. Calculations were done for both blade positions and interpolated linearly to the desired 15.3″ location, as seen in Table 1. Thus, the “critical” blade location in

the 2011 VENTURE model using ENDF/B-VII cross sections gives a calculated k_{eff} of about 0.980 -- which indicates that the model has a bias of about -2% Δk/k. This deviation from unity is larger than desired and the root cause of the error is unknown -- probably due to a combination of many factors such as the cross section processing procedure, the homogenization procedure and rough treatment of the axial reflectors within the 3-D VENTURE model, and the base uncertainties in the nuclear data, physical dimensions, and material compositions within the system. One should note however, that, although undesirable, a 1-2% Δk/k bias in the absolute reactivity is not uncommon, and it does not adversely affect the overall usefulness of the computational model (note that the 1999 model over-predicted the core reactivity by almost 1% Δk/k).

Table 1 Reactivity level versus control blade location (with regulating blade at 8.96″ out).

Control Blade Position (inches withdrawn)	k_{eff}
14.86	0.97652
16.04	0.98484
15.3	0.9796 (interpolated)

Blade Worth Evaluations: Calibration of the control blades and regulating blade using the stable positive period method (often referred to as the doubling time method) was performed as part of the startup tests for the new LEU core in August 2000. After each discrete movement of a test blade, the midpoint of the motion was recorded and the associated change in reactivity was determined from the measured period using the 6-delayed group reactivity equation. Several of these differential worth measurements were made, fit to a mathematical model, and then integrated to give the desired integral worth curves for each of the blades within the UMLRR.

Historically, the reactor staff have used a simple cosine model to do the curve fits (see Ref. 11, for example), but this assumes a symmetric axial worth distribution -- which is not really valid since, during normal operation, the blades are usually inserted 8 – 11 inches into the top of the core, leading to a bottom peaked flux and differential worth profile. Several years ago (see Ref. 1), an alternative cubic polynomial + cosine model was proposed, and this has been shown to give significantly better curve fits if a sufficient number of data points evenly spaced over the full 26″ range of the blades is available. Here we will show results using both curve fit models to illustrate the type of differences that are typically observed -- however, it should be emphasized that, if the above conditions are met (i.e. sufficient coverage of the experimental data), the cubic polynomial + cosine model generally is a much better choice.

The blade worth results from the startup test program for the M-1-3 core are summarized in Table 2. As noted above, the "theoretical model" refers to a symmetric cosine-only differential blade worth curve and the "new model" represents a 3rd-order polynomial + cosine model for fitting the differential worth data. The measured critical height had Blades 1 – 4 banked at 15.3 inches withdrawn with the regulating blade at 8 inches out. The tabulated excess reactivity is the remaining worth associated with the movable blade length above the critical height (full out is roughly 26 inches withdrawn).

Table 2 Measured results from M-1-3 startup core (August 2000).

	Theoretical Model (simple cosine fit)			New Model (3^{rd} order polynomial + cosine fit)		
Blade #	**Total Worth % Δk/k**	**Fit Quality R^2 Value**	**Excess Reactivity % Δk/k**	**Total Worth % Δk/k**	**Fit Quality R^2 Value**	**Excess Reactivity % Δk/k**
Blade 1	2.53	0.90	0.83	2.63	0.98	0.66
Blade 2	2.38	0.78	0.78	2.47	0.90	0.57
Blade 3	3.34	0.89	1.09	3.32	0.96	0.80
Blade 4	3.19	0.83	1.04	3.20	0.91	0.79
Total Worth Blades 1 – 4	11.4	--	3.74	11.6	--	2.82
Regulating Blade	0.28	--	0.23	--	--	--
Total Worth All Blades	11.7	--	3.97	11.9	--	3.05

Because of the low total worth, only two data points were taken for the regulating blade. Therefore, the new model could not be used with the limited experimental data available for the regulating blade (need a minimum of 5 data points). Thus, for the total worth and total excess reactivity of all blades, the regulating blade data using the cosine-only fit was used for both cases reported here.

Concerning the curve fits, there is a fair amount of experimental uncertainty in the raw differential worth data, especially for Blades 2 and 4 -- as apparent from visual inspection of the curve fits (see Fig. 12 below for Blade 4, for example) and via the R^2 correlation coefficient noted in the above table. In all cases, the new model gives significantly better fits relative to the theoretical model due mainly to the real asymmetric nature of the measured data. This difference in the two models, forced symmetry for the theoretical model versus potential asymmetry within the new model, accounts for much of the difference in the prediction of the total excess reactivity for the UMLRR M-1-3 startup core. However, the poor comparison for the excess reactivity values is also due to the overall poor curve fits (that are due to the large variation in the measured data). Thus, neither excess reactivity value is overly reliable, but it is expected that the real excess reactivity in the LEU startup core was closer to 4% Δk/k than the 3% Δk/k value (as observed from operational experience).

Note that the experimental approach for determining the blade worth curve can be easily simulated with the 3-D VENTURE model by simply doing a series of k_{eff} calculations with the blades at different locations. In practice, the VENTURE blade worth calculations were done with the goal of keeping the reactor roughly "near critical" (which in this case was k = 0.980 ±0.01). Once the VENTURE raw k_{eff} data were collected for several blade positions, +0.020 was added to the computed k values from VENTURE to give values closer to unity (to account for

the known bias in k_{eff}). These were then used to compute the differential worth estimates and to generate the blade worth curves (i.e. using the adjusted % Δk/k values).

The simulated blade worth data obtained from the VENTURE model are summarized in Table 3. The data shown here should be compared to the measured results given in Table 2. In general, the blade worth predictions from the 3-D VENTURE model agree reasonably well with the measured data, but they are generally a little on the high side (part of this may be due to the treatment of the -2% Δk/k bias associated with the nearly critical configuration). Other factors are also important, however, such as there is now much less variability in the simulated raw data, which gives better overall curve fits (i.e. compare the R^2 values and the simulated Blade 4 worth curves in Fig. 13 versus the measured data in Fig. 12).

Table 3 Computed results for M-1-3 startup core using the 2011 3-D VENTURE model.

	Theoretical Model (simple cosine fit)			**New Model (3^{rd} order polynomial + cosine fit)**		
Blade #	**Total Worth % Δk/k**	**Fit Quality R^2 Value**	**Excess Reactivity % Δk/k**	**Total Worth % Δk/k**	**Fit Quality R^2 Value**	**Excess Reactivity % Δk/k**
Blade 1	2.71	0.83	0.89	2.95	0.99	0.72
Blade 2	2.61	0.88	0.85	2.80	0.99	0.71
Blade 3	3.14	0.90	1.03	3.32	0.98	0.88
Blade 4	3.24	0.90	1.06	3.43	0.98	0.91
Total Worth Blades 1 – 4	11.7	--	3.83	12.5	--	3.22
Regulating Blade	0.39	0.71	0.33	0.44	0.99	0.30
Total Worth All Blades	12.1	--	4.16	12.9	--	3.52

Finally, we note that the VENTURE model for the regulating blade has traditionally over-predicted the regulating blade worth because of the homogenization procedure used in the model. Although the current 2011 model, with its finer mesh grid layout has allowed for a better geometry treatment than in previous models, the predicted total regulating blade worth is still somewhat high. Thus, although better than previous models, the 2011 VENTURE regulating blade worth data is still suspect, and probably should not be used directly as given in the above table (total worth is about 30 – 40% too large).

Axial Thermal Flux Profiles: A combination of gold foils and copper wires were used to perform thermal flux mapping in selected locations of the LEU startup core as illustrated in Fig. 14. Cadmium-covered and bare gold foils were used to provide an absolute determination of neutron fluence rate, while copper wires provided an axial flux distribution at the chosen locations. The gold foils and some comparison copper wires were installed near the axial midpoint of two standard sample bayonets and then lowered into the radiation baskets in grid locations C2 and E2. Five long copper flux wires (nearly 3 feet long in some cases) were placed

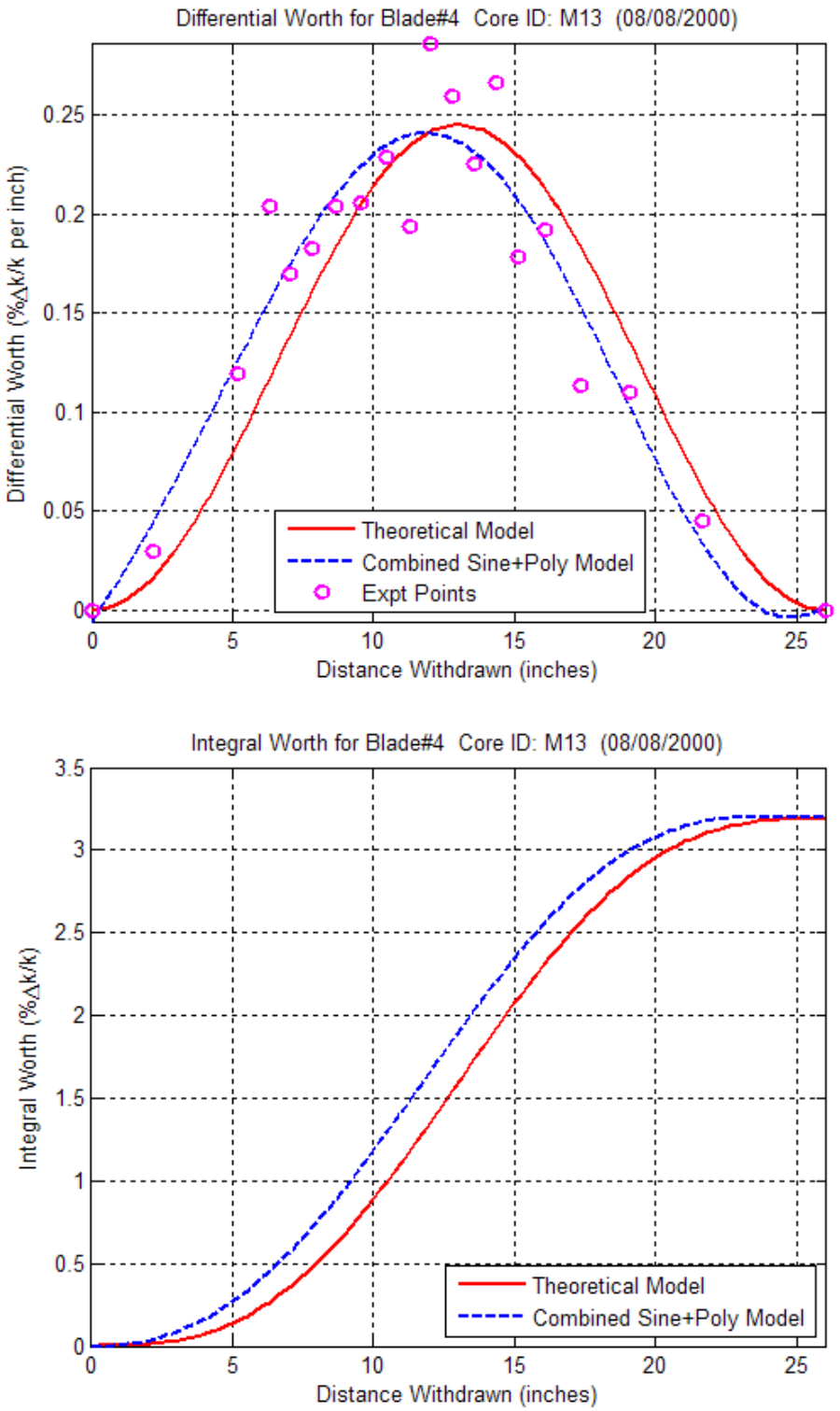

Fig. 12 Typical example of the raw measured data and resultant curve fits for the differential and integral blade worth curves.

(These data show the measured results for Blade 4 in the M-1-3 startup core. Note also that this case has an unusually large number of data points, where 8 – 10 points is more typical.)

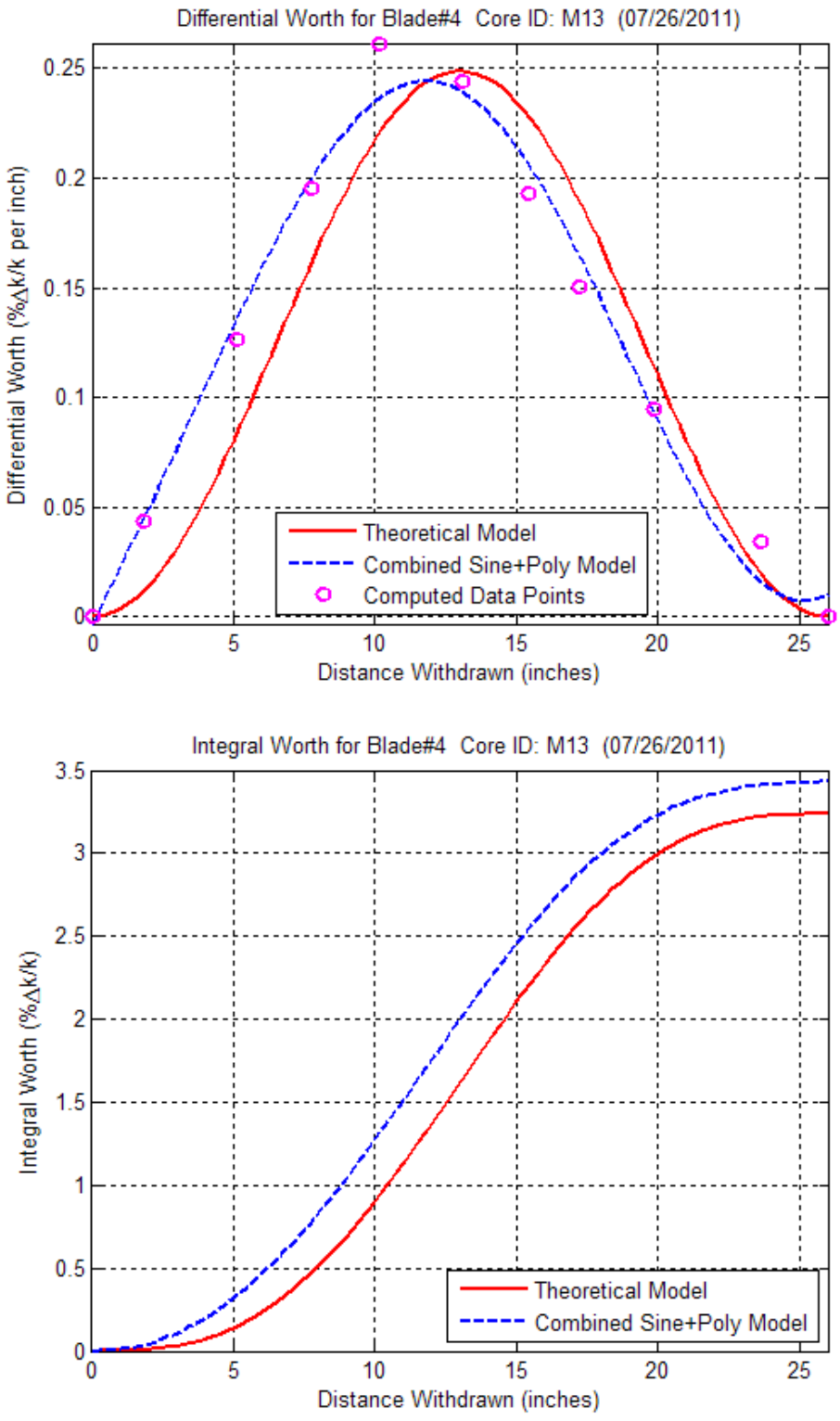

Fig. 13 Typical example of the raw data from the 3-D VENTURE calculations and the resultant curve fits for the differential and integral blade worth curves.

between the fuel plates of un-irradiated fuel elements in positions D6 and E6 and into the D2 and D5 irradiation positions as shown. The irradiations were then performed at an indicated power level of 100 watts for 30 minutes.

After irradiation, the wires and foils were removed and counted on a gamma spectrometer. An inter-calibration between the gold foils and copper wires provided an absolute flux distribution at the five wire locations indicated in Fig. 14. All the measured flux distribution data were then normalized to a nominal power level of 1 MW and compared to the results from the 3-D VENTURE computational model for the M-1-3 core. However, because of the discrete modeling of the axial material distribution in the VENTURE models, the blades were banked at 14.86 inches withdrawn for the VENTURE calculations instead of the actual 15.3 inch level associated with the actual measurements.

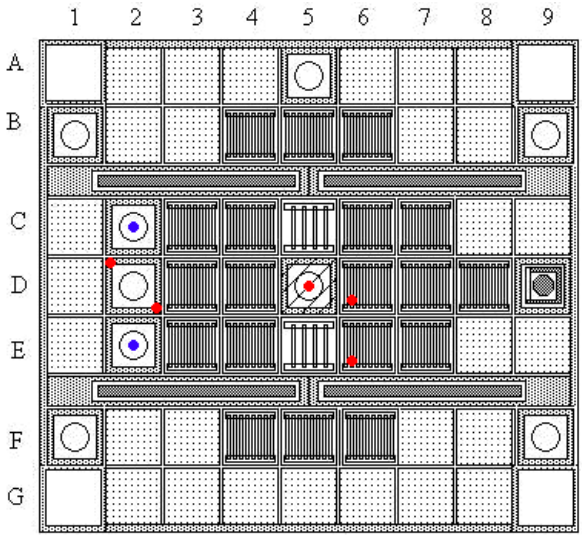

Fig. 14 Location of the gold foils (blue) and copper wires (red) for the flux mapping measurements.

Summary results from these comparisons are shown in Fig. 15. The individual points on these curves represent the experimental values of the absolute thermal flux and the continuous lines are associated with the VENTURE results. The top two plots highlight the two copper wires in the D2 position, with relatively good agreement in both cases. In particular, the VENTURE thermal flux profile in the upper left location gives a near perfect match with the measured profile and, for the lower right wire in D2, the worst case difference in the peak fluxes is only in the 10-15% range.

The results for the wires in the two fuel assemblies are shown in the middle plots in Fig. 15. The particular locations for the wires in the D6 and E6 fuel assemblies were chosen because these were near the locations of the peak power density from the VENTURE calculations. As apparent, the VENTURE results are quite reasonable, with a somewhat better representation of the full axial distribution in the D6 location relative to the E6 position. This is consistent with expectations since the copper wire in E6 is very close to Blade #4 which is inserted to a depth of about 15.3+2.5 = 17.8 inches above the grid box. The large flux gradient observed in this area is hard to model exactly with two-group diffusion theory. However, even with the large flux

gradients in this locations, the VENTURE profiles are quite reasonable. Finally, we note that the LEU fuel assembly height is 30 inches, with 23.5 inches of fuel meat and 3.25 inches of aluminum structure and water just above and below the active fuel region. The VENTURE calculations clearly show the expected thermal flux peak near the fuel/reflector interface (although there are limited experimental data to validate the computed profile).

Finally, the bottom curve in Fig. 15 shows the computed and measured thermal flux profiles in the center of the flux trap assembly in location D5. The agreement here is excellent; probably due to the fact that it is a relatively large homogeneous centrally located region that is easily modeled with few-group diffusion theory. This experimental location has the highest flux magnitude within the UMLRR and it is used whenever high fluence or fluence rates are needed.

Worth of an Empty Bayonet in D5: A new experimental facility associated with the HEU to LEU core conversion effort was the central flux trap irradiation location. Note also that the UMLRR technical specifications limit the maximum reactivity of movable samples to 0.1% $\Delta k/k$ and secured samples to 0.5% $\Delta k/k$. Thus, since most in-core samples are placed in a water-tight bayonet, a reactivity evaluation of an air-filled bayonet was made in the M-1-3 startup core. The worth associated with the insertion of an empty bayonet was measured to be about 0.25% $\Delta k/k$ by simply comparing the critical blade heights with and without the bayonet installed (Ref. 3). This result clearly indicates that samples to be irradiated in the flux trap will have to be treated as secured samples under the technical specifications.

A similar simulated test was performed with the 2011 3-D VENTURE model, where the composition of an air-filled bayonet was homogenized within the inner region of the 2-region flux trap model, instead of having the inner tube filled with water. The computed reactivity worth of this composition change was -0.04% $\Delta k/k$ -- which is not even close to the measured value (i.e. we do not even have the correct sign relative to the measured value).

A separate study with MCNP and the XSDRN code within SCALE tried to isolate the cause of this discrepancy. In particular, MCNP was used to compare the behavior of a 2-region homogeneous model and a detailed heterogeneous model of the flux trap -- and both models showed the same trend as observed with the experimental data. Thus, the discrepancy observed here is not due to a homogenization effect.

As an additional test, the result of a similar composition change in the 1-D XSDRN core model used to collapse the cross sections to 2-groups (see Ref. 7) also showed a similar (but larger) increase in reactivity with a corresponding reduction in the water content of a radiation basket located in the center of the core. Thus, it appears that the discrepancy observed here with the VENTURE model is a spectrum hardening effect that cannot be properly treated with a simple 2-group approximation. This observation is clearly an important deficiency within the current model and it suggests that a code such as MCNP, for example, should be used to evaluate sample worths within the UMLRR, rather than the 2-group VENTURE model (actually this was one of the main reasons for developing the current MCNP model of the UMLRR as noted in Ref. 12). Or, as another option, it also suggests that we may want to consider adding a few additional groups to the existing cross sections for use within the VENTURE 3-D model. For now, however, the VENTURE 2-group model is the main working computational model for general physics studies of the UMLRR, and it is simply acknowledged here that this model does indeed have some deficiencies -- along with its many positive predictive capabilities (as noted above).

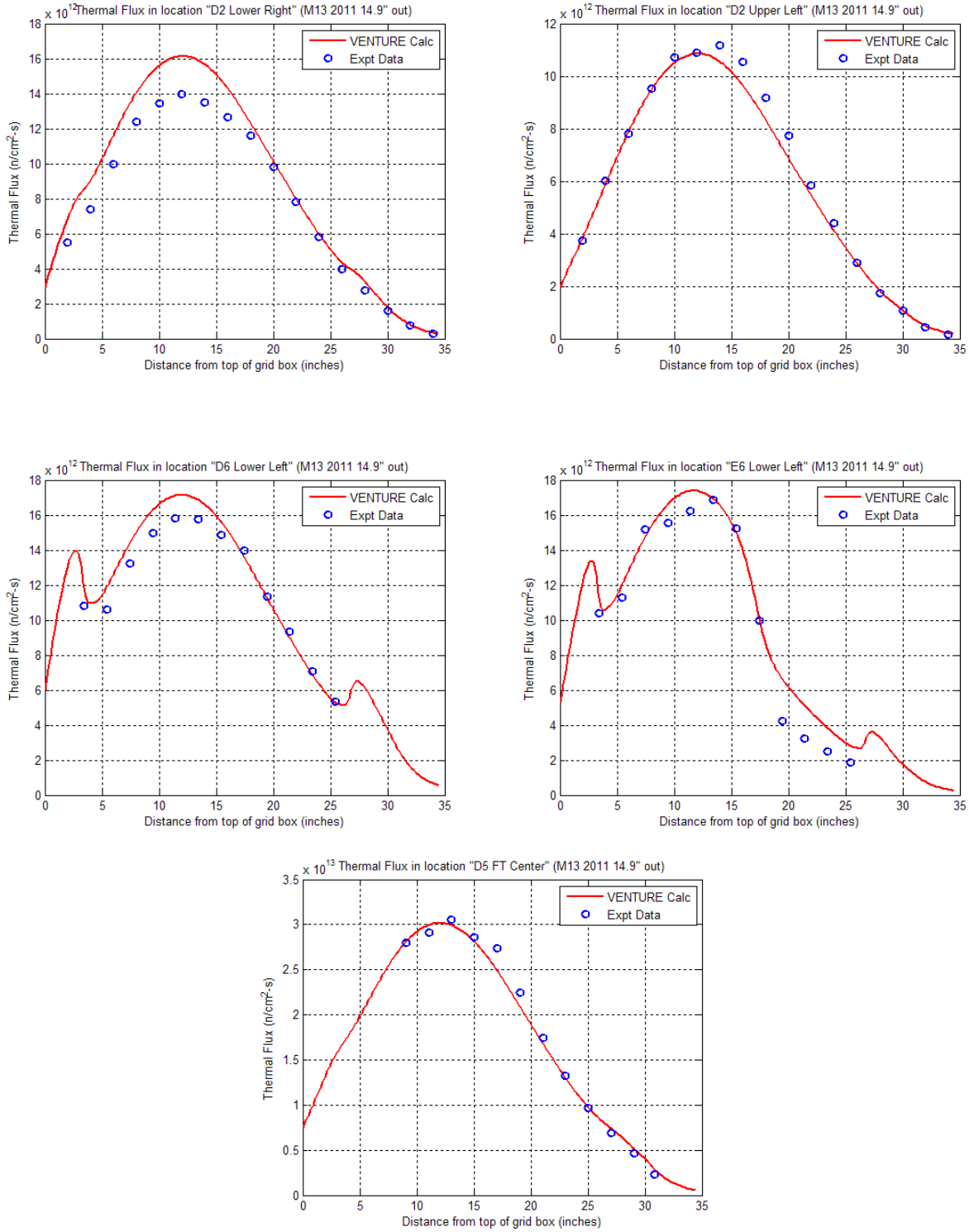

Fig. 15 Calculated vs. measured axial thermal flux profiles at various locations (M-1-3).

Summary Results/Validation for the M-2-5 BOL Configuration

As mentioned previously, there was less than 4 MWD of burnup when the fast neutron irradiator (FNI) was installed within the UMLRR in 2001. The post-FNI configuration was designated as the M-2-5 core and this is the same configuration used in current operations (in August 2012). For the initial M-2-5 calculations, our VENTURE models assume no burnup -- that is, they use the same BOL material composition for each of the individual assemblies as used in the M-1-3 computations.

As for any new core configuration, the operations staff recorded the critical height of the blades and completed a new set of blade calibration runs for the initial M-2-5 core configuration, and these results are used here to help evaluate and validate our BOL M-2-5 VENTURE model. In particular, the initial M-2-5 configuration was critical with the four large control blades at about 14.9 inches withdrawn and the regulating blade at 10.0 inches withdrawn (note that the 14.9 inches represents a backward linear extrapolation from 15.0 inches withdrawn to account for the shift backward from 4 MWD to 0 MWD). For these blade locations, however, the VENTURE model gives a multiplication factor of only 0.978 -- which, although low, is fully consistent with the -2% bias observed with the M-1-3 VENTURE models. Thus, this result was expected based on the above M-1-3 results.

Concerning the blade worth measurements, the worth distribution among the four large control blades in the M-2-5 core is much more asymmetric than in the M-1-3 core, due primarily to the movement of the two partial fuel elements to the left side of the core and the replacement of five graphite reflector elements in row A with lead-void elements (compare the M-1-3 and M-2-5 core layouts as shown in Figs 1 and 2). These configuration changes caused the flux to tilt in the direction of the lower right quadrant relative to the core sketches given in Figs. 1 and 2. And, since Blade 4 is the blade in the lower right location, it was expected to have the largest total worth of all the blades. Using similar arguments, Blade 2, which is located in the upper left quadrant in Figs. 1 and 2, was expected to have the lowest total worth.

As apparent, Table 4, which summarizes both the measured and computed blade worths, shows that these expectations were indeed observed for the M-2-5 configuration. Blade 2 has the lowest worth at about 2.2 - 2.4% $\Delta k/k$ and Blade 4 has the highest worth at roughly 3.5 - 3.9% $\Delta k/k$. Overall, the VENTURE model predicted the magnitude and relative worth distribution quite well, with less than 10% uncertainty -- which is well within the experimental uncertainty of the measured data. Finally, we note that the regulating blade worth estimate is still over-predicted because of the relatively complicated physical geometry and spatial homogenization that was required for representing the regulating blade within the 3-D VENTURE model.

Summary Results/Validation for the 50 MWD M-2-5 Configuration

Developing a computational model for the current UMLRR core configuration with roughly 50 MWD burnup is where the previous discussion of the fuel depletion model and the fission product treatment comes into play. In particular, the BOL M-2-5 core was depleted in 5 day intervals out to 25 MWD. At this point, the blades were moved from 14.9 inches withdrawn (their BOL position) to 16.0 inches out to counter the reactivity loss over time, and then the depletion was continued to 50 MWD with this blade configuration. With the material compositions at 50 MWD, two additional flux computations were made, one with the blades at the 16.0 position and another at 17.2 inches withdrawn.. The regulating blade was left at about 9.0 inches out for all the calculations. Additionally, it should be noted that the yields for I135

and Xe135 were set to zero for these full power depletion cases, since the UMLRR operational history never allows for the buildup of equilibrium xenon within the system. For our low duty cycle, most reactor startups either have no xenon initially present or only have small residual effects from the previous day's operation -- and most Monday morning startups are completely xenon-free. Thus, a xenon-free depletion model makes sense for the UMLRR.

Table 4 Comparison of measured and calculated M-2-5 BOL blade worths using the 2011 VENTURE 3-D model with data from the SCALE6 v7n238 library.

	Measured %Δk/k		VENTURE %Δk/k	
Parameter	**Theoretical Model**	**New Model**	**Theoretical Model**	**New Model**
Blade 1 Worth	2.69	2.82	2.71	2.91
Blade 2 Worth	2.17	2.19	2.19	2.35
Blade 3 Worth	3.15	3.19	2.96	3.16
Blade 4 Worth	3.81	3.93	3.52	3.72
Total Worth Blades 1-4	11.7	12.1	11.9	12.1
Excess Reactivity	4.13	3.46	4.06	3.45
Reg. Blade Worth	0.30	--	0.40	0.45

To elaborate a little on the discrete blade movements, one should first recall that the current 3-D model has 13 pre-determined distinct layers to allow blade movement, so the repositioning from 14.9 to 16.0 inches out, for example, represents the movement of the blades from layer 9 to layer 8 in the 3-D model. In practice, of course, the actual critical blade height increases slowly with burnup to counter the reactivity loss due to fuel depletion and fission product buildup as shown in Fig. 16, but the single discrete step made during the VENTURE/ BURNER 50 MWD burn is the best treatment that can be done with the current mathematical model. For the current core after about 50 MWD, the critical height is about 16.5 to 16.6 inches withdrawn. Thus, since this exact level cannot be modeled, the final VENTURE flux computation with the blades at 17.2 inches was completed so that a linear interpolation can be performed to estimate the VENTURE-predicted critical height for the 50 MWD M-2-5 core.

As apparent, both linear and quadratic fits were made to the measured critical height vs. burnup data given in Fig. 16. The early data suggests a rough linear behavior, and the critical height of about 14.9 inches out for the BOL M-2-5 core that was noted in the previous section was obtained from these data. However the more recent burnup data suggests some curvature in the critical height vs. burnup profile, which would suggest a slightly lower initial critical height. The nonlinear behavior, however, is closer to the expected behavior, due primarily to the saturating nature of the Sm149 isotope (and other saturating fission products that are built up over time).

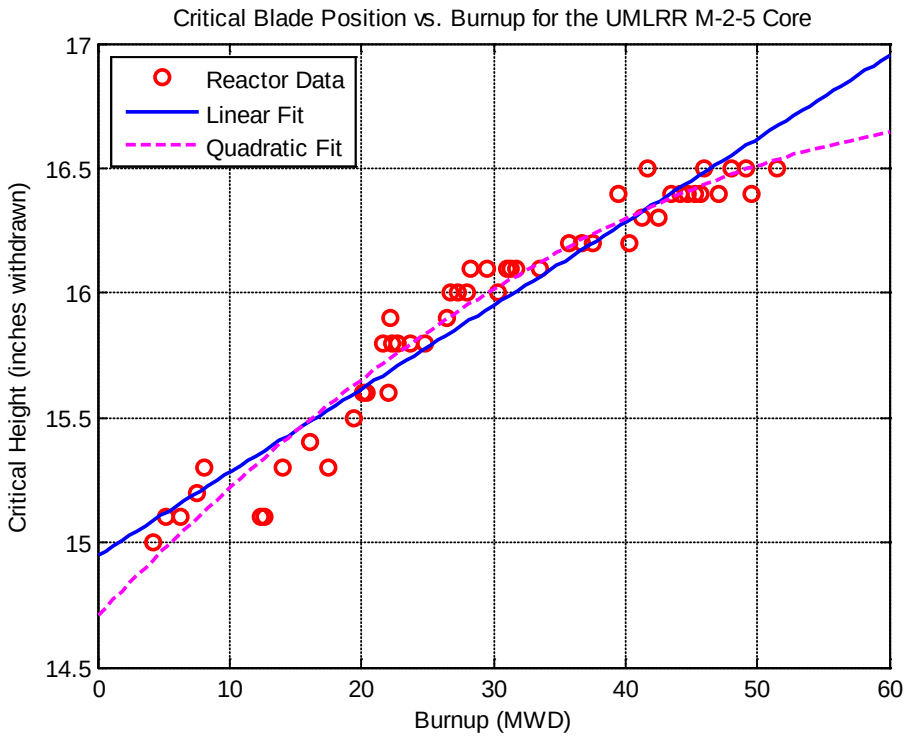

Fig. 16 Critical blade height vs. burnup for the UMLRR M-2-5 core. Much of the variability that is apparent in the raw data is due to a changing regulating blade position and differing pool temperatures. The data was collected on days when the residual Xe reactivity was negligible.

To compare the reactor data in Fig. 16 with the VENTURE prediction of reactivity loss vs. burnup, we first needed to convert the changing critical blade heights to reactivity. Since there has only been small changes in the blade worth curves over time (see below discussion), the measured blade worth curves at a single time point (from March 2011) were used to modify the curve fits in Fig. 16 to give reactivity vs. burnup. These data, along with the VENTURE predictions, are given in Fig. 17. As apparent, the VENTURE data gives a good estimate of reality and, furthermore, it indeed shows the expected nonlinear behavior seen in the quadratic fit to the experimental data (thus, we conclude that the quadratic fit is probably the better of the two empirical representations). In all cases, however, the data shows that there has been a decrease in reactivity of about 1.2 - 1.3% $\Delta k/k$ over the first 50 MWD of operation of the UMLRR M-2-5 core and that this change is predicted reasonably well with the 3-D VENTURE model.

Focusing now on the M-2-5 50 MWD core configuration, a series of blade worth curve calculations was made and compared to the measured data from the Jan. 2011 evaluation using the traditional doubling time method for determining blade worth curves. These data are summarized in Table 5 and they show similar variations as seen in the previous comparisons given for the M-1-3 and M-2-5 BOL configurations (see Tables 2 - 4). In addition, in March 2011, another experimental evaluation was performed using a newly developed inverse kinetics method,[13] and these data are also included in the last column of Table 5. The inverse kinetics method, in particular, significantly reduces the relatively large uncertainty that is inherent in the

doubling time approach using only a few measurement points. Thus, concerning the experimental data, we have more confidence in the new inverse kinetics data than in the previously available results obtained using doubling time approach.

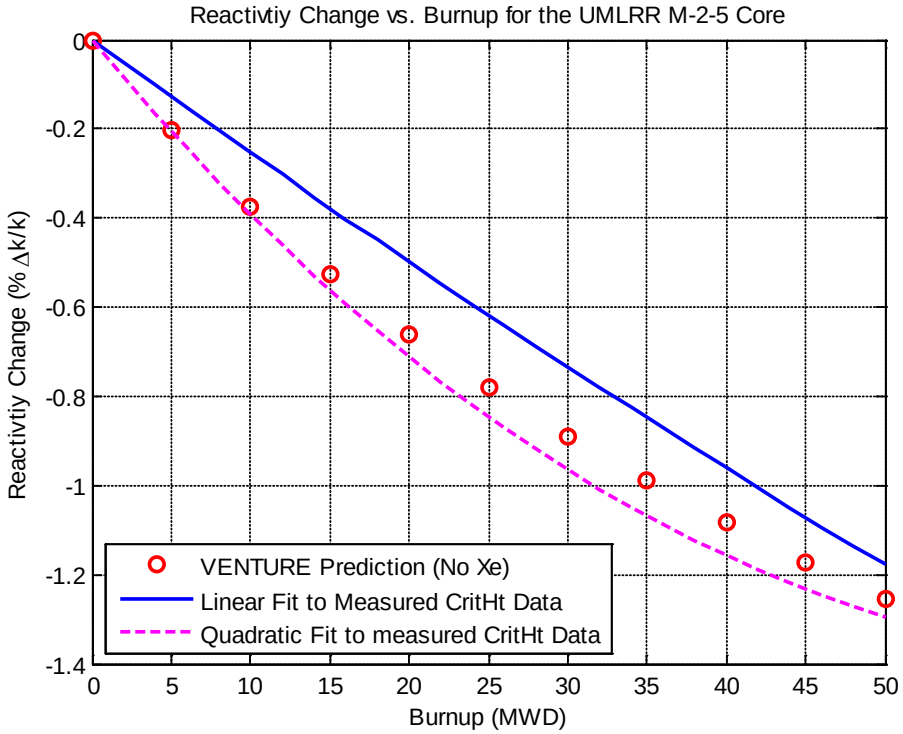

Fig. 17 Reactivity change vs. burnup for the UMLRR M-2-5 core.

Table 5 Comparison of measured and calculated M-2-5 50 MWD blade worths.

	Measured %Δk/k (DT method)		VENTURE %Δk/k (SCALE6 v7n238 data)		Measured %Δk/k (Inverse Kinetics)
Parameter	**Theoretical Model**	**New Model**	**Theoretical Model**	**New Model**	**New Model**
Blade 1 Worth	2.48	2.55	2.69	2.86	2.66
Blade 2 Worth	2.06	2.23	2.15	2.29	2.24
Blade 3 Worth	3.18	3.64	2.90	3.06	3.32
Blade 4 Worth	3.60	4.19	3.52	3.74	3.64
Total Blades 1-4	11.3	12.6	11.3	12.0	11.9
Excess Reactivity	2.86	2.41	2.84	2.71	2.68
Reg. Blade Worth	0.32	0.31	0.41	0.45	0.30

First we note that all the blade worth distributions noted in Table 5 are similar and they also resemble the distributions obtained at the beginning of life -- that is, Blade 2 still has the lowest worth and Blade 4 still has the largest value, with Blades 1 and 3 falling between these limits. In addition, the total worth has not changed significantly, still having a value close to 12 %Δk/k in most cases. There is still a lot of variability in the doubling time experimental results, but the VENTURE data compares quite well to the data from the new inverse kinetics method (which is probably the closest estimate of reality that we have). Thus, it appears that the VENTURE model after 50 MWD of burnup still gives a good representation of the worth data within the UMLRR (except, of course, for the regulating blade worth, which has always been over predicted by the VENTURE model).

Summary

This report provides summary documentation of the 2011/2012 3-D VENTURE model of the UMass-Lowell Research Reactor (UMLRR), along with a number of comparisons to measured data to evaluate the overall utility of the model to accurately predict core behavior. In particular, the model validation effort has looked at critical blade heights, total blade worths, and selected thermal flux profiles in the M-1-3 and M-2-5 cores, including an evaluation of the current M-2-5 configuration after roughly 50 MWD of operation. In most cases, the computational results are quite reasonable and they consistently exhibit the expected behavior of the system. There are some areas that could use improvement (such as the negative reactivity bias in the VENTURE-calculated k_{eff} values and the over prediction of the regulating blade worth), but generally, the comparisons have been quite favorable.

Thus, the 2011/2012 VENTURE model has successfully passed its first set of validation tests. Of course, model validation is a never-ending process -- so we plan to continually evaluate the real predictive capability of the existing computer models as they are used to support future operations within the UMLRR facility. In particular, the current model has been used to perform all the required physics analyses associated with the WPI fuel transfer project and, once permission to actually use the WPI fuel is received from the NRC, a series of reactivity evaluations using a combination of both the original UMLRR U_3Si_2-Al fuel and the WPI UAl_x-Al fuel will be made. These tests will significantly enhance our overall validation effort -- and hopefully add further evidence that supports the utility of the current VENTURE models.

As a final note, it should be mentioned that, in parallel with the current effort to develop and validate the VENTURE model, a comprehensive MCNP model of the UMLRR has also been under development (see Refs. 12 and 14, for example). As part of these combined modeling efforts, a short paper and poster[15] was presented at a recent research reactor topical meeting that summarized both the VENTURE and MCNP results for the validation tests mentioned herein -- thus, this paper also serves as summary documentation for the work reported here.

References

1. J. R. White, et. al., "Calculational Support for the Startup of the LEU-Fueled UMass-Lowell Research Reactor," Advances in Reactor Physics and Mathematics and Computation, Pittsburgh, PA (May 2000).

2. J. R. White, et. al., "Preliminary Characterization of the Irradiation Facilities within the LEU-Fueled UMass-Lowell Research Reactor," Advances in Reactor Physics and Mathematics and Computation, Pittsburgh, PA (May 2000).

3. "Report on the HEU to LEU Conversion of the University of Massachusetts Lowell Research Reactor," submitted to the US Nuclear Regulatory Commission in fulfillment of Amendment No. 12 to License No. R-125 (April 2001).
4. J. R. White and L. Bobek, "Startup Test Results and Model Evaluation for the HEU to LEU Conversion of the UMass-Lowell Research," 24th International Meeting on Reduced Enrichment for Research and Test Reactors (RERTR 2002), San Carlos de Bariloche, Argentina (Nov. 2002).
5. J. R. White, et. al., "Design and Initial Testing of an Ex-Core Fast Neutron Irradiator for the UMass-Lowell Research Reactor," 2002 ANS Radiation Protection and Shielding Topical Conference, Santa Fe, NM (April 2002).
6. J. R. White, L. Bobek, and T. Regan, "Initial Testing of the New Ex-Core Fast Neutron Irradiator at the UMass-Lowell Research Reactor," UMass-Lowell informal in-house project documentation (June 2002).
7. J. R. White, "Cross Section Libraries and Preliminary Modeling for the Reference UMLRR LEU Core Configuration," UMass-Lowell informal in-house project documentation (Jan. 1999).
8. J. R. White and J. Marcyoniak, "Comparison of the WPI and UMLRR Fuel Assembly Models," UMass-Lowell informal in-house project documentation (July 2011).
9. Michael Pike, "Development of Computational Tools for the Expansion of Simulation Capabilities for the University of Massachusetts Lowell Research Reactor," Nuclear Engineering M.S Thesis, UMass-Lowell (anticipated completion in Dec. 2012).
10. "Updates Scale from Version 6.0 to 6.1," part of the SCALE 6.1 documentation (June 2011).
11. J. R. Lamarsh and A. J. Baratta, ***Introduction to Nuclear Engineering***, 3rd Edition, Prentice Hall (2001).
12. J. R. White, R. Gocht, and M. Ducey "Final Report on MCNP Modeling for the UMLRR and Selected Gamma Irradiation Facilities," UMass-Lowell informal in-house project documentation (Sept. 2011).
13. Thomas Michaud, "Implementation of the Inverse Kinetics Method for Reactivity Calculations at the UMLRR," Nuclear Engineering M.S Thesis, UMass-Lowell (Dec. 2011).
14. Russell Gocht, "Monte Carlo Simulation of the Steady State Neutronics for The University of Massachusetts Lowell Research Reactor," Nuclear Engineering MS Thesis, UMass-Lowell (anticipated completion in Dec. 2012).
15. J. R. White, R. Gocht, M. Pike, and J. Marcyoniak, "Validation of the 3-D VENTURE and MCNP UMLRR Core Models used in Support of the WPI Fuel Transfer Project", Research Reactor Fuel Management Conference (RRFM2012), Prague, Czech Republic (March 2012)

Appendix I -- Geometry Data for the Pre-FNI 3-D VENTURE Model (2011 version)

The purpose of this appendix is to summarize the detailed geometry information for the 2011 version of the **3-D pre-FNI VENTURE model** for the UMLRR. A complete set of information was originally developed and recorded in an Excel spreadsheet file (stored with file name **prefni_leugeo_3d19_2011.xls**), so the reader is referred to this file for all the details. Here the goal is to summarize the primary information in this report for archival purposes and to give the reader easy access to the data.

There are three types of data tables given in the remainder of this appendix, as follows:

1. **Region boundaries and fine mesh by region information (Tables I.1 – I.3)** -- There are separate tables with the dimensions and mesh layout for each of the three coordinate directions. These tables define the model geometry including the details of the x-y grid layout and the thickness of each axial layer. A typical user, for example, may need to know the location of each axial layer for proper placement of the control and regulating blades for a particular simulation and Table I.3 contains this information.
2. **Zone assignment information (Tables I.4 – I.5)** -- These tables were used to help organize the assignment of zone numbers to specific locations in the core. There are five radial assembly types containing 1, 2, 3, or 6 radial zones per locations, with the 2-zone model having two styles (these are referred to as type 2a and 2b to model an inside/outside scheme or a center/side model, respectively). Table I.4 shows a rough sketch of the zone numbering scheme for each of the radial assembly types. In addition, there are four axial zone models containing 1, 2, 6 or 15 separate zones within the 30″ core region. Overall, the zone assignment approach used is actually rather complicated and the zone assignment table (Table I.5) given here tries to organize all this information in a useful way. This table would be useful to a typical user to help define how a particular zone or set of zones map to a grid location within the UMLRR. For example, in the M-1-3 configuration, grid location D6 often contains the assembly with the peak power density -- which includes fuel center zone numbers 309 – 314 (as seen in Table I.5).
3. **Zone by region map (Table I.6)** -- There are a set of 19 zone by region maps for the full 3-D VENTURE model (one for each layer in the model). This information is essentially the same as given in Table I.5, but it is in the form actually used within the VENTURE input stream (and the format given here gives a better visualization of the actual physical layout). Here we only show the middle layer (Layer 11) in Table I.6 as an example. All 19 layers are contained in the base Excel file.

Table I.1 X-direction region boundaries for the pre- and post-FNI VENTURE models.

	Data for constructing detailed 3-D model of UMass-Lowell Research Reactor								
	Reference LEU Model including capability for both beam ports and the FNI above Row A				(Reg Rod Model in only D9)				
		X-Direction Region Boundaries	**NOTE: Mesh spacing about 0.5 - 1.0 cm (about 1.5 cm in outer graphite)**						
			Dimensions in cm		Dimensions in inches				
Col #	Primary Region Description	Secondary Region Description	Thickness	Total Dist.	Thickness	Total Dist.	# Mesh	Delta x (cm)	Total Mesh
1	water reflector	water + beam ports	4.00000	4.0000	1.5748	1.5748	4	1.000	4
2		water + beam ports	4.00000	8.0000	1.5748	3.1496	4	1.000	8
3		water + beam ports	4.00000	12.0000	1.5748	4.7244	4	1.000	12
4		water + beam ports	4.00000	16.0000	1.5748	6.2992	4	1.000	16
5		water + beam ports	4.00000	20.0000	1.5748	7.8740	4	1.000	20
6		water + beam ports	4.00000	24.0000	1.5748	9.4488	4	1.000	24
7		water + beam ports	4.00000	28.0000	1.5748	11.0236	4	1.000	28
8		water + beam ports	4.00000	32.0000	1.5748	12.5984	4	1.000	32
9		water + beam ports	4.00000	36.0000	1.5748	14.1732	4	1.000	36
10		water + beam ports	4.00000	40.0000	1.5748	15.7480	4	1.000	40
11		water + beam ports	4.00000	44.0000	1.5748	17.3228	4	1.000	44
12		water + beam ports	2.73000	46.7300	1.0748	18.3976	3	0.910	47
13	water refl + core box	water(0.5) + Al(0.5)	1.27000	48.0000	0.5000	18.8976	2	0.635	49
14	grid location #1	rad basket or graphite refl	0.49950	48.4995	0.1967	19.0943	1	0.500	50
15		rad basket or graphite refl	3.38670	51.8862	1.3333	20.4276	4	0.847	54
16		rad basket or graphite refl	3.38670	55.2729	1.3333	21.7610	4	0.847	58
17	7.7724	basket/refl & control shroud end	0.49950	55.7724	0.1967	21.9576	1	0.500	59
18	grid location #2	fuel edge	0.49950	56.2719	0.1967	22.1543	1	0.500	60
19		fuel center	3.38670	59.6586	1.3333	23.4876	4	0.847	64
20	7.7724	fuel center	3.38670	63.0453	1.3333	24.8210	4	0.847	68
21		fuel edge	0.49950	63.5448	0.1967	25.0176	1	0.500	69
22	grid location #3	fuel edge	0.49950	64.0443	0.1967	25.2143	1	0.500	70
23		fuel center	3.38670	67.4310	1.3333	26.5476	4	0.847	74
24	7.7724	fuel center	3.38670	70.8177	1.3333	27.8810	4	0.847	78
25		fuel edge	0.49950	71.3172	0.1967	28.0776	1	0.500	79
26	grid location #4	fuel edge	0.49950	71.8167	0.1967	28.2743	1	0.500	80
27		fuel center	3.38670	75.2034	1.3333	29.6076	4	0.847	84
28	7.7724	fuel center	3.38670	78.5901	1.3333	30.9410	4	0.847	88
29		fuel edge	0.49950	79.0896	0.1967	31.1376	1	0.500	89
30	grid location #5	fuel edge	0.49950	79.5891	0.1967	31.3343	1	0.500	90
31	7.7724	fuel center	2.73480	82.3239	1.0767	32.4110	4	0.684	94
32		fuel center + control center Al	1.30380	83.6277	0.5133	32.9243	2	0.652	96
33		fuel center	2.73480	86.3625	1.0767	34.0010	4	0.684	100
34		fuel edge	0.49950	86.8620	0.1967	34.1976	1	0.500	101
35	grid location #6	fuel edge	0.49950	87.3615	0.1967	34.3943	1	0.500	102
36		fuel center	3.38670	90.7482	1.3333	35.7276	4	0.847	106
37	7.7724	fuel center	3.38670	94.1349	1.3333	37.0610	4	0.847	110
38		fuel edge	0.49950	94.6344	0.1967	37.2576	1	0.500	111
39	grid location #7	fuel edge	0.49950	95.1339	0.1967	37.4543	1	0.500	112
40		fuel center	3.38670	98.5206	1.3333	38.7876	4	0.847	116
41	7.7724	fuel center	3.38670	101.9073	1.3333	40.1210	4	0.847	120
42		fuel edge	0.49950	102.4068	0.1967	40.3176	1	0.500	121
43	grid location #8	fuel edge	0.49950	102.9063	0.1967	40.5143	1	0.500	122
44		fuel center	3.38670	106.2930	1.3333	41.8476	4	0.847	126
45	7.7724	fuel center	3.38670	109.6797	1.3333	43.1810	4	0.847	130
46		fuel edge	0.49950	110.1792	0.1967	43.3776	1	0.500	131
47	grid location #9 (reg rod)	control shroud end	0.49950	110.6787	0.1967	43.5743	1	0.500	132
48		control shroud end	0.68795	111.3667	0.2708	43.8451	1	0.688	133
49		control region	0.63500	112.0017	0.2500	44.0951	1	0.635	134
50		control region	2.06375	114.0654	0.8125	44.9076	3	0.688	137
51		control region	2.06375	116.1292	0.8125	45.7201	3	0.688	140
52		control region	0.63500	116.7642	0.2500	45.9701	1	0.635	141
53		control shroud end	0.68795	117.4521	0.2708	46.2410	1	0.688	142
54	7.7724	control shroud end	0.49950	117.9516	0.1967	46.4376	1	0.500	143
55	core box+gap+shield clad	water(0.400) + Al(0.600)	1.58750	119.5391	0.6250	47.0626	2	0.794	145
56	lead shield	pure lead	3.81000	123.3491	1.5000	48.5626	4	0.953	149
57	lead shield	pure lead	3.81000	127.1591	1.5000	50.0626	4	0.953	153
58	shield clad + water gap	water(0.6666) + Al(0.3334)	0.95250	128.1116	0.3750	50.4376	1	0.953	154
59	Thermal column clad	Al clad	1.90500	130.0166	0.7500	51.1876	2	0.953	156
60	Thermal column	graphite + water + beam ports	3.93500	133.9516	1.5492	52.7369	4	0.984	160
61		graphite + water + beam ports	4.00000	137.9516	1.5748	54.3117	4	1.000	164
62		graphite + water + beam ports	4.00000	141.9516	1.5748	55.8865	4	1.000	168
63		graphite + water + beam ports	4.00000	145.9516	1.5748	57.4613	4	1.000	172
64		graphite + water + beam ports	4.00000	149.9516	1.5748	59.0361	4	1.000	176
65		graphite + water + beam ports	4.00000	153.9516	1.5748	60.6109	4	1.000	180
66		graphite + water + beam ports	4.00000	157.9516	1.5748	62.1857	4	1.000	184
67		graphite + water + beam ports	4.00000	161.9516	1.5748	63.7605	4	1.000	188
68		graphite + water + beam ports	4.00000	165.9516	1.5748	65.3353	4	1.000	192
69		graphite + water + beam ports	59.04840	225.0000	23.2474	88.5827	40	1.476	232

Table I.2 Y-direction region boundaries for the pre- and post-FNI VENTURE models.

	Reference LEU Model including capability for both beam ports and the FNI above Row A				(Reg Rod Model in only D9)				
		Y-Direction Region Boundaries		**NOTE: Mesh spacing about 0.5 - 1.0 cm**					
			Dimensions in cm		Dimensions in inches				
Row #	Primary Region Description	Secondary Region Decription	Thickness	Total Dist.	Thickness	Total Dist.	# Mesh	Delta y (cm)	Total Mesh
1	water reflector	water reflector + beam ports (BP)	1.41280	1.4128	0.5562	0.5562	1	1.413	1
2		water reflector + beam ports (BP)	4.00000	5.4128	1.5748	2.1310	4	1.000	5
3		water reflector + beam ports (BP)	4.00000	9.4128	1.5748	3.7058	4	1.000	9
4		water reflector + beam ports (BP)	4.00000	13.4128	1.5748	5.2806	4	1.000	13
5		water reflector + beam ports (BP)	4.00000	17.4128	1.5748	6.8554	4	1.000	17
6		water reflector + beam ports (BP)	4.00000	21.4128	1.5748	8.4302	4	1.000	21
7		water reflector + beam ports (BP)	4.00000	25.4128	1.5748	10.0050	4	1.000	25
8		water reflector + beam ports (BP)	4.00000	29.4128	1.5748	11.5798	4	1.000	29
9		water reflector + beam ports (BP)	4.00000	33.4128	1.5748	13.1546	4	1.000	33
10		water reflector + beam ports (BP)	4.00000	37.4128	1.5748	14.7294	4	1.000	37
11		water reflector + beam ports (BP)	4.00000	41.4128	1.5748	16.3043	4	1.000	41
12		water reflector + beam ports (BP)	4.00000	45.4128	1.5748	17.8791	4	1.000	45
13	FNI region (3 rows)	water + BP or FNI Pb shield side	0.90800	46.3208	0.3575	18.2365	1	0.908	46
14		water + BP or FNI Pb shield center	2.97820	49.2990	1.1725	19.4091	3	0.993	49
15		water + BP or FNI Pb shield center	2.97820	52.2772	1.1725	20.5816	3	0.993	52
16		water + BP or FNI Pb shield side	0.90800	53.1852	0.3575	20.9391	1	0.908	53
17		water + BP or FNI Pb shield side	0.90800	54.0932	0.3575	21.2965	1	0.908	54
18		water + BP or FNI Pb shield center	2.97820	57.0714	1.1725	22.4691	3	0.993	57
19		water + BP or FNI Pb shield center	2.97820	60.0496	1.1725	23.6416	3	0.993	60
20		water + BP or FNI Pb shield side	0.90800	60.9576	0.3575	23.9991	1	0.908	61
21		water + BP or FNI Pb shield side	0.90800	61.8656	0.3575	24.3565	1	0.908	62
22		water + BP or FNI Pb shield center	2.97820	64.8438	1.1725	25.5291	3	0.993	65
23		water + BP or FNI Pb shield center	2.97820	67.8220	1.1725	26.7016	3	0.993	68
24		water + BP plate or FNI Pb shield sid	0.90800	68.7300	0.3575	27.0591	1	0.908	69
25	water refl + core box	water(0.5) + Al(0.5)	1.27000	70.0000	0.5000	27.5591	2	0.635	71
26	grid location A	rad basket/graphite refl/void box	1.82250	71.8225	0.7175	28.2766	2	0.911	73
27	7.7724	rad basket/graphite refl/void box	4.12740	75.9499	1.6250	29.9015	5	0.825	78
28		rad basket/graphite refl/void box	1.82250	77.7724	0.7175	30.6191	2	0.911	80
29	grid location B	side	0.84370	78.6161	0.3322	30.9512	1	0.844	81
30	7.7724	center	6.08500	84.7011	2.3957	33.3469	7	0.869	88
31		side	0.84370	85.5448	0.3322	33.6791	1	0.844	89
32	control location	control shroud	0.97160	86.5164	0.3825	34.0616	1	0.972	90
33	2.8957	control center	0.95250	87.4689	0.3750	34.4366	1	0.953	91
34		control shroud	0.97160	88.4405	0.3825	34.8191	1	0.972	92
35	grid location C	fuel side	0.84370	89.2842	0.3322	35.1513	1	0.844	93
36	7.7724	fuel center	6.08500	95.3692	2.3957	37.5469	7	0.869	100
37		fuel side	0.84370	96.2129	0.3322	37.8791	1	0.844	101
38	grid location D (reg rod)	fuel side or control shroud	0.84370	97.0566	0.3322	38.2113	1	0.844	102
39		fuel center or control shroud	0.34375	97.4004	0.1353	38.3466	1	0.344	103
40		fuel center or control matl	0.63500	98.0354	0.2500	38.5966	1	0.635	104
41	7.7724	fuel center or control center	4.12750	102.1629	1.6250	40.2216	5	0.826	109
42		fuel center or control matl	0.63500	102.7979	0.2500	40.4716	1	0.635	110
43		fuel center or control shroud	0.34375	103.1416	0.1353	40.6069	1	0.344	111
44		fuel side or control shroud	0.84370	103.9853	0.3322	40.9391	1	0.844	112
45	grid location E	fuel side	0.84370	104.8290	0.3322	41.2713	1	0.844	113
46	7.7724	fuel center	6.08500	110.9140	2.3957	43.6669	7	0.869	120
47		fuel side	0.84370	111.7577	0.3322	43.9991	1	0.844	121
48	control location	control shroud	0.97160	112.7293	0.3825	44.3816	1	0.972	122
49	2.8957	control center	0.95250	113.6818	0.3750	44.7566	1	0.953	123
50		control shroud	0.97160	114.6534	0.3825	45.1391	1	0.972	124
51	grid location F	fuel side	0.84370	115.4971	0.3322	45.4713	1	0.844	125
52	7.7724	fuel center	6.08500	121.5821	2.3957	47.8670	7	0.869	132
53		fuel side	0.84370	122.4258	0.3322	48.1991	1	0.844	133
54	grid location G	rad basket or graphite refl	7.77240	130.1982	3.0600	51.2591	8	0.972	141
55	water refl + core box	water(0.5) + Al(0.5)	1.27000	131.4682	0.5000	51.7591	2	0.635	143
56	beam port plate	pure Al	0.63500	132.1032	0.2500	52.0091	1	0.635	144
57	water refl or thermal col	water or graphite	2.41500	134.5182	0.9508	52.9599	3	0.805	147
58	water refl or thermal col	water or graphite	2.41500	136.9332	0.9508	53.9107	3	0.805	150
59	water refl or graphite refl clad	water or Al clad	1.90500	138.8382	0.7500	54.6607	2	0.953	152
60	water reflector	water + beam ports	4.00000	142.8382	1.5748	56.2355	4	1.000	156
61		water + beam ports	4.00000	146.8382	1.5748	57.8103	4	1.000	160
62		water + beam ports	4.00000	150.8382	1.5748	59.3851	4	1.000	164
63		water + beam ports	4.00000	154.8382	1.5748	60.9599	4	1.000	168
64		water + beam ports	4.00000	158.8382	1.5748	62.5347	4	1.000	172
65		water + beam ports	4.00000	162.8382	1.5748	64.1095	4	1.000	176
66		water + beam ports	4.00000	166.8382	1.5748	65.6843	4	1.000	180
67		water + beam ports	4.00000	170.8382	1.5748	67.2591	4	1.000	184
68		water + beam ports	4.00000	174.8382	1.5748	68.8339	4	1.000	188
69		water + beam ports	4.00000	178.8382	1.5748	70.4087	4	1.000	192
70		water + beam ports	4.00000	182.8382	1.5748	71.9835	4	1.000	196
71		water + beam ports	4.00000	186.8382	1.5748	73.5583	4	1.000	200
72		water + beam ports	4.00000	190.8382	1.5748	75.1331	4	1.000	204
73		water + beam ports	4.00000	194.8382	1.5748	76.7080	4	1.000	208
74		water + beam ports	4.00000	198.8382	1.5748	78.2828	4	1.000	212
75		water + beam ports	1.16180	200.0000	0.4574	78.7402	1	1.162	213

Table I.3 Z-direction region boundaries for the pre- and post-FNI VENTURE models.

	Data for constructing detailed 3-D model of UMass-Lowell Research Reactor											
	Reference LEU Model including capability for both beam ports and the FNI above Row A				(Reg Rod Model in only D9)							
		Z-Direction Region Boundaries		**NOTE: Mesh spacing about 1.0 - 1.5 cm**								
			Dimensions in cm		Dimensions in inches							
Layer #	Primary Region Description	Secondary Region Decription	Thickness	Total Dist.	Thickness	Total Dist.	# Mesh	Delta z (cm)	Total Mesh			
1	water reflector	top water refl + control	37.935	37.935	14.935	14.935	26	1.459	26			
2	water + Al reflector	water + Al + control	12.065	50.000	4.750	19.685	10	1.207	36			
3	side plate, graphite refl, radbasket	water + Al + graphite + control	3.810	53.810	1.500	21.185	3	1.270	39			
4	just above active fuel region	water + Al + graphite + cntl blade	4.445	58.255	1.750	22.935	4	1.111	43			
5	active fuel region	fuel + radbask + graphite + cntl blade	7.445	65.700	2.931	25.866	6	1.241	49			
6	active fuel region	fuel + radbask + graphite + cntl blade	7.400	73.100	2.913	28.780	6	1.233	55			
7	active fuel region	fuel + radbask + graphite + cntl blade	3.000	76.100	1.181	29.961	3	1.000	58			
8	active fuel region	fuel + radbask + graphite + cntl blade	3.000	79.100	1.181	31.142	3	1.000	61			
9	active fuel region	fuel + radbask + graphite + cntl blade	3.000	82.100	1.181	32.323	3	1.000	64			
10	active fuel region	fuel + radbask + graphite + cntl blade	3.000	85.100	1.181	33.504	3	1.000	67	23.5"	26"	30"
11	active fuel region (corecenter)	fuel + radbask + graphite + cntl blade	6.000	91.100	2.362	35.866	5	1.200	72			
12	active fuel region	fuel + radbask + graphite + cntl blade	6.000	97.100	2.362	38.228	5	1.200	77			
13	active fuel region	fuel + radbask + graphite + cntl blade	6.000	103.100	2.362	40.591	5	1.200	82			
14	active fuel region	fuel + radbask + graphite + cntl blade	7.400	110.500	2.913	43.504	6	1.233	88			
15	active fuel region	fuel + radbask + graphite + cntl blade	7.445	117.945	2.931	46.435	6	1.241	94			
16	just below active fuel region	water + Al + graphite + cntl blade	1.905	119.850	0.750	47.185	2	0.953	96			
17	side plate, graphite refl, radbasket	water + Al + graphite	6.350	126.200	2.500	49.685	5	1.270	101			
18	water + Al reflector	water + Al + grid plate	15.240	141.440	6.000	55.685	12	1.270	113			
19	water reflector	bot water refl	33.560	175.000	13.213	68.898	23	1.459	136			

Position of Blade Tip	
Layer #	Withdrawn
3	26.000
4	24.250
5	21.319
6	18.406
7	17.224
8	16.043
9	14.862
10	13.681
11	11.319
12	8.957
13	6.594
14	3.681
15	0.750
16	0.000

Table I.4 Description of the various radial assembly types.

Visualization of Radial Assy Types

1	1	1	1
1	1	1	1
1	1	1	1

Type #1

1 homo zone

corner post, graphite refl, homo rad basket

2	2	2	2
2	1	1	2
2	2	2	2

Type #2a

inside & outside zones

inside/outside rad basket model

2	2	2	2
1	1	1	1
2	2	2	2

Type #2b

center & side zones

center/side model for lead-void box

3	3	3	3
2	1	1	2
3	3	3	3

Type #3

center, edge & side zones

center/edges/sides model for fuel element

3	3	3	3	3	3
2	6	6	6	5	2
2	4	1	1	5	2
2	4	6	6	6	2
3	3	3	3	3	3

Type #6

center, edge, side, left, right, & top/bot zones

reg blade element

Table I.5 Zone assignment information for the pre-FNI VENTURE model.

	Data for constructing detailed 3-D model of UMass-Lowell Research Reactor (LEU Core + Beam Ports + Thermal Column -- **this is the Pre-FNI Model**)															
	This model represents a major update (in June 2011) with several new features/modifications -- some on the main ones are noted below.															
	This model reduces the mesh size in all three directions. The main motivation here was so that the single Al edge plate on each side of the assembly could be modeled explicily (in prior															
	models, some center fuel material was homogenized within this region). The model dimensions now are 232x214x136 which gives about 6.8 million mesh points!!!															
	The D9 location is now the only location where the regulating blade can be modeled (prior models had both D8 and D9). There appears to be no interest in moving the reg blade location.															
	The regblade has been modeled in more detail, with the individual boral segments modeled separately (no water homogenized in this region).															
	The axial model has also been adjusted to allow 26" blade movement with the "full in" position 2.5 inches above the grid (instead of 2.0 inches). This was actually measured in June 2011.															
	This model also changes the zone description quite significantly. In particular, the detailed sample region model with 5 radial zones and 8 axial zones was never used, so it was abandoned.															
	Now there are only 5 radial assy types and 4 axial region types, as follows:															
	radial type	1	only 1 zone per ass (corner post/graphite refl/homo rad basket)					see "radial assy types" sheet								
		2a	2 zones per assy (inside/outside radbasket model)													
		2b	2 zones per assy (center/side model for lead-void box)													
		3	3 zones per assy (center/edges/sides model for fuel element)													
		6	6 zones per assy (reg blade element)													
	axial types:	see separate Matlab plot for visual description of the 4 axial models for the 30" core region (1, 2, 6, and 15 region models)														
		Axial Zone Model by radial zone within the assembly								actual zone numbers by radial zone within assembly						
		inside/center	outside/edge	sides	left	right	top/bot			inside/center	outside/edge	sides	left	right	top/bot	
Row A	radial assy type	1	2	3	4	5	6	zones needed	zones so far	1	2	3	4	5	6	
1	1	1						1	1	1						
2	2b	1	1					2	3	2	3					
3	2b	1	1					2	5	4	5					
4	2b	1	1					2	7	6	7					
5	2b	1	1					2	9	8	9					
6	2b	1	1					2	11	10	11					
7	2b	1	1					2	13	12	13					
8	2b	1	1					2	15	14	15					
9	1	1						1	16	16						
						future flexibility		14	30	**zones 17 - 30 not used in current model (future capability for Row A)**						
Row B	radial assy type	1	2	3	4	5	6	zones needed	zones so far	1	2	3	4	5	6	
1	2a	6	2					8	38	31 - 36	37 - 38					
2	3	6	6	2				14	52	39 - 44	45 - 50	51 - 52				
3	3	6	6	2				14	66	53 - 58	59 - 64	65 - 66				
4	3	6	6	2				14	80	67 - 72	73 - 78	79 - 80				
5	3	6	6	2				14	94	81 - 86	87 - 92	93 - 94				
6	3	6	6	2				14	108	95 - 100	101 - 106	107 - 108				
7	3	6	6	2				14	122	109 - 114	115 - 120	121 - 122				
8	3	6	6	2				14	136	123 - 128	129 - 134	135 - 136				
9	1	1						1	137	137						
Row C	radial assy type	1	2	3	4	5	6	zones needed	zones so far	1	2	3	4	5	6	
1	2a	6	2					8	145	138 - 143	144 - 145					
2	3	6	6	2				14	159	146 - 151	152 - 157	158 - 159				
3	3	6	6	2				14	173	160 - 165	166 - 171	172 - 173				
4	3	6	6	2				14	187	174 - 179	180 - 185	186 - 187				
5	3	6	6	2				14	201	188 - 193	194 - 199	200 - 201				
6	3	6	6	2				14	215	202 - 207	208 - 213	214 - 215				
7	3	6	6	2				14	229	216 - 221	222 - 227	228 - 229				
8	3	6	6	2				14	243	230 - 235	236 - 241	242 - 243				
9	1	1						1	244	244						

Row D	radial assy type	1	2	3	4	5	6	zones needed	zones so far	1	2	3	4	5	6
1	2a	6	2					8	252	245 - 250	251 - 252				
2	3	6	6	2				14	266	253 - 258	259 - 264	265 - 266			
3	3	6	6	2				14	280	267 - 272	273 - 278	279 - 280			
4	3	6	6	2				14	294	281 - 286	287 - 292	293 - 294			
5	3	6	6	2				14	308	295 - 300	301 - 306	307 - 308			
6	3	6	6	2				14	322	309 - 314	315 - 320	321 - 322			
7	3	6	6	2				14	336	323 - 328	329 - 334	335 - 336			
8	3	6	6	2				14	350	337 - 342	343 - 348	349 - 350			
9	6	15	1	1	15	15	15	62	412	351 - 365	366	367	368 - 382	383 - 397	398 - 412
Row E	radial assy type	1	2	3	4	5	6	zones needed	zones so far	1	2	3	4	5	6
1	2a	6	2					8	420	413 - 418	419 - 420				
2	3	6	6	2				14	434	421 - 426	427 - 432	433 - 434			
3	3	6	6	2				14	448	435 - 440	441 - 446	447 - 448			
4	3	6	6	2				14	462	449 - 454	455 - 460	461 - 462			
5	3	6	6	2				14	476	463 - 468	469 - 474	475 - 476			
6	3	6	6	2				14	490	477 - 482	483 - 488	489 - 490			
7	3	6	6	2				14	504	491 - 496	497 - 502	503 - 504			
8	3	6	6	2				14	518	505 - 510	511 - 516	517 - 518			
9	1	1						1	519	519					
Row F	radial assy type	1	2	3	4	5	6	zones needed	zones so far	1	2	3	4	5	6
1	2a	6	2					8	527	520 - 525	526 - 527				
2	3	6	6	2				14	541	528 - 533	534 - 539	540 - 541			
3	3	6	6	2				14	555	542 - 547	548 - 553	554 - 555			
4	3	6	6	2				14	569	556 - 561	562 - 567	568 - 569			
5	3	6	6	2				14	583	570 - 575	576 - 581	582 - 583			
6	3	6	6	2				14	597	584 - 589	590 - 595	596 - 597			
7	3	6	6	2				14	611	598 - 603	604 - 609	610 - 611			
8	3	6	6	2				14	625	612 - 617	618 - 623	624 - 625			
9	1	1						1	626	626					
Row G	radial assy type	1	2	3	4	5	6	zones needed	zones so far	1	2	3	4	5	6
1	1	1						1	627	627					
2	1	1						1	628	628					
3	1	1						1	629	629					
4	1	1						1	630	630					
5	1	1						1	631	631					
6	1	1						1	632	632					
7	1	1						1	633	633					
8	1	1						1	634	634					
9	1	1						1	635	635					
						future flexibility		15	650	**zones 636 - 650 not used in current model (future capability for Row G)**					

Misc Edit Zones	Zone #	Control Zones	Zone #	Radial Structure/Ref Zones	Zone #	Axial Reflector Zones	Zone #
BeamPort top #1	651	Blade #1	661 - 675	Core Box + H2O	741	Top Axial Refl (inside)	751
BeamPort top # 2	652	Blade #2	676 - 690	Core Box + Gap + Pb Liner	742	Top Axial Refl (outside)	752
BeamPort top #3	653	Blade #3	691 - 705	Pb Shield	743	Top Axial Refl (homo)	753
BeamPort bot #1	654	Blade #4	706 - 720	Pb Liner + Gap	744	Bot Axial Refl (inside)	754
BeamPort bot # 2	655	Cntrl Ends (Al + H2O)	721	Thm Column Liner	745	Bot Axial Refl (outside)	755
BeamPort bot #3	656	Cntrl Center (Al + H2O)	722	Thm Column Graphite	746	Bot Axial Refl (homo)	756
		Cntrl Shroud (Al + H2O)	723	BP End Plate	747		
Thm Col #1	657			BP Tube	748	Top Axial Refl (D9-1)	757 - 760
Thm Col #2	658	**unused zones (future capability)**	724 - 740	BP Inside (low density water)	749	Top Axial Refl (D9-2)	761 - 764
				Water Refl	750		
Rabbit #1	659						
Rabbit #2	660						

Table I.6 Zone by region map for Level 11 for the pre-FNI VENTURE model.

Data for constructing detailed 3-D model of UMass-Lowell Research Reactor
Reference Pre-FNI LEU Model (June 2011)

Reference zone map by region for axial LAYER #11

This is axial LAYER #11

column	1	2	3	4	5	6	7	8	9	10	11	12	13	14	15	16	17	18	19	20	21	22	23	24	25	26	27	28	29	30	31	32	33	34	35
row																																			
1	750	750	750	750	749	749	749	749	749	750	750	750	750	750	750	750	750	750	750	750	750	750	750	750	750	748	749	749	749	749	749	749	749	749	749
2	750	750	750	750	749	749	749	749	749	750	750	750	750	750	750	750	750	750	750	750	750	750	750	750	750	748	749	749	749	749	749	749	749	749	749
3	750	750	750	750	750	749	749	749	749	749	750	750	750	750	750	750	750	750	750	750	750	750	750	750	750	748	749	749	749	749	749	749	749	749	749
4	750	750	750	750	750	749	749	749	749	749	750	750	750	750	750	750	750	750	750	750	750	750	750	750	750	748	749	749	749	749	749	749	749	749	749
5	750	750	750	750	750	750	749	749	749	749	749	750	750	750	750	750	750	750	750	750	750	750	750	750	750	748	749	749	749	749	749	749	749	749	749
6	750	750	750	750	750	750	750	749	749	749	749	749	750	750	750	750	750	750	750	750	750	750	750	750	750	748	749	749	749	749	749	749	749	749	749
7	750	750	750	750	750	750	750	749	749	749	749	749	750	750	750	750	750	750	750	750	750	750	750	750	750	748	749	749	749	749	749	749	749	749	749
8	750	750	750	750	750	750	750	749	749	749	749	749	749	749	750	750	750	750	750	750	750	750	750	750	750	748	749	749	749	749	749	749	749	749	749
9	750	750	750	750	750	750	750	750	749	749	749	749	749	749	749	750	750	750	750	750	750	750	750	750	750	748	749	749	749	749	749	749	749	749	749
10	750	750	750	750	750	750	750	750	749	749	749	749	749	749	749	749	750	750	750	750	750	750	750	750	750	748	749	749	749	749	749	749	749	749	749
11	750	750	750	750	750	750	750	750	750	749	749	749	749	749	749	749	749	749	750	750	750	750	750	750	750	748	749	749	749	749	749	749	749	749	749
12	750	750	750	750	750	750	750	750	750	750	749	749	749	749	749	749	749	749	749	750	750	750	750	750	750	748	749	749	749	749	749	749	749	749	749
13	750	750	750	750	750	750	750	750	750	750	749	749	749	749	749	749	749	749	749	750	750	750	750	750	750	748	749	749	749	749	749	749	749	749	749
14	750	750	750	750	750	750	750	750	750	750	750	749	749	749	749	749	749	749	749	749	750	750	750	750	750	748	749	749	749	749	749	749	749	749	749
15	750	750	750	750	750	750	750	750	750	750	750	749	749	749	749	749	749	749	749	749	749	750	750	750	750	748	749	749	749	749	749	749	749	749	749
16	750	750	750	750	750	750	750	750	750	750	750	749	749	749	749	749	749	749	749	749	749	749	750	750	750	748	749	749	749	749	749	749	749	749	749
17	750	750	750	750	750	750	750	750	750	750	750	749	749	749	749	749	749	749	749	749	749	749	750	750	750	748	749	749	749	749	749	749	749	749	749
18	750	750	750	750	750	750	750	750	750	750	750	750	749	749	749	749	749	749	749	749	749	749	750	750	750	748	749	749	749	749	749	749	749	749	749
19	750	750	750	750	750	750	750	750	750	750	750	750	749	749	749	749	749	749	749	749	749	749	749	750	750	748	749	749	749	749	749	749	749	749	749
20	750	750	750	750	750	750	750	750	750	750	750	750	750	750	749	749	749	749	749	749	749	749	749	750	750	748	749	749	749	749	749	749	749	749	749
21	750	750	750	750	750	750	750	750	750	750	750	750	750	750	749	749	749	749	749	749	749	749	749	750	750	748	749	749	749	749	749	749	749	749	749
22	750	750	750	750	750	750	750	750	750	750	750	750	750	750	750	749	749	651	651	651	651	749	749	749	750	748	749	749	749	652	652	652	652	652	749
23	750	750	750	750	750	750	750	750	750	750	750	750	750	750	750	749	749	651	651	651	651	749	749	749	750	748	749	749	749	652	652	652	652	652	749
24	750	750	750	750	750	750	750	750	750	750	750	750	747	747	747	747	747	747	747	747	747	747	747	747	747	747	747	747	747	747	747	747	747	747	747
25	750	750	750	750	750	750	750	750	750	750	750	750	741	741	741	741	741	741	741	741	741	741	741	741	741	741	741	741	741	741	741	741	741	741	741
26	750	750	750	750	750	750	750	750	750	750	750	750	741	1	1	1	1	3	3	3	3	5	5	5	5	7	7	7	7	9	9	9	9	9	11
27	750	750	750	750	750	750	750	750	750	750	750	750	741	1	1	1	1	2	2	2	2	4	4	4	4	6	6	6	6	8	8	8	8	8	10
28	750	750	750	750	750	750	750	750	750	750	750	750	741	1	1	1	1	3	3	3	3	5	5	5	5	7	7	7	7	9	9	9	9	9	11
29	750	750	750	750	750	750	750	750	750	750	750	750	741	38	38	38	38	52	52	52	52	66	66	66	66	80	80	80	80	94	94	94	94	94	108
30	750	750	750	750	750	750	750	750	750	750	750	750	741	38	34	34	38	48	42	42	48	62	56	56	62	76	70	70	76	90	84	84	84	90	104
31	750	750	750	750	750	750	750	750	750	750	750	750	741	38	38	38	38	52	52	52	52	66	66	66	66	80	80	80	80	94	94	94	94	94	108
32	750	750	750	750	750	750	750	750	750	750	750	750	741	721	721	721	723	723	723	723	723	723	723	723	723	723	723	723	723	723	723	722	723	723	723
33	750	750	750	750	750	750	750	750	750	750	750	750	741	721	721	721	684	684	684	684	684	684	684	684	684	684	684	684	684	684	684	722	699	699	699
34	750	750	750	750	750	750	750	750	750	750	750	750	741	721	721	721	723	723	723	723	723	723	723	723	723	723	723	723	723	723	723	722	723	723	723
35	750	750	750	750	750	750	750	750	750	750	750	750	741	145	145	145	145	159	159	159	159	173	173	173	173	187	187	187	187	201	201	201	201	201	215
36	750	750	750	750	750	750	750	750	750	750	750	750	741	145	141	141	145	155	149	149	155	169	163	163	169	183	177	177	183	197	191	191	191	197	211
37	750	750	750	750	750	750	750	750	750	750	750	750	741	145	145	145	145	159	159	159	159	173	173	173	173	187	187	187	187	201	201	201	201	201	215
38	750	750	750	750	750	750	750	750	750	750	750	750	741	252	252	252	252	266	266	266	266	280	280	280	280	294	294	294	294	308	308	308	308	308	322
39	750	750	750	750	750	750	750	750	750	750	750	750	741	252	248	248	252	262	256	256	262	276	270	270	276	290	284	284	290	304	298	298	298	304	318
40	750	750	750	750	750	750	750	750	750	750	750	750	741	252	248	248	252	262	256	256	262	276	270	270	276	290	284	284	290	304	298	298	298	304	318
41	750	750	750	750	750	750	750	750	750	750	750	750	741	252	248	248	252	262	256	256	262	276	270	270	276	290	284	284	290	304	298	298	298	304	318
42	750	750	750	750	750	750	750	750	750	750	750	750	741	252	248	248	252	262	256	256	262	276	270	270	276	290	284	284	290	304	298	298	298	304	318
43	750	750	750	750	750	750	750	750	750	750	750	750	741	252	248	248	252	262	256	256	262	276	270	270	276	290	284	284	290	304	298	298	298	304	318
44	750	750	750	750	750	750	750	750	750	750	750	750	741	252	252	252	252	266	266	266	266	280	280	280	280	294	294	294	294	308	308	308	308	308	322
45	750	750	750	750	750	750	750	750	750	750	750	750	741	420	420	420	420	434	434	434	434	448	448	448	448	462	462	462	462	476	476	476	476	476	490
46	750	750	750	750	750	750	750	750	750	750	750	750	741	420	416	416	420	430	424	424	430	444	438	438	444	458	452	452	458	472	466	466	466	472	486
47	750	750	750	750	750	750	750	750	750	750	750	750	741	420	420	420	420	434	434	434	434	448	448	448	448	462	462	462	462	476	476	476	476	476	490
48	750	750	750	750	750	750	750	750	750	750	750	750	741	721	721	721	723	723	723	723	723	723	723	723	723	723	723	723	723	723	723	722	723	723	723
49	750	750	750	750	750	750	750	750	750	750	750	750	741	721	721	721	669	669	669	669	669	669	669	669	669	669	669	669	669	669	669	722	714	714	714
50	750	750	750	750	750	750	750	750	750	750	750	750	741	721	721	721	723	723	723	723	723	723	723	723	723	723	723	723	723	723	723	722	723	723	723
51	750	750	750	750	750	750	750	750	750	750	750	750	741	527	527	527	527	541	541	541	541	555	555	555	555	569	569	569	569	583	583	583	583	583	597
52	750	750	750	750	750	750	750	750	750	750	750	750	741	527	523	523	527	537	531	531	537	551	545	545	551	565	559	559	565	579	573	573	573	579	593
53	750	750	750	750	750	750	750	750	750	750	750	750	741	527	527	527	527	541	541	541	541	555	555	555	555	569	569	569	569	583	583	583	583	583	597
54	750	750	750	750	750	750	750	750	750	750	750	750	741	627	627	627	627	628	628	628	628	629	629	629	629	630	630	630	630	631	631	631	631	631	632
55	750	750	750	750	750	750	750	750	750	750	750	750	741	741	741	741	741	741	741	741	741	741	741	741	741	741	741	741	741	741	741	741	741	741	741
56	750	750	750	750	750	750	750	750	750	750	750	750	747	747	747	747	747	747	747	747	747	747	747	747	747	747	747	747	747	747	747	747	747	747	747
57	750	750	750	750	750	750	750	750	750	750	750	750	750	750	750	749	749	654	654	654	654	749	749	749	750	748	749	749	749	655	655	655	655	655	749
58	750	750	750	750	750	750	750	750	750	750	750	750	750	750	750	749	749	654	654	654	654	749	749	749	750	748	749	749	749	655	655	655	655	655	749
59	750	750	750	750	750	750	750	750	750	750	750	750	750	750	749	749	749	749	749	749	749	749	749	750	750	748	749	749	749	749	749	749	749	749	749
60	750	750	750	750	750	750	750	750	750	750	750	750	750	750	749	749	749	749	749	749	749	749	749	750	750	748	749	749	749	749	749	749	749	749	749
61	750	750	750	750	750	750	750	750	750	750	750	750	749	749	749	749	749	749	749	749	749	749	750	750	750	748	749	749	749	749	749	749	749	749	749
62	750	750	750	750	750	750	750	750	750	750	750	749	749	749	749	749	749	749	749	749	750	750	750	750	750	748	749	749	749	749	749	749	749	749	749
63	750	750	750	750	750	750	750	750	750	750	749	749	749	749	749	749	749	749	749	750	750	750	750	750	750	748	749	749	749	749	749	749	749	749	749
64	750	750	750	750	750	750	750	750	750	750	749	749	749	749	749	749	749	749	749	750	750	750	750	750	750	748	749	749	749	749	749	749	749	749	749
65	750	750	750	750	750	750	750	750	750	749	749	749	749	749	749	749	749	750	750	750	750	750	750	750	750	748	749	749	749	749	749	749	749	749	749
66	750	750	750	750	750	750	750	750	750	749	749	749	749	749	749	749	750	750	750	750	750	750	750	750	750	748	749	749	749	749	749	749	749	749	749
67	750	750	750	750	750	750	750	750	749	749	749	749	749	749	749	750	750	750	750	750	750	750	750	750	750	748	749	749	749	749	749	749	749	749	749
68	750	750	750	750	750	750	750	750	749	749	749	749	749	749	750	750	750	750	750	750	750	750	750	750	750	748	749	749	749	749	749	749	749	749	749
69	750	750	750	750	750	750	750	749	749	749	749	749	750	750	750	750	750	750	750	750	750	750	750	750	750	748	749	749	749	749	749	749	749	749	749
70	750	750	750	750	750	750	749	749	749	749	749	750	750	750	750	750	750	750	750	750	750	750	750	750	750	748	749	749	749	749	749	749	749	749	749
71	750	750	750	750	750	750	749	749	749	749	749	750	750	750	750	750	750	750	750	750	750	750	750	750	750	748	749	749	749	749	749	749	749	749	749
72	750	750	750	750	750	749	749	749	749	749	750	750	750	750	750	750	750	750	750	750	750	750	750	750	750	748	749	749	749	749	749	749	749	749	749
73	750	750	750	750	750	749	749	749	749	749	750	750	750	750	750	750	750	750	750	750	750	750	750	750	750	748	749	749	749	749	749	749	749	749	749
74	750	750	750	750	749	749	749	749	749	750	750	750	750	750	750	750	750	750	750	750	750	750	750	750	750	748	749	749	749	749	749	749	749	749	749
75	750	750	750	750	749	749	749	749	749	750	750	750	750	750	750	750	750	750	750	750	750	750	750	750	750	748	749	749	749	749	749	749	749	749	749

column	36	37	38	39	40	41	42	43	44	45	46	47	48	49	50	51	52	53	54	55	56	57	58	59	60	61	62	63	64	65	66	67	68	69
row																																		
1	749	749	748	750	750	750	750	750	750	750	750	750	750	750	750	750	750	750	750	750	750	750	750	750	749	749	749	749	749	750	750	750	750	750
2	749	749	748	750	750	750	750	750	750	750	750	750	750	750	750	750	750	750	750	750	750	750	750	750	749	749	749	749	749	750	750	750	750	750
3	749	749	748	750	750	750	750	750	750	750	750	750	750	750	750	750	750	750	750	750	750	750	749	749	749	749	749	749	750	750	750	750	750	750
4	749	749	748	750	750	750	750	750	750	750	750	750	750	750	750	750	750	750	750	750	750	749	749	749	749	749	749	749	750	750	750	750	750	750
5	749	749	748	750	750	750	750	750	750	750	750	750	750	750	750	750	750	750	750	750	750	749	749	749	749	749	749	750	750	750	750	750	750	750
6	749	749	748	750	750	750	750	750	750	750	750	750	750	750	750	750	750	750	750	750	749	749	749	749	749	749	750	750	750	750	750	750	750	750
7	749	749	748	750	750	750	750	750	750	750	750	750	750	750	750	750	750	750	750	749	749	749	749	749	749	749	750	750	750	750	750	750	750	750
8	749	749	748	750	750	750	750	750	750	750	750	750	750	750	750	750	749	749	749	749	749	749	749	749	749	750	750	750	750	750	750	750	750	750
9	749	749	748	750	750	750	750	750	750	750	750	750	750	750	750	749	749	749	749	749	749	749	749	749	749	750	750	750	750	750	750	750	750	750
10	749	749	748	750	750	750	750	750	750	750	750	750	750	749	749	749	749	749	749	749	749	749	749	749	750	750	750	750	750	750	750	750	750	750
11	749	749	748	750	750	750	750	750	750	750	750	749	749	749	749	749	749	749	749	749	749	749	749	749	750	750	750	750	750	750	750	750	750	750
12	749	749	748	750	750	750	750	750	750	749	749	749	749	749	749	749	749	749	749	749	749	749	750	750	750	750	750	750	750	750	750	750	750	750
13	749	749	748	750	750	750	750	750	750	749	749	749	749	749	749	749	749	749	749	749	749	749	750	750	750	750	750	750	750	750	750	750	750	750
14	749	749	748	750	750	750	750	750	750	749	749	749	749	749	749	749	749	749	749	749	749	750	750	750	750	750	750	750	750	750	750	750	750	750
15	749	749	748	750	750	750	750	750	749	749	749	749	749	749	749	749	749	749	749	749	749	750	750	750	750	750	750	750	750	750	750	750	750	750
16	749	749	748	750	750	750	749	749	749	749	749	749	749	749	749	749	749	749	749	749	749	750	750	750	750	750	750	750	750	750	750	750	750	750
17	749	749	748	750	750	750	749	749	749	749	749	749	749	749	749	749	749	749	749	749	750	750	750	750	750	750	750	750	750	750	750	750	750	750
18	749	749	748	750	750	750	749	749	749	749	749	749	749	749	749	749	749	749	749	749	750	750	750	750	750	750	750	750	750	750	750	750	750	750
19	749	749	748	750	750	749	749	749	749	749	749	749	749	749	749	749	749	749	749	750	750	750	750	750	750	750	750	750	750	750	750	750	750	750
20	749	749	748	750	750	749	749	749	749	749	749	749	749	749	749	749	749	749	750	750	750	750	750	745	745	745	745	745	745	745	745	745	745	745
21	749	749	748	750	750	749	749	749	749	749	749	749	749	749	749	749	749	749	750	750	750	750	750	745	745	745	745	745	745	745	745	745	745	745
22	749	749	748	750	749	749	749	653	653	653	653	749	749	749	749	749	750	750	750	750	750	750	750	745	746	746	746	746	746	746	746	746	746	746
23	749	749	748	750	749	749	749	653	653	653	653	749	749	749	749	750	750	750	750	750	750	750	750	745	746	746	746	746	746	746	746	746	746	746
24	747	747	747	747	747	747	747	747	747	747	747	747	747	747	747	747	747	747	747	747	750	750	750	745	746	746	746	746	746	746	746	746	746	746
25	741	741	741	741	741	741	741	741	741	741	741	741	741	741	741	741	741	741	741	742	741	741	744	745	746	746	746	746	746	746	746	746	746	746
26	11	11	11	13	13	13	13	15	15	15	15	16	16	16	16	16	16	16	16	742	743	743	744	745	746	746	746	746	746	746	746	746	746	746
27	10	10	10	12	12	12	12	14	14	14	14	16	16	16	16	16	16	16	16	742	743	743	744	745	746	746	746	746	746	746	746	746	746	746
28	11	11	11	13	13	13	13	15	15	15	15	16	16	16	16	16	16	16	16	742	743	743	744	745	746	746	746	746	746	746	746	746	746	746
29	108	108	108	122	122	122	122	136	136	136	136	137	137	137	137	137	137	137	137	742	743	743	744	745	746	746	746	746	746	746	746	746	746	746
30	98	98	104	118	112	112	118	132	126	126	132	137	137	137	137	137	137	137	137	742	743	743	744	745	746	746	746	746	746	746	746	746	746	746
31	108	108	108	122	122	122	122	136	136	136	136	137	137	137	137	137	137	137	137	742	743	743	744	745	746	746	746	746	746	746	746	746	746	746
32	723	723	723	723	723	723	723	723	723	723	723	723	721	721	721	721	721	721	721	742	743	743	744	745	746	746	746	746	746	746	746	746	746	746
33	699	699	699	699	699	699	699	699	699	699	699	699	721	721	721	721	721	721	721	742	743	743	744	745	746	746	746	746	746	746	746	746	746	746
34	723	723	723	723	723	723	723	723	723	723	723	723	721	721	721	721	721	721	721	742	743	743	744	745	746	746	746	746	746	746	746	746	746	746
35	215	215	215	229	229	229	229	243	243	243	243	244	244	244	244	244	244	244	244	742	743	743	744	745	746	746	746	746	746	746	746	746	746	746
36	205	205	211	225	219	219	225	239	233	233	239	244	244	244	244	244	244	244	244	742	743	743	744	745	746	746	746	746	746	746	746	746	746	746
37	215	215	215	229	229	229	229	243	243	243	243	244	244	244	244	244	244	244	244	742	743	743	744	745	746	746	746	746	746	746	746	746	746	746
38	322	322	322	336	336	336	336	350	350	350	350	367	367	367	367	367	367	367	367	742	743	743	744	745	746	746	746	746	746	746	746	746	746	746
39	312	312	318	332	326	326	332	346	340	340	346	367	367	367	367	367	367	367	367	742	743	743	744	745	746	657	746	746	658	746	746	746	746	746
40	312	312	318	332	326	326	332	346	340	340	346	366	366	406	406	406	391	366	366	742	743	743	744	745	746	657	746	746	658	746	746	746	746	746
41	312	312	318	332	326	326	332	346	340	340	346	366	366	376	359	359	391	366	366	742	743	743	744	745	746	657	746	746	658	746	746	746	746	746
42	312	312	318	332	326	326	332	346	340	340	346	366	366	376	406	406	406	366	366	742	743	743	744	745	746	657	746	746	658	746	746	746	746	746
43	312	312	318	332	326	326	332	346	340	340	346	367	367	367	367	367	367	367	367	742	743	743	744	745	746	657	746	746	658	746	746	746	746	746
44	322	322	322	336	336	336	336	350	350	350	350	367	367	367	367	367	367	367	367	742	743	743	744	745	746	746	746	746	746	746	746	746	746	746
45	490	490	490	504	504	504	504	518	518	518	518	519	519	519	519	519	519	519	519	742	743	743	744	745	746	746	746	746	746	746	746	746	746	746
46	480	480	486	500	494	494	500	514	508	508	514	519	519	519	519	519	519	519	519	742	743	743	744	745	746	746	746	746	746	746	746	746	746	746
47	490	490	490	504	504	504	504	518	518	518	518	519	519	519	519	519	519	519	519	742	743	743	744	745	746	746	746	746	746	746	746	746	746	746
48	723	723	723	723	723	723	723	723	723	723	723	723	721	721	721	721	721	721	721	742	743	743	744	745	746	746	746	746	746	746	746	746	746	746
49	714	714	714	714	714	714	714	714	714	714	714	714	721	721	721	721	721	721	721	742	743	743	744	745	746	746	746	746	746	746	746	746	746	746
50	723	723	723	723	723	723	723	723	723	723	723	723	721	721	721	721	721	721	721	742	743	743	744	745	746	746	746	746	746	746	746	746	746	746
51	597	597	597	611	611	611	611	625	625	625	625	626	626	626	626	626	626	626	626	742	743	743	744	745	746	746	746	746	746	746	746	746	746	746
52	587	587	593	607	601	601	607	621	615	615	621	626	626	626	626	626	626	626	626	742	743	743	744	745	746	746	746	746	746	746	746	746	746	746
53	597	597	597	611	611	611	611	625	625	625	625	626	626	626	626	626	626	626	626	742	743	743	744	745	746	746	746	746	746	746	746	746	746	746
54	632	632	632	633	633	633	633	634	634	634	634	635	635	635	635	635	635	635	635	742	743	743	744	745	746	746	746	746	746	746	746	746	746	746
55	741	741	741	741	741	741	741	741	741	741	741	741	741	741	741	741	741	741	741	742	741	741	744	745	746	746	746	746	746	746	746	746	746	746
56	747	747	747	747	747	747	747	747	747	747	747	747	747	747	747	747	747	747	747	747	750	750	750	745	746	746	746	746	746	746	746	746	746	746
57	749	749	748	750	749	749	749	656	656	656	656	749	749	749	749	750	750	750	750	750	750	750	750	745	746	746	746	746	746	746	746	746	746	746
58	749	749	748	750	749	749	749	656	656	656	656	749	749	749	749	750	750	750	750	750	750	750	750	745	746	746	746	746	746	746	746	746	746	746
59	749	749	748	750	750	749	749	749	749	749	749	749	749	749	749	749	749	749	750	750	750	750	750	745	745	745	745	745	745	745	745	745	745	745
60	749	749	748	750	750	749	749	749	749	749	749	749	749	749	749	749	749	749	750	750	750	750	750	750	750	750	750	750	750	750	750	750	750	750
61	749	749	748	750	750	750	749	749	749	749	749	749	749	749	749	749	749	749	749	749	750	750	750	750	750	750	750	750	750	750	750	750	750	750
62	749	749	748	750	750	750	750	750	749	749	749	749	749	749	749	749	749	749	749	749	750	750	750	750	750	750	750	750	750	750	750	750	750	750
63	749	749	748	750	750	750	750	750	750	749	749	749	749	749	749	749	749	749	749	749	749	750	750	750	750	750	750	750	750	750	750	750	750	750
64	749	749	748	750	750	750	750	750	750	749	749	749	749	749	749	749	749	749	749	749	749	750	750	750	750	750	750	750	750	750	750	750	750	750
65	749	749	748	750	750	750	750	750	750	750	750	749	749	749	749	749	749	749	749	749	749	749	749	750	750	750	750	750	750	750	750	750	750	750
66	749	749	748	750	750	750	750	750	750	750	750	750	749	749	749	749	749	749	749	749	749	749	749	749	750	750	750	750	750	750	750	750	750	750
67	749	749	748	750	750	750	750	750	750	750	750	750	750	750	750	749	749	749	749	749	749	749	749	749	749	750	750	750	750	750	750	750	750	750
68	749	749	748	750	750	750	750	750	750	750	750	750	750	750	750	750	750	750	749	749	749	749	749	749	749	750	750	750	750	750	750	750	750	750
69	749	749	748	750	750	750	750	750	750	750	750	750	750	750	750	750	750	750	750	750	749	749	749	749	749	749	750	750	750	750	750	750	750	750
70	749	749	748	750	750	750	750	750	750	750	750	750	750	750	750	750	750	750	750	750	750	749	749	749	749	749	749	750	750	750	750	750	750	750
71	749	749	748	750	750	750	750	750	750	750	750	750	750	750	750	750	750	750	750	750	750	749	749	749	749	749	749	750	750	750	750	750	750	750
72	749	749	748	750	750	750	750	750	750	750	750	750	750	750	750	750	750	750	750	750	750	750	749	749	749	749	749	749	750	750	750	750	750	750
73	749	749	748	750	750	750	750	750	750	750	750	750	750	750	750	750	750	750	750	750	750	750	749	749	749	749	749	749	750	750	750	750	750	750
74	749	749	748	750	750	750	750	750	750	750	750	750	750	750	750	750	750	750	750	750	750	750	750	750	749	749	749	749	749	750	750	750	750	750
75	749	749	748	750	750	750	750	750	750	750	750	750	750	750	750	750	750	750	750	750	750	750	750	750	749	749	749	749	749	750	750	750	750	750

Appendix II -- Geometry Data for the Post-FNI 3-D VENTURE Model (2011 version)

The purpose of this appendix is to summarize the detailed geometry information for the 2011 version of the **3-D post-FNI VENTURE model** for the UMLRR. A complete set of information was originally developed and recorded in an Excel spreadsheet file (stored with file name **postfni_leugeo_3d19_2011.xls**), so the reader is referred to this file for all the details.

The data tables contained in this appendix are similar to those given in Appendix I -- except, of course, these are specific to the post-FNI UMLRR configuration. Thus, a detailed description will not be repeated here. Note however, that there is indeed a lot of overlap in the pre-and post FNI configurations, where the primary differences are associated with the excore regions just outside of Row A of the core grid. For the post-FNI configuration, the three beam ports originally on this side of the core have been replaced with a simple representation of the first three rows of the fast neutron irradiator (FNI) shield and grid support structure. The x-y planar and axial representations of the remaining core and excore geometries should be identical in the pre- and post-FNI models. Thus, familiarity with one of these models automatically implies knowledge of both UMLRR configurations.

Note also that the x, y, and z region boundaries mesh grid layout and the radial assembly types are identical with the pre-FNI core description given in Appendix I. Thus, these tables are not repeated here -- leaving only the zone descriptions (Table II.1) and sample zone map for Layer 11 (Table II.2) as unique for the post-FNI model.

Table II.1 Zone assignment information for the post-FNI VENTURE model.

	Data for constructing detailed 3-D model of UMass-Lowell Research Reactor (LEU Core + FNI + Beam Ports + Thermal Column -- **this is the Post-FNI Model**)													
	This model only represents a minor modification to the Pre-FNI model. In particular, the only difference is the zone description outside the core box next to Row A.													
	This is the FNI region , which replaces the three beam ports on this side of the model. Here we only model the first three rows of the FNI (about 9 inches) since nothing													
	beyond this point has any affect on the core physics. Thus, only additional water reflector is modeled outside this core-excore buffer region.													
	Note that the x, y, and z region boundaries for the Post-FNI model are **exactly the same** as the Pre-FNI model and all the incore and excore zone descriptions are also the same													
	except for the excore regions above Row A.													
	Thus, this model is actually very similar to the Pre-FNI model…													
		Axial Zone Model by radial zone within the assembly								actual zone numbers by radial zone within assembly					
		inside/center	outside/edge	sides	left	right	top/bot			inside/center	outside/edge	sides	left	right	top/bot
Row A	radial assy type	1	2	3	4	5	6	zones needed	zones so far	1	2	3	4	5	6
1	1	1						1	1	1					
2	2b	1	1					2	3	2	3				
3	2b	1	1					2	5	4	5				
4	2b	1	1					2	7	6	7				
5	2b	1	1					2	9	8	9				
6	2b	1	1					2	11	10	11				
7	2b	1	1					2	13	12	13				
8	2b	1	1					2	15	14	15				
9	1	1						1	16	16					
						future flexibility		14	30	**zones 17 - 30 not used in current model (future capability for Row A)**					
Row B	radial assy type	1	2	3	4	5	6	zones needed	zones so far	1	2	3	4	5	6
1	2a	6	2					8	38	31 - 36	37 - 38				
2	3	6	6	2				14	52	39 - 44	45 - 50	51 - 52			
3	3	6	6	2				14	66	53 - 58	59 - 64	65 - 66			
4	3	6	6	2				14	80	67 - 72	73 - 78	79 - 80			
5	3	6	6	2				14	94	81 - 86	87 - 92	93 - 94			
6	3	6	6	2				14	108	95 - 100	101 - 106	107 - 108			
7	3	6	6	2				14	122	109 - 114	115 - 120	121 - 122			
8	3	6	6	2				14	136	123 - 128	129 - 134	135 - 136			
9	1	1						1	137	137					
Row C	radial assy type	1	2	3	4	5	6	zones needed	zones so far	1	2	3	4	5	6
1	2a	6	2					8	145	138 - 143	144 - 145				
2	3	6	6	2				14	159	146 - 151	152 - 157	158 - 159			
3	3	6	6	2				14	173	160 - 165	166 - 171	172 - 173			
4	3	6	6	2				14	187	174 - 179	180 - 185	186 - 187			
5	3	6	6	2				14	201	188 - 193	194 - 199	200 - 201			
6	3	6	6	2				14	215	202 - 207	208 - 213	214 - 215			
7	3	6	6	2				14	229	216 - 221	222 - 227	228 - 229			
8	3	6	6	2				14	243	230 - 235	236 - 241	242 - 243			
9	1	1						1	244	244					
Row D	radial assy type	1	2	3	4	5	6	zones needed	zones so far	1	2	3	4	5	6
1	2a	6	2					8	252	245 - 250	251 - 252				
2	3	6	6	2				14	266	253 - 258	259 - 264	265 - 266			
3	3	6	6	2				14	280	267 - 272	273 - 278	279 - 280			
4	3	6	6	2				14	294	281 - 286	287 - 292	293 - 294			
5	3	6	6	2				14	308	295 - 300	301 - 306	307 - 308			
6	3	6	6	2				14	322	309 - 314	315 - 320	321 - 322			
7	3	6	6	2				14	336	323 - 328	329 - 334	335 - 336			
8	3	6	6	2				14	350	337 - 342	343 - 348	349 - 350			
9	6	15	1	1	15	15	15	62	412	351 - 365	366	367	368 - 382	383 - 397	398 - 412

Row E	radial assy type	1	2	3	4	5	6	zones needed	zones so far	1	2	3	4	5	6
1	2a	6	2					8	420	413 - 418	419 - 420				
2	3	6	6	2				14	434	421 - 426	427 - 432	433 - 434			
3	3	6	6	2				14	448	435 - 440	441 - 446	447 - 448			
4	3	6	6	2				14	462	449 - 454	455 - 460	461 - 462			
5	3	6	6	2				14	476	463 - 468	469 - 474	475 - 476			
6	3	6	6	2				14	490	477 - 482	483 - 488	489 - 490			
7	3	6	6	2				14	504	491 - 496	497 - 502	503 - 504			
8	3	6	6	2				14	518	505 - 510	511 - 516	517 - 518			
9	1	1						1	519	519					
Row F	radial assy type	1	2	3	4	5	6	zones needed	zones so far	1	2	3	4	5	6
1	2a	6	2					8	527	520 - 525	526 - 527				
2	3	6	6	2				14	541	528 - 533	534 - 539	540 - 541			
3	3	6	6	2				14	555	542 - 547	548 - 553	554 - 555			
4	3	6	6	2				14	569	556 - 561	562 - 567	568 - 569			
5	3	6	6	2				14	583	570 - 575	576 - 581	582 - 583			
6	3	6	6	2				14	597	584 - 589	590 - 595	596 - 597			
7	3	6	6	2				14	611	598 - 603	604 - 609	610 - 611			
8	3	6	6	2				14	625	612 - 617	618 - 623	624 - 625			
9	1	1						1	626	626					
Row G	radial assy type	1	2	3	4	5	6	zones needed	zones so far	1	2	3	4	5	6
1	1	1						1	627	627					
2	1	1						1	628	628					
3	1	1						1	629	629					
4	1	1						1	630	630					
5	1	1						1	631	631					
6	1	1						1	632	632					
7	1	1						1	633	633					
8	1	1						1	634	634					
9	1	1						1	635	635					
						future flexibility		15	650	**zones 636 - 650 not used in current model (future capability for Row G)**					

Misc Edit Zones	Zone #	Control Zones	Zone #	Radial Structure/Ref Zones	Zone #	Axial Reflector Zones	Zone #
FNI #1	651	Blade #1	661 - 675	Core Box + H2O	741	Top Axial Refl (inside)	751
FNI #2	652	Blade #2	676 - 690	Core Box + Gap + Pb Liner	742	Top Axial Refl (outside)	752
FNI #3	653	Blade #3	691 - 705	Pb Shield	743	Top Axial Refl (homo)	753
BeamPort bot #1	654	Blade #4	706 - 720	Pb Liner + Gap	744	Bot Axial Refl (inside)	754
BeamPort bot # 2	655	Cntrl Ends (Al + H2O)	721	Thm Column Liner	745	Bot Axial Refl (outside)	755
BeamPort bot #3	656	Cntrl Center (Al + H2O)	722	Thm Column Graphite	746	Bot Axial Refl (homo)	756
		Cntrl Shroud (Al + H2O)	723	BP End Plate	747		
Thm Col #1	657			BP Tube	748	Top Axial Refl (D9-1)	757 - 760
Thm Col #2	658	**unused zones (future capability)**	724 - 740	BP Inside (low density water)	749	Top Axial Refl (D9-2)	761 - 764
				Water Refl	750		
Rabbit #1	659	FNI Pb Shield Blocks	Zone #			**unused zones (future capability)**	765 - 770
Rabbit #2	660	Shield Sides (layers 4-16)	771	FNI Pb-Void Assy	Zone #		
		Shield Center (layers 4-16)	772	no new zones here			
		Shield Top (layer 3))	773	use same incore zone layout as pre-FNI cores			
		Shield Bottom #1 (layer 17)	774				
		Shield Bottom #2 (layer 18)	775				

Table II.2 Zone by region map for Level 11 for the post-FNI VENTURE model.

Data for constructing detailed 3-D model of UMass-Lowell Research Reactor
Reference Post-FNI LEU Model (July 2011)

Reference zone map by region for axial LAYER #11

This is axial LAYER #11

column	1	2	3	4	5	6	7	8	9	10	11	12	13	14	15	16	17	18	19	20	21	22	23	24	25	26	27	28	29	30	31	32	33	34	35	36	37	38	39	40	41	42	43	44	45	46	47	48	49	50	51	52	53	54	55	56	57	58	59	60	61	62	63	64	65	66	67	68	69
row																																																																					
1	750	750	750	750	750	750	750	750	750	750	750	750	750	750	750	750	750	750	750	750	750	750	750	750	750	750	750	750	750	750	750	750	750	750	750	750	750	750	750	750	750	750	750	750	750	750	750	750	750	750	750	750	750	750	750	750	750	750	750	750	750	750	750	750	750	750	750	750	750
2	750	750	750	750	750	750	750	750	750	750	750	750	750	750	750	750	750	750	750	750	750	750	750	750	750	750	750	750	750	750	750	750	750	750	750	750	750	750	750	750	750	750	750	750	750	750	750	750	750	750	750	750	750	750	750	750	750	750	750	750	750	750	750	750	750	750	750	750	750
3	750	750	750	750	750	750	750	750	750	750	750	750	750	750	750	750	750	750	750	750	750	750	750	750	750	750	750	750	750	750	750	750	750	750	750	750	750	750	750	750	750	750	750	750	750	750	750	750	750	750	750	750	750	750	750	750	750	750	750	750	750	750	750	750	750	750	750	750	750
4	750	750	750	750	750	750	750	750	750	750	750	750	750	750	750	750	750	750	750	750	750	750	750	750	750	750	750	750	750	750	750	750	750	750	750	750	750	750	750	750	750	750	750	750	750	750	750	750	750	750	750	750	750	750	750	750	750	750	750	750	750	750	750	750	750	750	750	750	750
5	750	750	750	750	750	750	750	750	750	750	750	750	750	750	750	750	750	750	750	750	750	750	750	750	750	750	750	750	750	750	750	750	750	750	750	750	750	750	750	750	750	750	750	750	750	750	750	750	750	750	750	750	750	750	750	750	750	750	750	750	750	750	750	750	750	750	750	750	750
6	750	750	750	750	750	750	750	750	750	750	750	750	750	750	750	750	750	750	750	750	750	750	750	750	750	750	750	750	750	750	750	750	750	750	750	750	750	750	750	750	750	750	750	750	750	750	750	750	750	750	750	750	750	750	750	750	750	750	750	750	750	750	750	750	750	750	750	750	750
7	750	750	750	750	750	750	750	750	750	750	750	750	750	750	750	750	750	750	750	750	750	750	750	750	750	750	750	750	750	750	750	750	750	750	750	750	750	750	750	750	750	750	750	750	750	750	750	750	750	750	750	750	750	750	750	750	750	750	750	750	750	750	750	750	750	750	750	750	750
8	750	750	750	750	750	750	750	750	750	750	750	750	750	750	750	750	750	750	750	750	750	750	750	750	750	750	750	750	750	750	750	750	750	750	750	750	750	750	750	750	750	750	750	750	750	750	750	750	750	750	750	750	750	750	750	750	750	750	750	750	750	750	750	750	750	750	750	750	750
9	750	750	750	750	750	750	750	750	750	750	750	750	750	750	750	750	750	750	750	750	750	750	750	750	750	750	750	750	750	750	750	750	750	750	750	750	750	750	750	750	750	750	750	750	750	750	750	750	750	750	750	750	750	750	750	750	750	750	750	750	750	750	750	750	750	750	750	750	750
10	750	750	750	750	750	750	750	750	750	750	750	750	750	750	750	750	750	750	750	750	750	750	750	750	750	750	750	750	750	750	750	750	750	750	750	750	750	750	750	750	750	750	750	750	750	750	750	750	750	750	750	750	750	750	750	750	750	750	750	750	750	750	750	750	750	750	750	750	750
11	750	750	750	750	750	750	750	750	750	750	750	750	750	750	750	750	750	750	750	750	750	750	750	750	750	750	750	750	750	750	750	750	750	750	750	750	750	750	750	750	750	750	750	750	750	750	750	750	750	750	750	750	750	750	750	750	750	750	750	750	750	750	750	750	750	750	750	750	750
12	750	750	750	750	750	750	750	750	750	750	750	750	750	750	750	750	750	750	750	750	750	750	750	750	750	750	750	750	750	750	750	750	750	750	750	750	750	750	750	750	750	750	750	750	750	750	750	750	750	750	750	750	750	750	750	750	750	750	750	750	750	750	750	750	750	750	750	750	750
13	750	750	750	750	750	750	750	750	750	750	750	750	750	771	771	771	771	771	771	771	771	771	771	771	771	771	771	771	771	771	771	771	771	771	771	771	771	771	771	771	771	771	771	771	771	771	771	771	771	771	771	771	771	771	750	750	750	750	750	750	750	750	750	750	750	750	750	750	750
14	750	750	750	750	750	750	750	750	750	750	750	750	750	772	772	772	772	772	772	772	772	772	772	772	772	772	772	772	772	772	772	772	772	772	772	772	772	772	772	772	772	772	772	772	772	772	772	772	772	772	772	772	772	772	750	750	750	750	750	750	750	750	750	750	750	750	750	750	750
15	750	750	750	750	750	750	750	750	750	750	750	750	750	772	772	772	772	772	772	772	772	772	772	772	772	772	772	772	772	772	772	772	772	772	772	772	772	772	772	772	772	772	772	772	772	772	772	772	772	772	772	772	772	772	750	750	750	750	750	750	750	750	750	750	750	750	750	750	750
16	750	750	750	750	750	750	750	750	750	750	750	750	750	771	771	771	771	771	771	771	771	771	771	771	771	771	771	771	771	771	771	771	771	771	771	771	771	771	771	771	771	771	771	771	771	771	771	771	771	771	771	771	771	771	750	750	750	750	750	750	750	750	750	750	750	750	750	750	750
17	750	750	750	750	750	750	750	750	750	750	750	750	750	771	771	771	771	771	771	771	771	771	771	771	771	771	771	771	771	771	771	771	771	771	771	771	771	771	771	771	771	771	771	771	771	771	771	771	771	771	771	771	771	771	750	750	750	750	750	750	750	750	750	750	750	750	750	750	750
18	750	750	750	750	750	750	750	750	750	750	750	750	750	772	772	772	772	772	772	772	772	772	772	772	772	772	772	772	772	772	772	772	772	772	772	772	772	772	772	772	772	772	772	772	772	772	772	772	772	772	772	772	772	772	750	750	750	750	750	750	750	750	750	750	750	750	750	750	750
19	750	750	750	750	750	750	750	750	750	750	750	750	750	772	772	772	772	772	772	772	772	772	772	772	772	772	772	772	772	772	772	772	772	772	772	772	772	772	772	772	772	772	772	772	772	772	772	772	772	772	772	772	772	772	750	750	750	750	750	750	750	750	750	750	750	750	750	750	750
20	750	750	750	750	750	750	750	750	750	750	750	750	750	771	771	771	771	771	771	771	771	771	771	771	771	771	771	771	771	771	771	771	771	771	771	771	771	771	771	771	771	771	771	771	771	771	771	771	771	771	771	771	771	771	750	750	750	750	745	745	745	745	745	745	745	745	745	745	745
21	750	750	750	750	750	750	750	750	750	750	750	750	750	771	771	771	771	771	771	771	771	771	771	771	771	771	771	771	771	771	771	771	771	771	771	771	771	771	771	771	771	771	771	771	771	771	771	771	771	771	771	771	771	771	750	750	750	750	745	745	745	745	745	745	745	745	745	745	745
22	750	750	750	750	750	750	750	750	750	750	750	750	750	772	772	772	772	651	651	651	651	772	772	772	772	772	772	772	772	652	652	652	652	652	772	772	772	772	772	772	772	772	653	653	653	653	772	772	772	772	772	772	772	772	750	750	750	750	745	746	746	746	746	746	746	746	746	746	746
23	750	750	750	750	750	750	750	750	750	750	750	750	750	772	772	772	772	651	651	651	651	772	772	772	772	772	772	772	772	652	652	652	652	652	772	772	772	772	772	772	772	772	653	653	653	653	772	772	772	772	772	772	772	772	750	750	750	750	745	746	746	746	746	746	746	746	746	746	746
24	750	750	750	750	750	750	750	750	750	750	750	750	750	771	771	771	771	771	771	771	771	771	771	771	771	771	771	771	771	771	771	771	771	771	771	771	771	771	771	771	771	771	771	771	771	771	771	771	771	771	771	771	771	771	750	750	750	750	745	746	746	746	746	746	746	746	746	746	746
25	750	750	750	750	750	750	750	750	750	750	750	750	741	741	741	741	741	741	741	741	741	741	741	741	741	741	741	741	741	741	741	741	741	741	741	741	741	741	741	741	741	741	741	741	741	741	741	741	741	741	741	741	741	741	742	741	741	744	745	746	746	746	746	746	746	746	746	746	746
26	750	750	750	750	750	750	750	750	750	750	750	750	741	1	1	1	1	3	3	3	3	5	5	5	5	7	7	7	7	9	9	9	9	9	11	11	11	11	13	13	13	13	15	15	15	15	16	16	16	16	16	16	16	16	742	743	743	744	745	746	746	746	746	746	746	746	746	746	746
27	750	750	750	750	750	750	750	750	750	750	750	750	741	1	1	1	1	2	2	2	2	4	4	4	4	6	6	6	6	8	8	8	8	8	10	10	10	10	12	12	12	12	14	14	14	14	16	16	16	16	16	16	16	16	742	743	743	744	745	746	746	746	746	746	746	746	746	746	746
28	750	750	750	750	750	750	750	750	750	750	750	750	741	1	1	1	1	3	3	3	3	5	5	5	5	7	7	7	7	9	9	9	9	9	11	11	11	11	13	13	13	13	15	15	15	15	16	16	16	16	16	16	16	16	742	743	743	744	745	746	746	746	746	746	746	746	746	746	746
29	750	750	750	750	750	750	750	750	750	750	750	750	741	38	38	38	38	52	52	52	52	66	66	66	66	80	80	80	80	94	94	94	94	94	108	108	108	108	122	122	122	122	136	136	136	136	137	137	137	137	137	137	137	137	742	743	743	744	745	746	746	746	746	746	746	746	746	746	746
30	750	750	750	750	750	750	750	750	750	750	750	750	741	38	34	34	38	48	42	42	48	62	56	56	62	76	70	70	76	90	84	84	84	90	104	98	98	104	118	112	112	118	132	126	126	132	137	137	137	137	137	137	137	137	742	743	743	744	745	746	746	746	746	746	746	746	746	746	746
31	750	750	750	750	750	750	750	750	750	750	750	750	741	38	38	38	38	52	52	52	52	66	66	66	66	80	80	80	80	94	94	94	94	94	108	108	108	108	122	122	122	122	136	136	136	136	137	137	137	137	137	137	137	137	742	743	743	744	745	746	746	746	746	746	746	746	746	746	746
32	750	750	750	750	750	750	750	750	750	750	750	750	741	721	721	721	723	723	723	723	723	723	723	723	723	723	723	723	723	723	723	722	723	723	723	723	723	723	723	723	723	723	723	723	723	723	723	721	721	721	721	721	721	721	742	743	743	744	745	746	746	746	746	746	746	746	746	746	746
33	750	750	750	750	750	750	750	750	750	750	750	750	741	721	721	721	684	684	684	684	684	684	684	684	684	684	684	684	684	684	684	722	699	699	699	699	699	699	699	699	699	699	699	699	699	699	699	721	721	721	721	721	721	721	742	743	743	744	745	746	746	746	746	746	746	746	746	746	746
34	750	750	750	750	750	750	750	750	750	750	750	750	741	721	721	721	723	723	723	723	723	723	723	723	723	723	723	723	723	723	723	722	723	723	723	723	723	723	723	723	723	723	723	723	723	723	723	721	721	721	721	721	721	721	742	743	743	744	745	746	746	746	746	746	746	746	746	746	746
35	750	750	750	750	750	750	750	750	750	750	750	750	741	145	145	145	145	159	159	159	159	173	173	173	173	187	187	187	187	201	201	201	201	201	215	215	215	215	229	229	229	229	243	243	243	243	244	244	244	244	244	244	244	244	742	743	743	744	745	746	746	746	746	746	746	746	746	746	746
36	750	750	750	750	750	750	750	750	750	750	750	750	741	145	141	141	145	155	149	149	155	169	163	163	169	183	177	177	183	197	191	191	191	197	211	205	205	211	225	219	219	225	239	233	233	239	244	244	244	244	244	244	244	244	742	743	743	744	745	746	746	746	746	746	746	746	746	746	746
37	750	750	750	750	750	750	750	750	750	750	750	750	741	145	145	145	145	159	159	159	159	173	173	173	173	187	187	187	187	201	201	201	201	201	215	215	215	215	229	229	229	229	243	243	243	243	244	244	244	244	244	244	244	244	742	743	743	744	745	746	746	746	746	746	746	746	746	746	746
38	750	750	750	750	750	750	750	750	750	750	750	750	741	252	252	252	252	266	266	266	266	280	280	280	280	294	294	294	294	308	308	308	308	308	322	322	322	322	336	336	336	336	350	350	350	350	367	367	367	367	367	367	367	367	742	743	743	744	745	746	746	746	746	746	746	746	746	746	746
39	750	750	750	750	750	750	750	750	750	750	750	750	741	252	248	248	252	262	256	256	262	276	270	270	276	290	284	284	290	304	298	298	298	304	318	312	312	318	332	326	326	332	346	340	340	346	367	367	367	367	367	367	367	367	742	743	743	744	745	746	657	746	746	658	746	746	746	746	746
40	750	750	750	750	750	750	750	750	750	750	750	750	741	252	248	248	252	262	256	256	262	276	270	270	276	290	284	284	290	304	298	298	298	304	318	312	312	318	332	326	326	332	346	340	340	346	366	366	406	406	406	391	366	366	742	743	743	744	745	746	657	746	746	658	746	746	746	746	746
41	750	750	750	750	750	750	750	750	750	750	750	750	741	252	248	248	252	262	256	256	262	276	270	270	276	290	284	284	290	304	298	298	298	304	318	312	312	318	332	326	326	332	346	340	340	346	366	366	376	359	359	391	366	366	742	743	743	744	745	746	657	746	746	658	746	746	746	746	746
42	750	750	750	750	750	750	750	750	750	750	750	750	741	252	248	248	252	262	256	256	262	276	270	270	276	290	284	284	290	304	298	298	298	304	318	312	312	318	332	326	326	332	346	340	340	346	366	366	376	406	406	406	366	366	742	743	743	744	745	746	657	746	746	658	746	746	746	746	746
43	750	750	750	750	750	750	750	750	750	750	750	750	741	252	248	248	252	262	256	256	262	276	270	270	276	290	284	284	290	304	298	298	298	304	318	312	312	318	332	326	326	332	346	340	340	346	367	367	367	367	367	367	367	367	742	743	743	744	745	746	657	746	746	658	746	746	746	746	746
44	750	750	750	750	750	750	750	750	750	750	750	750	741	252	252	252	252	266	266	266	266	280	280	280	280	294	294	294	294	308	308	308	308	308	322	322	322	322	336	336	336	336	350	350	350	350	367	367	367	367	367	367	367	367	742	743	743	744	745	746	746	746	746	746	746	746	746	746	746
45	750	750	750	750	750	750	750	750	750	750	750	750	741	420	420	420	420	434	434	434	434	448	448	448	448	462	462	462	462	476	476	476	476	476	490	490	490	490	504	504	504	504	518	518	518	518	519	519	519	519	519	519	519	519	742	743	743	744	745	746	746	746	746	746	746	746	746	746	746
46	750	750	750	750	750	750	750	750	750	750	750	750	741	420	416	416	420	430	424	424	430	444	438	438	444	458	452	452	458	472	466	466	466	472	486	480	480	486	500	494	494	500	514	508	508	514	519	519	519	519	519	519	519	519	742	743	743	744	745	746	746	746	746	746	746	746	746	746	746
47	750	750	750	750	750	750	750	750	750	750	750	750	741	420	420	420	420	434	434	434	434	448	448	448	448	462	462	462	462	476	476	476	476	476	490	490	490	490	504	504	504	504	518	518	518	518	519	519	519	519	519	519	519	519	742	743	743	744	745	746	746	746	746	746	746	746	746	746	746
48	750	750	750	750	750	750	750	750	750	750	750	750	741	721	721	721	723	723	723	723	723	723	723	723	723	723	723	723	723	723	723	722	723	723	723	723	723	723	723	723	723	723	723	723	723	723	723	721	721	721	721	721	721	721	742	743	743	744	745	746	746	746	746	746	746	746	746	746	746
49	750	750	750	750	750	750	750	750	750	750	750	750	741	721	721	721	669	669	669	669	669	669	669	669	669	669	669	669	669	669	669	722	714	714	714	714	714	714	714	714	714	714	714	714	714	714	714	721	721	721	721	721	721	721	742	743	743	744	745	746	746	746	746	746	746	746	746	746	746
50	750	750	750	750	750	750	750	750	750	750	750	750	741	721	721	721	723	723	723	723	723	723	723	723	723	723	723	723	723	723	723	722	723	723	723	723	723	723	723	723	723	723	723	723	723	723	723	721	721	721	721	721	721	721	742	743	743	744	745	746	746	746	746	746	746	746	746	746	746
51	750	750	750	750	750	750	750	750	750	750	750	750	741	527	527	527	527	541	541	541	541	555	555	555	555	569	569	569	569	583	583	583	583	583	597	597	597	597	611	611	611	611	625	625	625	625	626	626	626	626	626	626	626	626	742	743	743	744	745	746	746	746	746	746	746	746	746	746	746
52	750	750	750	750	750	750	750	750	750	750	750	750	741	527	523	523	527	537	531	531	537	551	545	545	551	565	559	559	565	579	573	573	573	579	593	587	587	593	607	601	601	607	621	615	615	621	626	626	626	626	626	626	626	626	742	743	743	744	745	746	746	746	746	746	746	746	746	746	746
53	750	750	750	750	750	750	750	750	750	750	750	750	741	527	527	527	527	541	541	541	541	555	555	555	555	569	569	569	569	583	583	583	583	583	597	597	597	597	611	611	611	611	625	625	625	625	626	626	626	626	626	626	626	626	742	743	743	744	745	746	746	746	746	746	746	746	746	746	746
54	750	750	750	750	750	750	750	750	750	750	750	750	741	627	627	627	627	628	628	628	628	629	629	629	629	630	630	630	630	631	631	631	631	631	632	632	632	632	633	633	633	633	634	634	634	634	635	635	635	635	635	635	635	635	742	743	743	744	745	746	746	746	746	746	746	746	746	746	746
55	750	750	750	750	750	750	750	750	750	750	750	750	741	741	741	741	741	741	741	741	741	741	741	741	741	741	741	741	741	741	741	741	741	741	741	741	741	741	741	741	741	741	741	741	741	741	741	741	741	741	741	741	741	741	742	741	741	744	745	746	746	746	746	746	746	746	746	746	746
56	750	750	750	750	750	750	750	750	750	750	750	750	747	747	747	747	747	747	747	747	747	747	747	747	747	747	747	747	747	747	747	747	747	747	747	747	747	747	747	747	747	747	747	747	747	747	747	747	747	747	747	747	747	747	747	750	750	750	745	746	746	746	746	746	746	746	746	746	746
57	750	750	750	750	750	750	750	750	750	750	750	750	750	750	750	749	749	654	654	654	654	749	749	749	750	748	749	749	749	655	655	655	655	655	749	749	749	748	750	749	749	749	656	656	656	656	749	749	749	749	750	750	750	750	750	750	750	750	745	746	746	746	746	746	746	746	746	746	746
58	750	750	750	750	750	750	750	750	750	750	750	750	750	750	750	749	749	654	654	654	654	749	749	749	750	748	749	749	749	655	655	655	655	655	749	749	749	748	750	749	749	749	656	656	656	656	749	749	749	749	750	750	750	750	750	750	750	750	745	746	746	746	746	746	746	746	746	746	746
59	750	750	750	750	750	750	750	750	750	750	750	750	750	750	749	749	749	749	749	749	749	749	749	750	750	748	749	749	749	749	749	749	749	749	749	749	749	748	750	750	749	749	749	749	749	749	749	749	749	749	749	749	749	750	750	750	750	750	745	745	745	745	745	745	745	745	745	745	745
60	750	750	750	750	750	750	750	750	750	750	750	750	750	750	749	749	749	749	749	749	749	749	749	750	750	748	749	749	749	749	749	749	749	749	749	749	749	748	750	750	749	749	749	749	749	749	749	749	749	749	749	749	749	750	750	750	750	750	750	750	750	750	750	750	750	750	750	750	750
61	750	750	750	750	750	750	750	750	750	750	750	750	749	749	749	749	749	749	749	749	749	749	750	750	750	748	749	749	749	749	749	749	749	749	749	749	749	748	750	750	750	749	749	749	749	749	749	749	749	749	749	749	749	749	749	750	750	750	750	750	750	750	750	750	750	750	750	750	750
62	750	750	750	750	750	750	750	750	750	750	750	749	749	749	749	749	749	749	749	749	750	750	750	750	750	748	749	749	749	749	749	749	749	749	749	749	749	748	750	750	750	750	750	749	749	749	749	749	749	749	749	749	749	749	749	750	750	750	750	750	750	750	750	750	750	750	750	750	750
63	750	750	750	750	750	750	750	750	750	750	749	749	749	749	749	749	749	749	749	750	750	750	750	750	750	748	749	749	749	749	749	749	749	749	749	749	749	748	750	750	750	750	750	750	749	749	749	749	749	749	749	749	749	749	749	749	750	750	750	750	750	750	750	750	750	750	750	750	750
64	750	750	750	750	750	750	750	750	750	750	749	749	749	749	749	749	749	749	750	750	750	750	750	750	750	748	749	749	749	749	749	749	749	749	749	749	749	748	750	750	750	750	750	750	749	749	749	749	749	749	749	749	749	749	749	749	750	750	750	750	750	750	750	750	750	750	750	750	750
65	750	750	750	750	750	750	750	750	750	749	749	749	749	749	749	749	749	750	750	750	750	750	750	750	750	748	749	749	749	749	749	749	749	749	749	749	749	748	750	750	750	750	750	750	750	750	749	749	749	749	749	749	749	749	749	749	749	749	750	750	750	750	750	750	750	750	750	750	750
66	750	750	750	750	750	750	750	750	750	749	749	749	749	749	749	749	750	750	750	750	750	750	750	750	750	748	749	749	749	749	749	749	749	749	749	749	749	748	750	750	750	750	750	750	750	750	750	749	749	749	749	749	749	749	749	749	749	749	749	750	750	750	750	750	750	750	750	750	750
67	750	750	750	750	750	750	750	750	749	749	749	749	749	749	749	750	750	750	750	750	750	750	750	750	750	748	749	749	749	749	749	749	749	749	749	749	749	748	750	750	750	750	750	750	750	750	750	750	750	750	749	749	749	749	749	749	749	749	749	749	750	750	750	750	750	750	750	750	750
68	750	750	750	750	750	750	750	750	749	749	749	749	749	749	750	750	750	750	750	750	750	750	750	750	750	748	749	749	749	749	749	749	749	749	749	749	749	748	750	750	750	750	750	750	750	750	750	750	750	750	750	750	750	749	749	749	749	749	749	749	750	750	750	750	750	750	750	750	750
69	750	750	750	750	750	750	750	749	749	749	749	749	750	750	750	750	750	750	750	750	750	750	750	750	750	748	749	749	749	749	749	749	749	749	749	749	749	748	750	750	750	750	750	750	750	750	750	750	750	750	750	750	750	750	750	749	749	749	749	749	749	750	750	750	750	750	750	750	750
70	750	750	750	750	750	750	749	749	749	749	749	750	750	750	750	750	750	750	750	750	750	750	750	750	750	748	749	749	749	749	749	749	749	749	749	749	749	748	750	750	750	750	750	750	750	750	750	750	750	750	750	750	750	750	750	750	749	749	749	749	749	749	750	750	750	750	750	750	750
71	750	750	750	750	750	750	749	749	749	749	749	750	750	750	750	750	750	750	750	750	750	750	750	750	750	748	749	749	749	749	749	749	749	749	749	749	749	748	750	750	750	750	750	750	750	750	750	750	750	750	750	750	750	750	750	750	749	749	749	749	749	749	750	750	750	750	750	750	750
72	750	750	750	750	750	749	749	749	749	749	750	750	750	750	750	750	750	750	750	750	750	750	750	750	750	748	749	749	749	749	749	749	749	749	749	749	749	748	750	750	750	750	750	750	750	750	750	750	750	750	750	750	750	750	750	750	750	749	749	749	749	749	749	750	750	750	750	750	750
73	750	750	750	750	750	749	749	749	749	749	750	750	750	750	750	750	750	750	750	750	750	750	750	750	750	748	749	749	749	749	749	749	749	749	749	749	749	748	750	750	750	750	750	750	750	750	750	750	750	750	750	750	750	750	750	750	750	749	749	749	749	749	749	750	750	750	750	750	750
74	750	750	750	750	749	749	749	749	749	750	750	750	750	750	750	750	750	750	750	750	750	750	750	750	750	748	749	749	749	749	749	749	749	749	749	749	749	748	750	750	750	750	750	750	750	750	750	750	750	750	750	750	750	750	750	750	750	750	749	749	749	749	749	749	750	750	750	750	750
75	750	750	750	750	749	749	749	749	749	750	750	750	750	750	750	750	750	750	750	750	750	750	750	750	750	748	749	749	749	749	749	749	749	749	749	749	749	748	750	750	750	750	750	750	750	750	750	750	750	750	750	750	750	750	750	750	750	750	749	749	749	749	749	749	750	750	750	750	750

Appendix III -- Material Composition Data for the M-1-3 and M-2-5 Configurations (2011 version)

This appendix documents the development of the 40 homogeneous material compositions used within the 2-D and 3-D VENTURE models of the UMLRR. The actual nuclide densities used are summarized in Table III.1 and III.2 for the fuel and non-fuel regions, respectively.

All the work associated with the development of the fuel materials for the UMLRR full fuel and partial assemblies and the WPI full fuel element (see Materials 11 – 19 in Table III.1) is documented in Ref. 8 and, for the non-fuel materials (see Materials 1 – 10 and 20 – 40 in Table III.2), a Matlab script file, called **umlrrden_nonfuel_2011.m**, contains sufficient internal comments along with the coding to fully describe each of the non-fuel compositions used within the models. Most of the non-fuel materials are simple combinations of aluminum structure and water to model a variety of regions -- such as the ¼ inch core box + ¼ inch of water gap surrounding the core, the 1-region and 2-region radiation baskets with and without a bayonet inserted, the control and regulating blade shroud regions, etc. -- as detailed in the **umlrrden_nonfuel_2011.m** file listed in Table III.3. There are several materials, however, that contain graphite, lead, and/or, of course, boron-10 within the control and Pb shield regions. The reader is simply referred to the Matlab code listing in Table III.3 for further details/explanation.

Table III.1 Fuel region material compositions for the 2-D and 3-D VENTURE models.

Materials 11 – 13: UMLRR LEU Full Fuel Assembly Densities (at/b-cm)

	CENTER	EDGE	SIDE
U235	2.0831e-004	0.0000e+000	0.0000e+000
U238	8.3571e-004	0.0000e+000	0.0000e+000
Al	1.5583e-002	1.5312e-002	4.1024e-002
Si	6.9601e-004	0.0000e+000	0.0000e+000
H	4.6798e-002	4.9868e-002	2.1343e-002
O	2.3399e-002	2.4934e-002	1.0671e-002

Materials 14 – 16: UMLRR LEU Partial Fuel Assembly Densities (at/b-cm)

	CENTER	EDGE	SIDE
U235	1.0415e-004	0.0000e+000	0.0000e+000
U238	4.1786e-004	0.0000e+000	0.0000e+000
Al	1.6832e-002	1.5312e-002	4.1024e-002
Si	3.4801e-004	0.0000e+000	0.0000e+000
H	4.6798e-002	4.9868e-002	2.1343e-002
O	2.3399e-002	2.4934e-002	1.0671e-002

Materials 17 – 19: WPI LEU Full Fuel Assembly Densities (at/b-cm)

	CENTER	EDGE	SIDE
U235	1.5461e-004	1.3095e-004	0.0000e+000
U238	6.2028e-004	5.2534e-004	0.0000e+000
Al	1.9183e-002	1.6246e-002	3.9837e-002
Si	0.0000e+000	0.0000e+000	0.0000e+000
H	4.2786e-002	4.6470e-002	2.2659e-002
O	2.1393e-002	2.3235e-002	1.1330e-002

Table III.2 Non-fuel material compositions used in the 2-D and 3-D VENTURE models.

Non-Fuel Material Compositions (atoms/b-cm) for the 2-D & 3-D UMLRR LEU VENTURE models (2011 version)

Material	Al	H	O	C	B10	Pb
# 1 water	0.000e+000	6.686e-002	3.343e-002	0.000e+000	0.000e+000	0.000e+000
# 2 core box + water (50/50)	3.013e-002	3.343e-002	1.671e-002	0.000e+000	0.000e+000	0.000e+000
# 3 homo radbasket	1.164e-002	5.394e-002	2.697e-002	0.000e+000	0.000e+000	0.000e+000
# 4 radbasket outside	2.863e-002	3.509e-002	1.755e-002	0.000e+000	0.000e+000	0.000e+000
# 5 radbasket inside H2O	3.727e-003	6.272e-002	3.136e-002	0.000e+000	0.000e+000	0.000e+000
# 6 radbasket inside AIR	6.694e-003	4.423e-002	2.211e-002	0.000e+000	0.000e+000	0.000e+000
# 7 homo graphite refl	2.999e-003	4.636e-003	2.318e-003	7.950e-002	0.000e+000	0.000e+000
# 8 flux trap outside	2.863e-002	1.459e-002	7.295e-003	2.768e-002	0.000e+000	0.000e+000
# 9 flux trap inside H2O	3.727e-003	2.874e-002	1.437e-002	4.587e-002	0.000e+000	0.000e+000
#10 flux trap inside AIR	6.694e-003	1.025e-002	5.124e-003	4.587e-002	0.000e+000	0.000e+000
Note: Materials 11 - 19 are for the UMLRR full and partial assemblies and for the WPI fuel element						
#20 control blade end	4.950e-002	1.194e-002	5.970e-003	0.000e+000	0.000e+000	0.000e+000
#21 control blade center	5.207e-002	9.092e-003	4.546e-003	0.000e+000	0.000e+000	0.000e+000
#22 control blade shroud	1.851e-002	4.632e-002	2.316e-002	0.000e+000	0.000e+000	0.000e+000
#23 control in (control)	4.550e-002	0.000e+000	0.000e+000	7.787e-003	5.087e-003	0.000e+000
#24 regblade shroud	3.375e-002	2.942e-002	1.471e-002	0.000e+000	0.000e+000	0.000e+000
#25 regblade in (center)	5.671e-003	6.057e-002	3.028e-002	0.000e+000	0.000e+000	0.000e+000
#26 pure aluminum	6.026e-002	0.000e+000	0.000e+000	0.000e+000	0.000e+000	0.000e+000
#27 regblade in (control)	4.596e-002	0.000e+000	0.000e+000	7.540e-003	4.925e-003	0.000e+000
#28 Pb shield clad (core side)	3.616e-002	2.674e-002	1.337e-002	0.000e+000	0.000e+000	0.000e+000
#29 pure lead shield	0.000e+000	0.000e+000	0.000e+000	0.000e+000	0.000e+000	3.296e-002
#30 Pb shield clad (thm col)	2.009e-002	4.457e-002	2.229e-002	0.000e+000	0.000e+000	0.000e+000
#31 reactor graphite	0.000e+000	0.000e+000	0.000e+000	9.025e-002	0.000e+000	0.000e+000
#32 inside beam tube (5% H2O)	0.000e+000	3.343e-003	1.671e-003	0.000e+000	0.000e+000	0.000e+000
#33 top/bot nonfuel refl	6.722e-004	6.611e-002	3.306e-002	0.000e+000	0.000e+000	0.000e+000
#34 homo top refl	9.573e-003	5.624e-002	2.812e-002	0.000e+000	0.000e+000	0.000e+000
#35 homo bottom refl	1.915e-002	4.561e-002	2.281e-002	0.000e+000	0.000e+000	0.000e+000
#36 Pb void assy (sides)	1.503e-002	4.313e-003	2.157e-003	0.000e+000	0.000e+000	2.261e-002
#37 Pb void assy (center-void)	1.266e-002	1.311e-003	6.555e-004	0.000e+000	0.000e+000	0.000e+000
#38 Pb void assy (center-H2O)	1.266e-002	5.281e-002	2.641e-002	0.000e+000	0.000e+000	0.000e+000
#39 homo Pb void assy (c-void)	1.317e-002	1.954e-003	9.768e-004	0.000e+000	0.000e+000	4.840e-003
#40 Pb shield side/B-Al liner	5.337e-002	7.481e-003	3.740e-003	0.000e+000	4.560e-004	0.000e+000

Table III.3 Listing of Matlab code umlrrden_nonfuel_2011.m.

```
%
%   UMLRRDEN_NONFUEL_2011.M  Create densities for all the regions within
%              the UMLRR excluding the fuel assemblies (umlrrden.m does the fuel)
%
%   In updating the 3-D VENTURE model (in June 2011) a new set of nonfuel densities
%   is needed.  Instead of doing this by hand as done previously, I have decided to
%   put the generation of these into a Matlab file for formal documentation and
%   quality control considerations.
%
%   Note that because of the change in the fuel edge dimension in the June 2011
%   version of the VENTURE model, some of the nonfuel homogeneous region densities
%   will also change (because of a change in the structure vs water volume
%   fractions).  Thus, we will do all the nonfuel density calculations here...
%
%   The atom densities (at/b-cm) are computed for six isotopes, as follows:
%       Al, H, O, C, B10, and Pb
%
%   File prepared by J. R. White, UMass-Lowell (July 2011)
%


%
%   getting started
      clear all,   close all
%
%   set some constants (isotope order ->  Al, H, O, C, B10/Bnat, and Pb
      Na = 0.60221;                        % Avogadro's number (x 10^+24) (at/g-mole)
      MW = [26.982 1.0079 15.999 12.011 10.811 207.21];  % Molecular Wt (g/g-mole)
      MWW = 2*MW(2)+MW(3);                               % Molecular Wt for water
      assyarea = 7.7724*7.7724;                          % area of each unit in grid
%
%   calc Al, water, graphite, etc. nominal densities first
      ald = 2.70;  alad = ald*Na/MW(1);    % Al atom density (at/b-cm)
      wd = 1.0;  wad = wd*Na/MWW;          % water molecular density (molecules/b-cm)
      gd = 1.8;  gad = gd*Na/MW(4);        % graphite atom density (at/b-cm)
      pbd = 11.34; pbad = pbd*Na/MW(6);    % Pb atom density (at/b-cm)
%
%   allocate space for the atom densities for 40 different materials
      ad = zeros(40,6);                    % material atom densities for six isotopes
      name = zeros(40,30);                 % material names (up to 30 characters)
%
%   matl #1 water --  pure water at nominal density
      ad(1,2) = 2*wad;  ad(1,3) = wad;
      name(1,:) = '# 1 water                     ';
%   matl #2 core box + water  --  this is a 50/50 mix of Al + H20 since the core box
%     is 0.25" thick and the whole region modeled is 0.5" thick (1.27 cm).
      vfal = 0.5;   vfw = 1-vfal;
      ad(2,1) = vfal*alad;  ad(2,2) = vfw*ad(1,2);  ad(2,3) = vfw*ad(1,3);
      name(2,:) = '# 2 core box + water (50/50)  ';
%   matl #3 homo radbasket  --  this is a 1-region homogeneous model of the radiation
%     basket with no bayonet inserted.  The radbasket consists of a cylindrical inner
%     Al tube and an outer Al square can.  If there is no bayonet inserted, then
%     everything that is not Al is simply filled with water.
%     dimensions:  outside can = 2.952" = 7.4981 cm
%                  inside can = 2.702" = 6.8631 cm
%                  outside radius of tube = 2"/2 = 2.54 cm
%                  inside radius of tube = 1.87"/2 = 2.3749 cm
      can = 7.4981^2 - 6.8631^2;   tube = pi*(2.54^2 - 2.3749^2);
      vfal = (can+tube)/assyarea;  vfw = 1-vfal;
      ad(3,1) = vfal*alad;  ad(3,2) = vfw*ad(1,2);  ad(3,3) = vfw*ad(1,3);
      name(3,:) = '# 3 homo radbasket            ';
%   matl #4 radbasket outside  --  this is part of a 2-region model of the radiation
%     basket.  The inside/outside regions are defined by the fuel assembly model.
%     The outer side region area is 2(0.8437x7.7724) cm^2 and the outer edge
%     region is 2(0.4995x6.085) cm^2 and the outer Al can of the basket is in this
%     region.
      can = 7.4981^2 - 6.8631^2;   tarea = 2*(0.8437*7.7724 + 0.4995*6.085);
      vfal = can/tarea;  vfw = 1-vfal;
      ad(4,1) = vfal*alad;  ad(4,2) = vfw*ad(1,2);  ad(4,3) = vfw*ad(1,3);
```

```
      name(4,:) = '# 4 radbasket outside         ';
%   matl #5 radbasket inside  --  this is part of a 2-region model of the radiation
%     basket with no bayonet inserted.  The inside/outside regions are defined by the
%     fuel assembly model.  The inside region dimension is 6.085x(7.7724-2*0.4995)
%     cm^2 and the inside circular Al can of the basket is in this region.
      tube = pi*(2.54^2 - 2.3749^2);   tarea = 6.085*(7.7724-2*0.4995);
      vfal = tube/tarea;  vfw = 1-vfal;
      ad(5,1) = vfal*alad;  ad(5,2) = vfw*ad(1,2);  ad(5,3) = vfw*ad(1,3);
      name(5,:) = '# 5 radbasket inside H2O      ';
%   matl #6 radbasket inside with empty bayonet --  this is similar to matl #5
%     except an air filled bayonet is assumed to be in the radbasket. The bayonet
%     dimensions are: inside radius = 1.36"/2 = 1.7272 cm
%                     outside radius = 1.5"/2 = 1.905 cm
      tube = pi*(2.54^2 - 2.3749^2);   air = pi*1.7272^2;
      bayonet = pi*1.905^2 - air;   tarea = 6.085*(7.7724-2*0.4995);
      vfal = (tube+bayonet)/tarea;  vfair = air/tarea;   vfw = 1-vfal-vfair;
      ad(6,1) = vfal*alad;  ad(6,2) = vfw*ad(1,2);  ad(6,3) = vfw*ad(1,3);
      name(6,:) = '# 6 radbasket inside AIR      ';
%   matl #7 homo graphite refl  --  this is a 1-region homogeneous model of the
%     graphite reflector element.  This element is simply an outer square Al can
%     filled with graphite.  Water is on the outside of the can.
%     dims:  outside can = 2.952" = 7.4981 cm
%            inside can = 2.872" = 7.2949 cm
      g = 7.2949^2;   can = 7.4981^2 - g;
      vfal = can/assyarea;  vfg = g/assyarea;   vfw = 1-vfal-vfg;
      ad(7,1) = vfal*alad;  ad(7,2) = vfw*ad(1,2);  ad(7,3) = vfw*ad(1,3);
      ad(7,4) = vfg*gad;
      name(7,:) = '# 7 homo graphite refl        ';
%   Note:  The flux trap is similar to a radiation basket except that the material
%          between the inner and out can is graphite instead of water.  Thus the
%          development of matls #8 - #10 is similar to matls #4 - #6
%   matl #8 flux trap outside  --  this is part of a 2-region model of the flux trap.
%     The inside/outside regions are defined by the fuel assembly model (same as
%     radbasket).  The dimensions are the same as for the radbasket but only the
%     region outside the can has water, with the rest being graphite.
      can = 7.4981^2 - 6.8631^2;   water = assyarea-7.4981^2;
      tarea = 2*(0.8437*7.7724 + 0.4995*6.085);
      vfal = can/tarea;  vfw = water/tarea;  vfg = 1-vfal-vfw;
      ad(8,1) = vfal*alad;  ad(8,2) = vfw*ad(1,2);  ad(8,3) = vfw*ad(1,3);
      ad(8,4) = vfg*gad;
      name(8,:) = '# 8 flux trap outside         ';
%   matl #9 flux trap inside  --  this is part of a 2-region model of the flux trap
%     basket with no bayonet inserted.  The inside/outside regions are defined by the
%     fuel assembly model (same as for radbasket).  The dimensions are the same as
%     for the radbasket but only the region inside the inner tube has water, with
%     the rest being graphite.
      tube = pi*(2.54^2 - 2.3749^2);   water = pi*2.3749^2;
      tarea = 6.085*(7.7724-2*0.4995);
      vfal = tube/tarea;  vfw = water/tarea;  vfg = 1-vfal-vfw;
      ad(9,1) = vfal*alad;  ad(9,2) = vfw*ad(1,2);  ad(9,3) = vfw*ad(1,3);
      ad(9,4) = vfg*gad;
      name(9,:) = '# 9 flux trap inside H2O      ';
%   matl #10 flux trap inside with empty bayonet --  this is similar to matl #9
%     except an air filled bayonet is assumed to be in the flux trap. The bayonet
%     dimensions are given above in the matl #6 description.
      tube = pi*(2.54^2 - 2.3749^2);   air = pi*1.7272^2;
      bayonet = pi*1.905^2 - air;   water = pi*(2.3749^2 - 1.905^2);
      tarea = 6.085*(7.7724-2*0.4995);
      vfal = (tube+bayonet)/tarea;  vfair = air/tarea;
      vfw = water/tarea;  vfg = 1-vfal-vfair-vfw;
      ad(10,1) = vfal*alad;  ad(10,2) = vfw*ad(1,2);  ad(10,3) = vfw*ad(1,3);
      ad(10,4) = vfg*gad;
      name(10,:) = '#10 flux trap inside AIR      ';
%   Note: Materials 11 - 19 are for the UMLRR full and partial assemblies and for
%         the WPI fuel element
%   Note: The control region is fairly complicated and it is composed of several
%         parts. Because of the fuel edge dimension, we cannot model things exactly,
%         since the blades extend 0.4995 cm into columns 1 and 9. However, things are
%         very close and we will made sure that the blade length is modeled
%         correctly. The regions of interest here will be blade ends, blade center,
%         blade shroud, and blade in (control).  See notebook UMLRR Physics Analysis
```

```
%         starting on pg 5 for summer 2011 for the key dimensions.  The MCNP modeling
%         notebook pg.40 (9/2/10) also has a good sketch with of the real system
%         with the proper dimensions (in inches).
%   matl #20 control end  --  this is a mix of Al + water.  There is a little water
%     outside the structure and a small water hole for the blade to actually move
%     inside this portion of the shroud.
      tarea = 2.8957*7.2729;   block = 2.5019*7.2729 - 0.4709*1.905;
      vfal = block/tarea;  vfw = 1-vfal;
      ad(20,1) = vfal*alad;  ad(20,2) = vfw*ad(1,2);  ad(20,3) = vfw*ad(1,3);
      name(20,:) = '#20 control blade end          ';
%   matl #21 control center  --  another mix of Al + water, but mostly Al except for
%     the water outside the structure.
      tarea = 2.8957*1.3038;   block = 2.5019*1.3038;
      vfal = block/tarea;  vfw = 1-vfal;
      ad(21,1) = vfal*alad;  ad(21,2) = vfw*ad(1,2);  ad(21,3) = vfw*ad(1,3);
      name(21,:) = '#21 control blade center       ';
%   matl #22 control shroud  --  this is also a mix of Al + water.
      tarea = 0.9716*27.051;   block = 0.29845*27.051;
      vfal = block/tarea;  vfw = 1-vfal;
      ad(22,1) = vfal*alad;  ad(22,2) = vfw*ad(1,2);  ad(22,3) = vfw*ad(1,3);
      name(22,:) = '#22 control blade shroud       ';
%   matl #23 control in (control) --  this is the actual boral control blade.  This
%     material includes the boral (B4C-Al) and the Al clad. The dimensions are
%       boral region: 0.255x10.53 sq inches = 0.6477x26.7462 sq cm
%       full blade with clad: 0.375x10.65 sq inches = 0.9525x27.051 sq cm
%     For the boral densities, refer to pg. 110 of Bob Freeman's thesis (with
%     corrections).  The calculations assume 2.64 g of boral/cc with 35 w/o B4C in
%     the B4C-Al mix.  Also, they assume 75 w/o B in B4C instead of 78 w/o due to
%     impurities.  Finally, natural boron contains roughly 19.6 a/o B10.
      B10 = (2.64*0.35*0.75*Na/MW(5))*0.196;
      C12 = 2.64*0.35*0.25*Na/MW(4);   Al = 2.64*0.65*Na/MW(1);
      tarea = 0.9525*27.051;  contrl = 0.6477*26.7462;  clad = tarea-contrl;
      vfal = clad/tarea;  vfc = 1-vfal;
      ad(23,1) = vfal*alad+vfc*Al;    ad(23,4) = vfc*C12;   ad(23,5) = vfc*B10;
      name(23,:) = '#23 control in (control)       ';
%   Note: The regblade region is also fairly complicated and it is composed of four
%         parts.  The regions of interest here will be regrod shroud, regrod in
%         center, regrod in structure, and regrod in control.  See notebook UMLRR
%         Physics Analysis starting on pg 6 for summer 2011 for the key dimensions.
%   matl #24 regblade shroud -- this is a mix of Al + water.  The total area includes
%     the assembly area minus the control region and the Al shroud is a 2.965" square
%     (outside dim) Al can with a thickness of 0.25".
      tarea = assyarea - (2.125*2.54)^2;   can = (2.965*2.54)^2 - (2.465*2.54)^2;
      vfal = can/tarea;  vfw = 1-vfal;
      ad(24,1) = vfal*alad;  ad(24,2) = vfw*ad(1,2);  ad(24,3) = vfw*ad(1,3);
      name(24,:) = '#24 regblade shroud            ';
%   matl #25 regblade in (center)  --  another mix of Al + water.  The total area
%     includes the area inside the regrod control region.  This is all water except
%     for a 0.5625" diameter Al rod which allows the reg blade to move vertically.
%     Note that there are a couple of Al blocks within this region for structural
%     support at two different axial locations, but these have been ignored here.
      tarea = (1.625*2.54)^2;   rod = (pi/4)*(0.5625*2.54)^2;
      vfal = rod/tarea;  vfw = 1-vfal;
      ad(25,1) = vfal*alad;  ad(25,2) = vfw*ad(1,2);  ad(25,3) = vfw*ad(1,3);
      name(25,:) = '#25 regblade in (center)       ';
%   matl #26 regblade in (structure)  --  pure Al structure.  In the high worth
%     arrangement, this is the piece located away from the core.
      ad(26,1) = alad;
      name(26,:) = '#26 pure aluminum              ';
%   matl #27 regblade in (control) --  this is the actual boral control blade.  This
%     material includes the boral (B4C-Al) and the Al clad. This is very similar
%     to matl #23 but the dimensions are different, as follows:
%       boral region: 0.170x1.795 sq inches = 0.4318x4.5593 sq cm
%       full blade with clad: 0.250x1.875 sq inches = 0.635x4.7625 sq cm
%     The Al, C12, and B10 regions densities from matl #23 are used here.
      tarea = 0.635*4.7625;  contrl = 0.4318*4.5593;  clad = tarea-contrl;
      vfal = clad/tarea;  vfc = 1-vfal;
      ad(27,1) = vfal*alad+vfc*Al;    ad(27,4) = vfc*C12;   ad(27,5) = vfc*B10;
      name(27,:) = '#27 regblade in (control)      ';
%   matl #28 core box + gap + Pd shield clad  --  this is a mix of Al + water.  The
%     1-D x-direction cut includes the core box (0.25"), a water gap (0.25"), and
```

```
%     the clad on the Pb shield (0.125").
      tarea = (0.25+0.25+0.125)*2.54;   clad = (0.25+0.125)*2.54;
      vfal = clad/tarea;  vfw = 1-vfal;
      ad(28,1) = vfal*alad;  ad(28,2) = vfw*ad(1,2);  ad(28,3) = vfw*ad(1,3);
      name(28,:) = '#28 Pb shield clad (core side)';
%   matl #29 Pd shield  --  this is pure Pb.
      ad(29,6) = pbad;
      name(29,:) = '#29 pure lead shield          ';
%   matl #30 Pd shield clad + gap --  this is a mix of Al + water.  The 1-D x-dir
%   cut includes the clad on the Pb shield (0.125") and the water gap (0.25") before
%   the thermal column liner (which is pure Al, thue no new matl needed here).
      tarea = (0.125+0.25)*2.54;   clad = (0.125)*2.54;
      vfal = clad/tarea;  vfw = 1-vfal;
      ad(30,1) = vfal*alad;  ad(30,2) = vfw*ad(1,2);  ad(30,3) = vfw*ad(1,3);
      name(30,:) = '#30 Pb shield clad (thm col)  ';
%   matl #31 thermal column  --  this is pure graphite.
      ad(31,4) = gad;
      name(31,:) = '#31 reactor graphite          ';
%   matl #32 inside beam tube   --  this is modeled as low density (5%) water. Note
%     that this is really mostly void (air), but diffusion theory cannot treat this
%     (gives very large diffusion coeffs) --  thus the need for low density water
%     in this region.
      ad(32,2) = 0.05*ad(1,2);  ad(32,3) = 0.05*ad(1,3);
      name(32,:) = '#32 inside beam tube (5% H2O) ';
%   matl #33 top/bot nonfuel refl  --  this is a region of Al + water.  The axial
%     increment is 3.25" (layers 3 & 4 and 16 & 17).  This region is over/under the
%     center/edge regions of the fuel assemblies.  It contains mostly water, but the
%     nonfuel portion of the plates (above and below) the active fuel reion extend
%     into this region of the model.  This region plus the active fuel regions gives
%     the 30" standard height of most of the assemblies.  Note that the side plates
%     are treated separately --  which slightly over estimates the Al vol to roughly
%     compensate for the under estimation here (end box piece in this region is
%     ignored).
      tvol = 7.7724*(7.7724-2*0.8437)*(3.25*2.54);
      alvol = 18*0.127*(25-23.5)*2.54/2;
      vfal = alvol/tvol;  vfw = 1-vfal;
      ad(33,1) = vfal*alad;  ad(33,2) = vfw*ad(1,2);  ad(33,3) = vfw*ad(1,3);
      name(33,:) = '#33 top/bot nonfuel refl      ';
%   Note: There are two models for the top and bottom refl regions outside the
%         standard 30" height of the assemblies.  These include the end boxes on the
%         top (4.75" high) and the end box and grid structure on the bottom (6"
%         thick). There is a 1-region homogeneous model and a 2-region inside/outside
%         model.  The actual geometry is quite complicated, so only a rough
%         approximation is made here.
%         In particular, in the 2-region model, the inside region is pure water
%         (matl #1) in both the top and bottom regions.  For the outer region, on the
%         top we assume a 50/50 mix (same as matl #2), and on the bottom, with the
%         large grid structure, this is pure Al (matl #26) -- which actually
%         underestimates the amount of Al at the bottom (but we will go with this
%         approximation anyway for ease in modeling).  Thus, for the 2-region model,
%         no new materials are needed  --  we will use matls 1, 2, 26 as appropriate.
%         For the 1-region homogeneous model, the region densities as noted above
%         are simply weighted by the inside/outside volume fractions.  Two new
%         materials are needed here for the top and bottom homogenoeus reflectors.
      inside_area = (7.7724-2*0.4995)*(7.7724-2*0.8437);
      vfin = inside_area/assyarea;  vfout = 1-vfin;
%   matl #34 homo top refl
      ad(34,1) = vfout*ad(2,1);
      ad(34,2) = vfin*ad(1,2) + vfout*ad(2,2);
      ad(34,3) = vfin*ad(1,3) + vfout*ad(2,3);
      name(34,:) = '#34 homo top refl             ';
%   matl #35 homo bottom refl
      ad(35,1) = vfout*ad(26,1);
      ad(35,2) = vfin*ad(1,2);   ad(35,3) = vfin*ad(1,3);
      name(35,:) = '#35 homo bottom refl          ';
%   Note:  The above 35 materials are needed for modeling the 3-D BOL M-1-3 LEU core
%          within the UMLRR (also has the WPI BOL fuel densities).  For the M-2-5
%          configuration that includes the FNI, some additional materials are needed
%          to model the lead-void box (a 2-region assembly) and the lead shield
%          blocks in the first three rows of the FNI grid (the VENTURE 3-D model does
%          not model the full FNI  --  only that portion that has any effect on the
```

```
%         core neutron balance).
%   matl #36 Pb void assy (sides) --  this is a mix of Al + Pb + water.  The geometry
%   contains a C-shaped Al component 1/8" thick whose outside dimensions are 3" x
%   0.625".  A 0.5" thick lead block is inside this C-channel and outside this
%   component is the normal 0.03" water gap between assemblies.
      tarea = 7.7724*(0.625+0.03)*2.54;
      clad = 7.62*(0.125*2.54) + 2*(0.125*2.54)*(0.5*2.54);
      pb = (2.75*2.54)*(0.5*2.54);
      vfal = clad/tarea;  vfpb = pb/tarea;  vfw = 1-vfal-vfpb;
      ad(36,1) = vfal*alad;  ad(36,2) = vfw*ad(1,2);  ad(36,3) = vfw*ad(1,3);
      ad(36,6) = vfpb*pbad;
      name(36,:) = '#36 Pb void assy (sides)      ';
%   matl #37 Pb void assy (center void) -- this is a mix of Al +  water.  This region
%   contains a rectangular-shaped Al can 1/8" thick whose outside dimensions are 3" x
%   1.75".  The normal 0.03" water gap is only on this sides of this piece (since
%   matl #36 already accounts for this).
      tarea = 7.7724*(1.75*2.54);
      void = (2.75*2.54)*(1.5*2.54);
      clad = 7.62*(1.75*2.54) - void;
      vfal = clad/tarea;  vfv = void/tarea;  vfw = 1-vfal-vfv;
      ad(37,1) = vfal*alad;  ad(37,2) = vfw*ad(1,2);  ad(37,3) = vfw*ad(1,3);
      name(37,:) = '#37 Pb void assy (center-void)';
%   matl #38 Pb void assy (center H2O) -- this is a mix of Al +  water.  This is the
%   same as matl #37 except that we assume that the assembly has leaked and that the
%   center region has filled with water.
      tarea = 7.7724*(1.75*2.54);
      center = (2.75*2.54)*(1.5*2.54);
      clad = 7.62*(1.75*2.54) - center;
      vfal = clad/tarea;   vfw = 1-vfal;
      ad(38,1) = vfal*alad;  ad(38,2) = vfw*ad(1,2);  ad(38,3) = vfw*ad(1,3);
      name(38,:) = '#38 Pb void assy (center-H2O) ';
%   matl #39 homo Pb void assy (center voided) -- this is a homogenous mix of matl 36
%   and 37 so that we could insert this Pb void assy in a 1-region zone if desired.
      side = 7.7724*(0.625+0.03)*2.54;
      vfside = side/assyarea;   vfcenter = 1-vfside;
      ad(39,:) = vfside*ad(36,:) + vfcenter*ad(37,:);
      name(39,:) = '#39 homo Pb void assy (c-void)';
%   Note: The Pb void assy is 28" high with an additional 0.75" thick Al block on top
%         and a 0.375" Al cap on the bottom.  Also, on the bottom, the end box is a
%         solid Al block that just fits within the grid.  Thus, this region is
%         essentially pure Al.  Unfortunately, this geometry is somewhat inconsistent
%         with the 30" geometry and zone layout for all the other incore elements.
%         Thus, to keep the incore zone layout UNCHANGED, I have decided to make a
%         few rough approximations here, as follows:
%         1. We will treat the Pb-void region as 30" instead of 28" (1-zn axial model)
%         2. The top and bottom axial reflectors will be treated as the other
%            assemblies (puts slightly more Al in the top and less in the bottom).
%         Both these approximations are minor and only affect the densities above and
%         below the active core region  --  but they allow the use of the SAME zone
%         layout as the pre-FNI model. Okay --  go with this for the post-FNI cores.
%   matl #40 Pb shield sides -- this is a mix of water + Al + B-Al.  This region is
%   (0.04 + 0.2775 + 0.04) = 0.3575 inches thick and it will be treated as a single
%   homogeneous material.  The B-Al is 2.5 w/o fully enriched B-10 in the B-Al and
%   the mix has a density of about 2.71 g/cc (I think - this is the best info I have).
%   The region inside the sides is pure Pb (matl 29), so no new material is needed.
      tarea = 0.04+0.2775+0.04;
      can = 0.2775;  liner = 0.04;
      Al = 2.71*0.975*Na/MW(1);   B10 = 2.71*0.025*Na/10.01;
      vfal = can/tarea;   vfbal = liner/tarea;  vfw = 1-vfal-vfbal;
      ad(40,1) = vfal*alad+vfbal*Al;  ad(40,2) = vfw*ad(1,2);  ad(40,3) = vfw*ad(1,3);
      ad(40,5) = vfbal*B10;
      name(40,:) = '#40 Pb shield side/B-Al liner ';
%   Note: The Pb shield blocks are 26" high with additional 1.0" thick Al caps on top
%         and bottom (total of 28").  Also, on the bottom, the end box is a solid Al
%         block that just fits within the grid.  However, there are only 2 of these
%         blocks in the 1 x 3 element.  I plan to place the Pb shield portion in the
%         26" axial region associated with the blade movement (layers 4-16). In the
%         layers above and below these (layer 3 and 17), use matl 2 (50/50 mix)
%         and use matl 26 (pure Al) in layer 18 (use water in layers 1, 2, and 19).
%         This simplification offsets the real axial placement of the Pb shield by
%         about 1.25" with a 1.25" (homogenized) segment of water just above the
```

```
%         grid region.  This is pretty crude, but we are in the excore region and
%         already a few inches below the active active fuel --  thus, these approxs
%         should have minimal effect...
%
%   edit material atom densities
      fid = 1; name = char(name);
      isot = '             Al            H            O            C           B10          Pb
';
      fprintf(fid,'\n      Material Composition (atoms/b-cm) for the 2-D & 3-D UMLRR LEU VENTURE
models (2011 version) \n');
      fprintf(fid,'     Material         %s     \n',isot);
      for i = 1:10
        fprintf(fid,' %s  %11.3e  %11.3e  %11.3e  %11.3e  %11.3e  %11.3e\n', ...
                    name(i,:),ad(i,:));
      end
      fprintf(fid,'  Note: Materials 11 - 19 are for the UMLRR full and partial assemblies and
for the WPI fuel element \n');
      for i = 20:40
        fprintf(fid,' %s  %11.3e  %11.3e  %11.3e  %11.3e  %11.3e  %11.3e\n', ...
                    name(i,:),ad(i,:));
      end
%
%   end of program
```